UNIVERSITÀ
DEGLI STUDI
FIRENZE

DOTTORATO DI RICERCA TOSCANO IN NEUROSCIENZE

CICLO XXXI

COORDINATORE Prof. Renato Corradetti

IH LOSS OF FUNCTION AS A PATHOGENIC MECHANISM UNDERLYING THE SELECTIVE VULNERABILITY OF NIGRAL DOPAMINE NEURONS IN PARKINSON'S DISEASE

Settore Scientifico Disciplinare BIO/14

Dottoranda
Dott.ssa Carbone Carmen

Tutore
Prof. Mannaioni Guido

Supervisore
Dott. Masi Alessio

Coordinatore
Prof. Corradetti Renato

Anni 2015/2018

HO'OPONOPONO

CONTENTS

INTRODUCTION

1. PARKINSON'S DISEASE

Parkinson's disease (PD), is a progressive neurological disorder characterised by early prominent death of dopaminergic (DA) neurons in the substantia nigra pars compacta (SNpc). The resulting dopamine deficiency within the basal ganglia leads to the appearance of motor symptoms such as bradykinesia, resting tremor, rigidity, postural instability, as well as non-motor symptoms such as sleep disturbances, depression, and cognitive deficits (Rodriguez-Oroz et al. 2009). The prevalence of PD is approximately 1.5 to 2% of the population over the age of 55; in fact, PD is the second most common neurodegenerative disorder after Alzheimer's disease. The exact etiology of PD still remains elusive and the precise mechanisms that cause this disease remain to be identified (Obeso et al. 2010). The first detailed description of PD was made two centuries ago when the physician James Parkinson in 1817 described the first clear medical description in "The Shaking Palsy" where he described the daily lives and symptoms of six patients affected by problems such as constant shaking, rigidity and slowness of movement. Later, Jean-Martin Charcot was particularly influential in refining and expanding this early description and in disseminating information internationally about Parkinson's disease. Although PD was once considered a single disease entity, it is now recognised that many disease states can produce parkinsonism. Administration of the dopamine precursor levodopa (L-3,4-dihydroxyphenylaline) effectively, yet transiently, reverts motor deficit but does not stop disease progression and leads, in the long run, to the development of L-DOPA-induced dyskinesia, a condition characterized by the appearance of uncontrolled movements, perceived by patients nearly as disabling as Parkinson's symptoms. Disease-modifying treatments that reduce the rate of neurodegeneration or stop the disease process remain unavailable as yet, and are at present the greatest unmet therapeutic need in PD.

1.1. Clinical characteristics of PD

Parkinson's disease is primarily a disorder of voluntary movement. There are four cardinal features of PD that can be grouped under the acronym TRAP: Tremor at rest, Rigidity, Akinesia (or bradykinesia) and Postural instability. In addition, flexed posture and freezing (motor blocks) have been included among classic features of parkinsonism (Jankovic 2002).

Bradykinesia

Bradykinesia means literally slowness of movement. Given that bradykinesia is one of the most easily recognisable symptoms of PD, it may become apparent before any formal neurological

examination. Bradykinesia is a hallmark of basal ganglia disorders, and it encompasses difficulties with planning, initiating and executing movement and with performing sequential and simultaneous tasks (Berardelli et al. 2001). This is supported by the observation of decreased neuronal density in the SNpc in elderly patients with parkinsonism regardless of PD diagnosis (Ross et al. 2004).It is hypothesised that bradykinesia is the result of a disruption in normal motor cortex activity caused by reduced dopaminergic function.

Tremor

Rest tremor is the most common easily recognised symptom of PD. Tremors are unilateral, occur at a frequency between 4-6 Hz, and almost always are prominent in the distal part of an extremity. Hand tremors are described as supination–pronation ("pill-rolling") tremors that spread from one hand to the other. Rest tremor in patients with PD can also involve the lips, chin, jaw and legs but, unlike essential tremor, rarely involves the neck/head or voice. Characteristically, rest tremor disappears during action execution and during sleep. Some patients with PD have a history of postural tremor, phenomenologically identical to essential tremor, for many years or decades before the onset of parkinsonian tremor or other PD related features. In addition to rest tremor, many patients with PD also have postural tremor that is more prominent and disabling than rest tremor and may be the first manifestation of the disease (Jankovic, Schwartz and Ondo 1999, Jankovic 2002). Parkinson's related postural tremor ("re-emergent tremor") is differentiated from essential tremor in that the appearance of tremor is often delayed after the patient assumes an outstretched horizontal position. Because re-emergent tremor occurs at the same frequency as classical rest tremor and is responsive to dopaminergic therapy, it is likely that it represents a variant of the more typical rest tremor. The occurrence of rest tremor is variable among patients and during the course of the disease. Clinical–pathological studies have demonstrated that patients with PD and prominent tremor have degeneration of a subgroup of midbrain (A9) neurons, whereas this area is spared in PD patients without tremor.

Rigidity

Rigidity is a motor sign characterised by increased resistance to passive movement of a patient's limbs. It may occur proximally (eg, neck, shoulders, hips) or distally (eg, wrists, ankles). Rigidity may be associated with pain, and painful shoulder is one of the most frequent initial manifestations of PD although it is commonly misdiagnosed as arthritis, bursitis or rotator cuff injury (Riley et al. 1989). In addition, rigidity of the neck and trunk (axial rigidity) may occur, resulting in abnormal axial postures (eg, anterocollis, scoliosis).

Postural instability

Postural instability due to loss of postural reflexes is generally a manifestation of the late stages of PD and usually occurs after the onset of other clinical features. Postural instability (along with

freezing of gait) is the most common cause of falls and contributes significantly to the risk of hip fractures (Williams, Watt and Lees 2006).

Freezing

Freezing, also referred to as motor blocks, is a form of akinesia (loss of movement) and is one of the most disabling symptoms of PD (Giladi et al. 2001). Although freezing is a characteristic feature of PD, it does not occur universally. Freezing most commonly affects the legs during walking, but the arms and eyelids can also be involved (Boghen 1997). It typically manifests as a sudden and transient (usually <10 s) inability to move. It is transient, lasting for seconds or minutes, and suddenly abates. Freezing is associated with substantial social and clinical consequences for patients. In particular, it is a common cause of falls (Bloem et al. 2004). Risk factors for the development of freezing include the presence of rigidity, bradykinesia, postural instability and longer disease duration. Replenishment of striatal DA through the oral administration of the DA precursor levodopa alleviates most of the symptoms. Nonetheless, after several years of treatment with levodopa most patients develop involuntary movements, termed dyskinesia, which are difficult to control and impair the quality of life.

Non-motor features

Although PD is primarily a motor disorder, it is often complicated by cognitive and neuropsychiatric problems and careful examination often reveals abnormalities in other parts of the nervous system, including the visual, olfactory, somatosensory and autonomic systems. Failure to appreciate these non-motor problems is often the cause of distress to patients. For most patients with PD, the cognitive deficits are generally mild and subtle. However, up to 25 per cent of patients with parkinsonism will develop dementia over four years. Dementia occurs more commonly in patients with atypical parkinsonian syndromes, such as progressive supranuclear palsy (PSP) or corticobasal ganglionic degeneration (CBGD) (Zesiewicz, Sullivan and Hauser 2006). In addition to cognitive and affective disorders, many patients with PD exhibit features of obsessive–compulsive behaviour, sensory and sleep abnormalities.

1.2. Neurochemical and neuropathological features of PD

The pathologic hallmark of the disease is the progressive loss of nigral DA neurons and the presence of intracytoplasmic inclusions termed “Lewy bodies” (LBs). These are intracytoplasmic bodies consisting of an amorphous core surrounded by a less dense ‘halo’(Gibb, Esiri and Lees 1987).They contain a number of elements including ubiquitin, α-synuclein and proteases (Lennox and Lowe 1997, Spillantini et al. 1998). Their function is thought a consequence of a defect in the systems to involve of disposal of abnormal or damaged proteins (Jellinger 2010), through the ubiquitin-protease system. LBs are commonly observed in the brain region showing the most neuron loss in PD, including substancia nigra, locus coeruleus, the dorsal motor nucleus of the

vagus and the nucleus basalis of Meynert, but they are also observed in neocortex, diencephalon, spinal cord, and even peripheral autonomic ganglia. The role of LBs is controversial and moreover, they are not specific for PD, they are also found in Alzheimer disease, in a condition called "dementia with LBs disease". The cell bodies of nigrostriatal neurons are located in the SNpc, and they project primarily to the putamen. The loss of these neurons, which normally contain conspicuous amounts of neuro-melanin (Marsden 1983), produces the classic gross neuropathological finding of SNpc depigmentation. The pattern of SNpc cell loss appears to parallel the level of expression of the DA transporter (DAT) mRNA (Uhl et al. 1994) and is consistent with the finding that depletion of DA is most pronounced in the dorsolateral putamen (Bernheimer et al. 1973), the main site of projection for these neurons. At the onset of symptoms, putamen DA is depleted 80%, and 60% of SNpc DA neurons have already been lost. The mesolimbic DA neurons, the cell bodies of which reside adjacent to the SNpc in the ventral tegmental area (VTA), are much less affected (Uhl, Hedreen and Price 1985). Although some DA neurons are spared in PD, neurodegeneration is also found in noradrenergic (locus coeruleus), serotoninergic (raphe), and cholinergic (nucleus basalis of Meynert, dorsal motor nucleus of vagus) systems, as well as in the cerebral cortex (especially cingulate and entorhinal cortices), olfactory bulb, and anatomic nervous system (Hornykiewicz and Kish 1987) thus, while the involvement of these areas occurs in the most serious or late diseases, the temporal manifestation of the damage to specific neurochemical systems is not well established. For example, some patients develop depression months or years prior to the onset of PD motor symptoms, which could be due to early involvement of non-DA pathways. (Dauer and Przedborski 2003)

1.3. Anatomy and physiology of the basal ganglia

Basal ganglia are a complex network of nuclei in the forebrain strongly connected with the cerebral cortex, thalamus and other little brain areas. The basal ganglia and related nuclei consist of a variety of subcortical cell groups engaged primarily in motor control, together with a wider variety of roles such as motor learning, executive functions and behavior, and emotions. The term basal ganglia in the strictest sense refers to nuclei embedded deep in the brain hemispheres (striatum or caudate-putamen and globus pallidus), whereas related nuclei consist of structures located in the diencephalon (subthalamic nucleus), mesencephalon (substantia nigra), and pons (pedunculopontine nucleus) (Lanciego, Luquin and Obeso 2012). Several models of the functional anatomy of the basal ganglia have been proposed. The most popular model was introduced in the 1980's (Alexander, Crutcher and DeLong 1990). This model is based on the existence of separate parallel loops, mediating motor, cognitive and emotional functions, and running through the basal ganglia in a more or less uniform fashion. Two important properties of basal ganglia function included in this classical model are convergence and segregation. Convergence refers to the fact

that along the circuits the number of neurons decreases by each step, thus converging information following each relay. Segregation not only implies separation of the individual circuits along their path through the basal ganglia, but also the separation of information flow for motor functions of individual parts of the body (Santens et al. 2003). The basal ganglia and related nuclei can be broadly categorized as (1) input nuclei, (2) output nuclei, and (3) intrinsic nuclei. Input nuclei are those structures receiving incoming information from different sources, mainly cortical, thalamic, and nigral in origin. The caudate nucleus (CN), the putamen (Put), and the accumbens nucleus (NAc) are all considered input nuclei. The output nuclei are those structures that send basal ganglia information to the thalamus and consist of the internal segment of the globus pallidus (GPi) and the substantia nigra pars reticulata (SNr). Finally, intrinsic nuclei such as the external segment of the globus pallidus (GPe), the STN and SNpc are located between the input and output nuclei in the relay of information. Cortical and thalamic efferent information enters the striatum (CN, Put, and Acb) to be processed further within the basal ganglia system. The output nuclei (GPi and SNr) project mainly to the thalamus (ventral nuclei), which, in turn, project back to the cerebral cortex (mainly frontal lobe). The appropriate functioning of the basal ganglia system requires dopamine to be released at the input nuclei. DA cells are present in the SNpc and contain neuromelanin, a dark pigment derived from oxidized and polymerized DA, but also in the VTA, a medial extension of SNpc. DA neurons in the VTA primarily project to the ventral striatum (nucleus accumbens and olfactory tubercle) as part of the so-called Mesolimbic pathway, and to the prefrontal cortex (the mesolimbic pathway).The striatum is the major recipient of inputs to the basal ganglia. It contains two different types of neurons: projection neurons and interneurons (90% and 10% of striatal neurons, respectively). Projection or striatofugal neurons are also called medium-sized spiny neurons (MSNs) because these multipolar neurons have small to medium cellular somata (20 μm in diameter), and their dendritic processes are covered by postsynaptic specializations called dendritic spines. All striatal MSNs are inhibitory neurons that use GABA as the neurotransmitter. Striatofugal MSNs can be divided further, according to their projection targets, into those innervating the GPe nucleus and those projecting to the output nuclei GPi and SNr. Striatal MSNs innervating the GPe nucleus express the dopamine receptor subtype 2 (D_2R), which inhibits intracellular adenyl-cyclase trough G-protein signaling, and give rise to the indirect pathway (striato-GPe-STN-GPi/SNr). On the other hand, striatal MSNs projecting directly to GPi and SNr contain dopamine receptor subtype 1 (D_1R), which activate adenyl-cyclase signaling (D1-containing neurons), and give rise to the direct striatopallidal pathway. Furthermore, striatal MSNs projecting through the indirect pathway are known to contain the neuropeptide enkephalin, whereas the neuropeptides substance P and dynorphin are expressed in those MSNs projecting directly to the GPi and SNr. When DA binds to the D_1R, it facilitates the release of GABA on output nuclei, thus resulting in less tonic inhibition of thalamus which leads to the transient activation of cortical nuclei via glutamate. On the other hand, when DA binds to the D_2R, the release of inhibitory

GABA from the MSNs is reduced, thereby increasing GPe's output of GABA which results in decreased STN output of excitatory glutamate and in a subsequence reduction in GABA release from the output nuclei. This eventually leads to a reduction in the inhibition of thalamo-cortical glutamatergic neurons.

1.4. The Consequences of Dopaminergic Deficit in PD

According to the classic pathophysiologic model of basal ganglia dysfunction in PD dopaminergic depletion reduces the facilitation of MSNs in the direct pathway and increases the activation of indirect circuit neurons, which leads to increased activity of the STN, which, in turn, over activates inhibitory output neurons in the GPi/SNr. Similarly, the reduction of GABAergic inhibition of direct MSNs combined with an increased glutamatergic driving force from the disinhibited STN increases activity in the GPi/SNr , this effectively reduces the likelihood of phasic inhibitory activity in these output neurons, thus impeding movement initiation and execution. Interestingly, two recent in vivo optogenetics studies have provided strong support for the classical model. Kravitz et al. showed that selective stimulation of MSNs expressing D_2R (indirect circuit) provoked movement arrest, whereas activation of MSNs expressing D_1R led to movement activation. This essentially confirmed the notion that the indirect and direct circuits are in functional equilibrium, inhibiting and facilitating movement, respectively. Bateup et colleagues. found that the loss of DARPP-32 in the "direct" striatonigral projection abolished levodopa-induced dyskinesias, whereas in striatopallidal neurons produced a robust increase in locomotor activity and reduced cataleptic response to haloperidol. These two elegant studies, based on selective activation or inhibition of the direct and indirect striatopallidal circuits in vivo, corroborated the hypothesis of the existence of a functional balance between these projection systems (Lanciego et al. 2012).

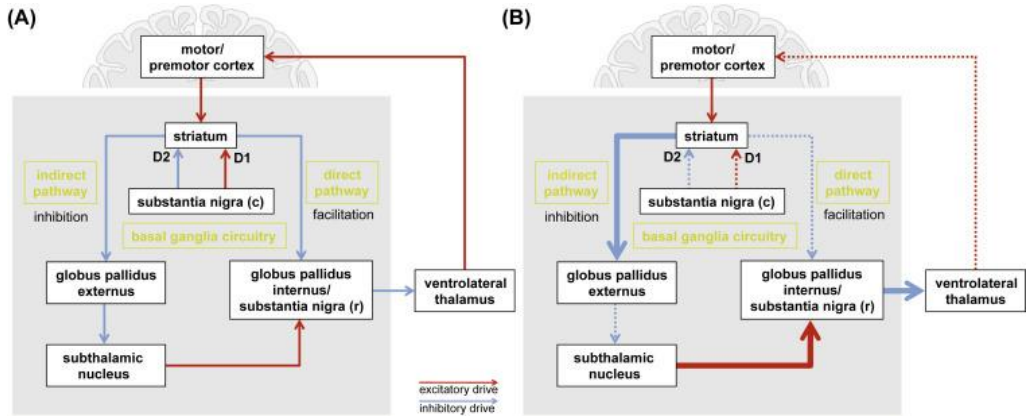

Figure 1**: Basal ganglia circuitry in normal conditions and in Parkinson's' disease.** Model of excitatory (red arrows) and inhibitory (blue arrows) influences within the basal ganglia circuitry under physiological conditions. (B) Changes within the basal ganglia circuitry in the Parkinsonian brain (bold arrows, increase in excitation/inhibition; dotted arrows, decrease in excitation/inhibition). (Adapted from J.Watson et al., 2017)

2. ETIOLOGY OF PD

PD is now widely accepted as a complex, multifactorial disease. Despite an intense research effort over many years, the exact causes aren't fully understood. Researchers have identified characteristics that increase a person's risk of developing Parkinson's, including gender, age, race, and genetic factors. Age is the largest risk factor for the development and progression of PD. Ageing affects many cellular processes that predispose to neurodegeneration, and age-related changes in cellular function predispose to the pathogenesis of PD. PD reflects a failure of the normal cellular compensatory mechanisms in vulnerable brain regions, and this vulnerability is increased by a genetic susceptibility acted upon by other genetic and environmental factors (Hindle 2010). In fact, the contributions of environmental toxins and genetic factors regarding the cause of PD have been hotly debated. The environmental toxin hypothesis was dominant for much of the 20th century, especially because of the example of post encephalitic PD (as described in the Oliver Sacks' book Awakenings) and the discovery of MPTP-induced parkinsonism. However, the discovery of PD-causing genes has renewed interest in hereditary susceptibility factors. Both probably play a role. The environmental hypothesis posits that PD-related neurodegeneration results from exposure to a dopaminergic neurotoxin. Theoretically, the progressive neurodegeneration of PD could be produced by chronic neurotoxin exposure or by limited exposure initiating a self-perpetuating cascade of deleterious events. The finding that people intoxicated with MPTP develop a syndrome nearly identical to PD (Langston et al. 1983) is a prototypic example of how brief exposure to an exogenous toxin can mimic the clinical and pathological features of PD. Paraquat is structurally similar to 1-methyl-4-phenylpyridinium (MPP^+), the active metabolite of MPTP, and has been used as a herbicide. Like MPP^+, rotenone is also a mitochondrial poison present in the environment, due to its use as an insecticide and to kill unwanted lake fish. Human epidemiological studies have implicated residence in a rural environment and related exposure to herbicides and pesticides with an elevated risk of PD (Tanner 1992). Yet, there are convincing data to implicate any specific toxin as a cause of sporadic PD, and chronic environmental exposure to MPP^+ or rotenone is likely to cause PD. Still, cigarette smoking and coffee drinking are inversely associated with the risk for development of PD (Hernán et al. 2002) reinforcing the concept that some environmental factors do modify PD susceptibility or affect disease progression. Another possibility, which does not fit neatly into a genetic or environmental category, is that an endogenous toxin may be responsible for PD neurodegeneration. Distortions of normal metabolism might create toxic substances because of environmental exposures or inherited differences in metabolic pathways. One source of endogenous toxins may be the normal metabolism of DA, which generates harmful reactive oxygen species (ROS) (Cohen 1984). Consistent with the endogenous toxin hypothesis is the report that patients harboring specific polymorphisms in the gene encoding the xenobiotic detoxifying enzyme cytochrome P450 may be at greater risk of developing young-onset PD (Sandy et al., 1996). Further, isoquinoline derivatives toxic to DA

neurons have been recovered from PD brains (Nagatsu 1997). However, the discovery of inherited form of PD shifted the emphasis back to genetic factors. Among the different genetic forms of PD, mutations in the gene encoding for α-synuclein have received most attention. Furthermore, Alpha-synuclein is one of the major components of Lewy bodies and Lewy neurites in sporadic PD (Spillantini et al. 1998), and two missense mutations in the alpha-synuclein gene (A53T and A30P) have been identified in several families with autosomal dominant parkinsonism (Polymeropoulos et al. 1997, Krüger et al. 1998).

2.1. Pathogenesis of PD

Whatever insult initially provokes neurodegeneration, studies of toxic PD models and the functions of genes implicated in inherited forms of PD suggest two major hypotheses regarding the pathogenesis of the disease. One hypothesis posits that misfolding and aggregation of proteins are instrumental in the death of SNpc DA neurons, while the other proposes that the culprit is mitochondrial dysfunction and the consequent oxidative stress, including toxic oxidized DA species. The pathogenic factors cited above are not mutually exclusive, and one of the key aims of current PD research is to elucidate the sequence in which they act and whether points of interaction between these pathways are key to the demise of SNpc DA neurons.

2.1.1. Misfolding and aggregation of proteins

The abnormal deposition of protein in brain tissue is a feature of several age-related neurodegenerative diseases, including PD. Although the composition and location (i.e., intra- or extracellular) of protein aggregates differ from disease to disease, this common feature suggests that protein deposition per se, or some related event, is toxic to neurons. Aggregated or soluble misfolded proteins could be neurotoxic through a variety of mechanisms. Protein aggregates could directly cause damage, perhaps by deforming the cell or interfering with intracellular trafficking in neurons. Protein inclusions might also sequester proteins that are important for cell survival. If so, there should be a direct correlation between inclusion formation and neurodegeneration. However, a growing body of evidence, particularly from studies of Huntington disease (HD) and other polyglutamine diseases (Saudou et al. 1998, Cummings et al. 1999), suggests that there is no correlation between inclusion formation and cell death. Cytoplasmic protein inclusions may not result simply from precipitated misfolded proteins but rather from an active process meant to sequester soluble misfolded proteins from the cellular milieu (Kopito 2000). Accordingly, while possibly indicative of a cell under attack, inclusion formation may be a defensive measure aimed at removing toxic soluble misfolded proteins (Warrick et al. 1999, Cummings et al. 1999, Cummings et al. 2001) the ability of chaperones such as Hsp-70 to protect against neurodegeneration provoked by disease-related proteins (including a-synuclein-mediated DA neuron loss) is consistent with the view that soluble misfolded proteins are neurotoxic (Muchowski 2002). In patients with inherited

PD, pathogenic mutations are thought to cause disease directly by inducing abnormal and possibly toxic protein conformations (e.g.,(Bussell and Eliezer 2001) or indirectly by interfering with the processes that normally recognize or process misfolded proteins. In sporadic PD, there is a similar focus both on direct protein-damaging modifications and on dysfunction of chaperones or the proteasome that may indirectly contribute to the accumulation of misfolded proteins. The triggers for dysfunctional protein metabolism in sporadic PD are only just beginning to be elucidated. One trigger may be oxidative stress, long thought to play a key role in the pathogenesis of PD through damage caused by ROS (Przedborski et al. 2000). The tissue content of abnormally oxidized proteins (which may misfolded) increases with age reviewed by (Beckman and Ames 1998), and neurons may be particularly susceptible because they are postmitotic. In PD, LBs contain oxidatively modified a-synuclein, which in vitro exhibits a greater propensity to aggregate than unmodified a-synuclein (Giasson et al. 2000). Several herbicides and pesticides induce misfolding or aggregation of a-synuclein (Uversky, Li and Fink 2001, Manning-Bog et al. 2002). There also appears to be an age-related decline in the ability of cells to handle misfolded proteins (Sherman and Goldberg 2001). Cells respond to misfolded proteins by inducing chaperones, but if not properly refolded they are targeted for proteasomal degradation by polyubiquitination. With aging, the ability of cells to induce a variety of chaperones is impaired as is the activity of the proteasome. Proteasomal dysfunction and the consequent accumulation of misfolded proteins may provoke a vicious cycle, with excess misfolded proteins further inhibiting an already compromised proteasome (Dauer and Przedborski 2003) .

2.1.2. Role of oxidative stress and deficits in energy metabolism in PD

In both idiopathic and genetic cases of PD, oxidative stress is thought to be the common underlying mechanism that leads to cellular dysfunction and demise. Oxidative stress occurs when an imbalance is formed between production of ROS and cellular antioxidant activity (Blesa et al. 2012). Oxidants and superoxide radicals are produced as products of oxidative phosphorylation, making mitochondria the main site of ROS generation within the cell. Because of the presence of ROS-generating enzymes such as tyrosine hydroxylase and monoamine oxidase, the DA neurons are particularly prone to oxidative stress. In addition, the nigral DA neurons contain iron, which catalyses the Fenton reaction, in which superoxide radicals and hydrogen peroxide can contribute to further oxidative stress (Halliwell 1992). Mitochondria-related energy failure may disrupt vesicular storage of DA, causing the free cytosolic concentration of DA to rise and allowing harmful DA-mediated reactions to damage cellular macromolecules. Thus, DA may be pivotal in rendering SNpc DA neurons particularly susceptible to oxidative attack. Because of this intrinsic sensitivity to reactive species, a moderate oxidative stress can trigger a cascade of events that lead to cell demise. The major sources of such oxidative stress generated for the nigral DA neurons are

thought to be the ROS produced during DA metabolism, neuroinflammation and mitochondrial dysfunction.

DA metabolism

Selective degeneration of the DA neurons of the SNpc suggests that DA itself may be a source of oxidative stress (Segura-Aguilar et al. 2014). DA is synthesized from tyrosine by tyrosine hydroxylase (TH) and aromatic amino acid decarboxylase. Following this, DA is stored in synaptic vesicles after uptake by the vesicular monoamine transporter 2 (VMAT2). However, when there is an excess amount of cytosolic DA outside of the synaptic vesicle in damaged neurons, i.e., after L-DOPA treatment, DA is easily metabolized via monoamine oxidase (MAO) or by auto-oxidation to cytotoxic ROS (Zucca et al. 2014). For example, mishandling of DA in mice with reduced VMAT2 expression was sufficient to cause DA-mediated toxicity and progressive loss of DA neurons (Caudle et al. 2007). This oxidative process alters mitochondrial respiration and induces a change in the permeability transition pores in brain mitochondria (Berman and Hastings 1999). Also, the auto-oxidation of DA produces electron-deficient DA quinones or DA semiquinones (Sulzer and Zecca 2000). Some studies have demonstrated a regulatory role for quinone formation in DA neurons in the L-DOPA-treated PD model induced by neurotoxins and in methamphetamine neurotoxicity (Asanuma, Miyazaki and Ogawa 2003, Ares-Santos et al. 2014) DA quinones can modify a number of PD-related proteins, such as α-synuclein , parkin, DJ-1, Superoxide dismutase-2 (SOD2), and UCH-L1 (Belluzzi et al. 2012, Girotto et al. 2012, da Silva et al. 2013, Hauser et al. 2013) and have been shown to cause inactivation of the DA transporter (DAT) and the TH enzyme (Kuhn et al. 1999), as well as mitochondrial dysfunction (Lee et al. 2003), alterations of brain mitochondria (Gluck and Zeevalk 2004) and dysfunction in Complex I activity (Jana et al. 2011, Van Laar et al. 2009). Additionally, DA quinones can be oxidized to amino chrome, whose redox-cycling leads to the generation of the superoxide radical and the depletion of cellular nicotinamide adenine dinucleotide phosphate-oxidase (NADPH), which ultimately forms the neuromelanin (Sulzer et al. 2000) known to be accumulated in the SNpc of the human brain (Plum et al. 2013).Significant increases in cysteinyl adducts of L-DOPA, DA, and DOPAC have been found in substantia nigra of PD patients, suggesting the cytotoxic nature of DA oxidation (Spencer et al. 1998). Also, DA terminals actively degenerated proportionally to increased levels of DA oxidation following a single injection of DA into the striatum (Rabinovic, Lewis and Hastings 2000). Recently, it has been shown that increased uptake of DA through the DAT in mice results in oxidative damage, neuronal loss and motor deficits (Masoud et al. 2015).

Neuroinflammation

Neuronal loss in PD is associated with chronic neuroinflammation, which is controlled primarily by microglia, the major resident immune cells in the brain (Barcia et al. 2003) and, to a lesser extent,

by (Perry 2012). Microglial activation has been found with a greater density in the SNpc (Lawson et al. 1990) and in the olfactory bulb of both sporadic and familial PD patients (McGeer et al. 1988). When activated, they release free radicals such as nitric oxide and superoxide, which can in turn contribute to oxidative stress in the microenvironment. This is thought to be exacerbated by inflammatory signals generated by molecules released from damaged neurons, leading to induction of reactive microgliosis. The oxidized or ROS-induced molecules that are released from damaged nigral DA neurons and trigger microglial activation include neuromelanin, α-synuclein. Neuromelanin confers the dark pigmentation that is produced from DA oxidation and is so characteristic of the SNpc appearance. High levels of catecholamine metabolism in the midbrain are associated with increased levels of neuromelanin in the same region and, it is neuromelanin that is thought to be one of the molecules responsible for inducing chronic neuroinflammation in PD. Neuromelanin released from dying DA neurons in the SNpc activate microglia, increasing the sensitivity of DA neurons to oxidative stress-mediated cell death (Halliday et al. 2005, Zhang et al. 2011). Neuromelanin appears to remain for a very long time in the extracellular space (Langston et al. 1999) and thus thought to be one of the molecules responsible for inducing chronic neuroinflammation in PD.

2.2. Mitochondrial Dysfunction

As neurons have a considerable energy need and are also highly equipped with mitochondria they are extremely sensitive to mitochondrial dysfunction. Several neurological disorders are associated with mitochondrial dysfunction and demonstrate enhanced production of free-radical species (Finsterer 2006, Lin and Beal 2006). The first line of evidence for a link between mitochondrial dysfunction and PD came from the description of Complex I (CI) deficiency in the postmortem SNpc of PD patients and has been suggested to be one of the fundamental causes of PD (Schapira et al. 1990, Mizuno et al. 1989). This CI deficiency was also seen in the frontal cortex in PD (Parker, Parks and Swerdlow 2008), and in peripheral tissues such as platelets (Haas et al. 1995) and skeletal muscle (Haas et al. 1995) suggesting that there is a global reduction in mitochondrial CI activity in PD. This inhibition of CI can lead to the degeneration of affected neurons by a number of mechanisms such as increased oxidative stress and excitotoxicity (Sherer et al. 2002b). A link between impairment of mitochondrial CIII assembly, an increase in free radical-production, and PD has also been identified (Rana et al. 2000). Complex I or III inhibition causes an increase in the release of electrons from the transport chain into the mitochondrial matrix which then react with oxygen to form ROS such as,·O2−, hydroxyl radicals (·OH) and nitric oxide (NO·). This increase in the normal electron leakage occurs by blockage of electron movement along the chain to the next acceptor molecule. The ROS formed can act as signaling molecules by causing lipid peroxidation or promote excitotoxicity, all leading to modification of proteins and eventual cell death. The main areas in which ROS cause damage in the cell include oxidative DNA damage,

lipid peroxidation, and protein oxidation and nitration. One target of these reactive species may be the electron transport chain itself (Cohen 2000), leading to mitochondrial damage and further promotion of ROS. Several Complex I inhibitors such as MPTP or rotenone show some of the key motor features of PD and are used in PD neurotoxic models. Interestingly, rotenone toxicity is involved in oxidative damage to proteins and Lewy body-like inclusions (Betarbet et al. 2000). Other evidence for mitochondrial dysfunction related to oxidative stress and DA cell damage comes from findings that mutations in genes of proteins like α-synuclein, parkin, DJ-1, or PINK are linked to familial forms of PD. The convergence of all of these proteins on mitochondrial dynamics uncovers a common function in the mitochondrial stress response that might provide a potential physiological basis for the pathology of PD (Norris et al. 2015, van der Merwe et al. 2015). Overall, these observations show that mutations in these genes affect mitochondrial function and integrity and, are associated with increases in oxidative stress (Zuo and Motherwell 2013). ROS influence proteasomal, lysosomal, and mitochondrial function, which, in turn, regulate the cellular response to oxidative damage (Cook, Stetler and Petrucelli 2012). The correct elimination of damaged proteins by effective proteolysis and the synthesis of new and protective proteins are vital in the preservation of brain homeostasis during periods of increased levels of ROS. Consequently, this can lead to protein misfolding (i.e., α-synuclein), preventing the ability of some of these proteins to be unfolded and degraded by the systems that regulate protein clearance, like the ubiquitin proteasome system or autophagy. Indeed, protein misfolding, together with the dysfunction of these protein degradation systems, may play a key role in the appearance of deleterious events implicated in the neurodegenerative process of PD (Schapira et al. 2014).

2.2.1. Involvement of Ca^{2+} in Mitochondrial Dysfunction

The cellular damage caused by electron transfer chain inhibition may contribute to neuronal excitotoxicity exacerbating neurotoxicity in PD. Several mechanisms for excitotoxicity in neurodegenerative conditions have been proposed (Albin and Greenamyre 1992). Excitotoxicity occurs when depolarisation of the neuronal cell membrane from −90 mV to between −60 and −30 mV leads to a decrease in the magnesium blockade of N-methyl-D-aspartate (NMDA) receptors. This, in turn, leads to NMDA receptor activation by latent levels of glutamate and causes an intracellular Ca^{2+}accumulation. This increase in Ca^{2+} is then thought to cause neurotoxicity by two main mechanisms. Firstly, Ca^{2+} causes an increase in intracellular via activation of nitric oxide synthase (NOS). The excess of in the cell can react with to form peroxynitrite (Dawson and Dawson 1996), which can cause cell death by mechanisms similar to those caused by ROS and mentioned above. Besides, the peroxynitrite, itself can lead to cell damage via nitrosylation of various proteins.

A second mechanism driven by intracellular Ca^{2+} increase causes toxicity in DA neurons by acting on mitochondria themselves. The Ca^{2+} influx is extensively accumulated in the mitochondria and

leads to effects on mitochondrial membrane potential and ATP synthesis as well as generation of ROS (Nicholls and Budd 1998) contributing to the oxidative damage discussed above. This also all feeds back causing further malfunction of the cell's Ca^{2+} homeostasis and additional cellular damage.

Mitochondrial dysfunction can lead to excitotoxicity and cause a reduction in cellular ATP levels, an increase in cellular Ca^{2+}, or a combination of both (Sherer, Betarbet and Greenamyre 2002a). Inhibition of Complex I, and consequently ATP generation, lowers intracellular ATP, leading to partial neuronal depolarisation, due to a reduction in the activity of Na^{+}/K^{+}-ATPase. The Na^{+}/K^{+}-ATPase acts to maintain the resting membrane potential of the cell. A reduction in ATP levels will compromise this function leading to depolarisation and, therefore, excitotoxicity via over activation of NMDA receptors. Intracellular Ca^{2+} can be increased by two methods, that is, either directly by mitochondrial impairment or by over activity of NMDA receptors. Mitochondria can take up Ca^{2+} from the cytosol via an uniporter transporter or a transient "rapid mode", both of which rely on the mitochondrial membrane potential, reviewed by (Gunter et al. 2000). The ROS generated by mitochondrial respiratory chain dysfunction can damage the mitochondrial membranes and disrupt this mechanism of Ca^{2+} uptake and storage, thereby raising intracellular Ca^{2+} levels and exacerbating the excitotoxicity. Sherer et al. showed that this could be a viable mechanism for cell death in PD by inhibiting Complex I in SH-SY5Y cells and showing a disruption in the mitochondrial membrane potential leading to an increased susceptibility to calcium overload (Sherer et al. 2003). It has also been shown that there is an increase in glutamate activity linked to excitotoxicity in the SNpc of mice treated with the Parkinsonian toxin MPTP, which may be linked to apoptosis and autophagy (Meredith et al. 2009). This evidence suggests that mitochondrially derived or driven excitotoxicity could be a major contributory factor in PD.

Further to being integrally involved in mitochondrially generated excitotoxic cell death in PD, Ca^{2+} has been implicated in other mechanisms of cell death in the disease that may involve compromise of the role of mitochondria as one of the major intracellular Ca^{2+} stores. Sheehan et al. reported that mitochondria from PD patients showed lower sequestration of calcium than age-matched controls suggesting a role for Ca^{2+}homeostasis dysfunction in PD (Sheehan et al. 1997). This would lead to higher intracellular Ca^{2+} levels, which has been shown to amplify free-radical production (Dykens 1994) and, therefore, an increase in ROS. An increase in cytosolic Ca^{2+}due to mitochondrial dysfunction has also been suggested to activate calpains and so raise levels of toxic α-synuclein proposing another link with PD (Esteves et al. 2010), a discovery supported by the protective effect of calpain inhibition in an MPTP model of PD (Crocker et al. 2003).

A role for Ca^{2+} and mitochondria has also been suggested in a mechanism of increased susceptibility to cell death specific to SNpc DA neurons and, therefore, relevant for PD. SNpc DA neurons are atypical in the brain in that they have self-generated pacemaker activity (Grace and Bunney 1983) mediated by Cav1.3, a rare L-type Ca^{2+} channel (Striessnig et al. 2006). This activity

means that the Cav1.3 channels are open for a higher proportion of time than Ca^{2+} channels in other neurons leading to an increased ATP usage in the cells to pump Ca^{2+} across the membrane up steep concentration gradients (Surmeier, Guzman and Sanchez-Padilla 2010). This elevated need for ATP would lead to an increase in the activity of the electron transport chain, therefore increasing ROS production so exacerbating any mitochondrial dysfunction and making SNpc DA neurons more prone to cell death.

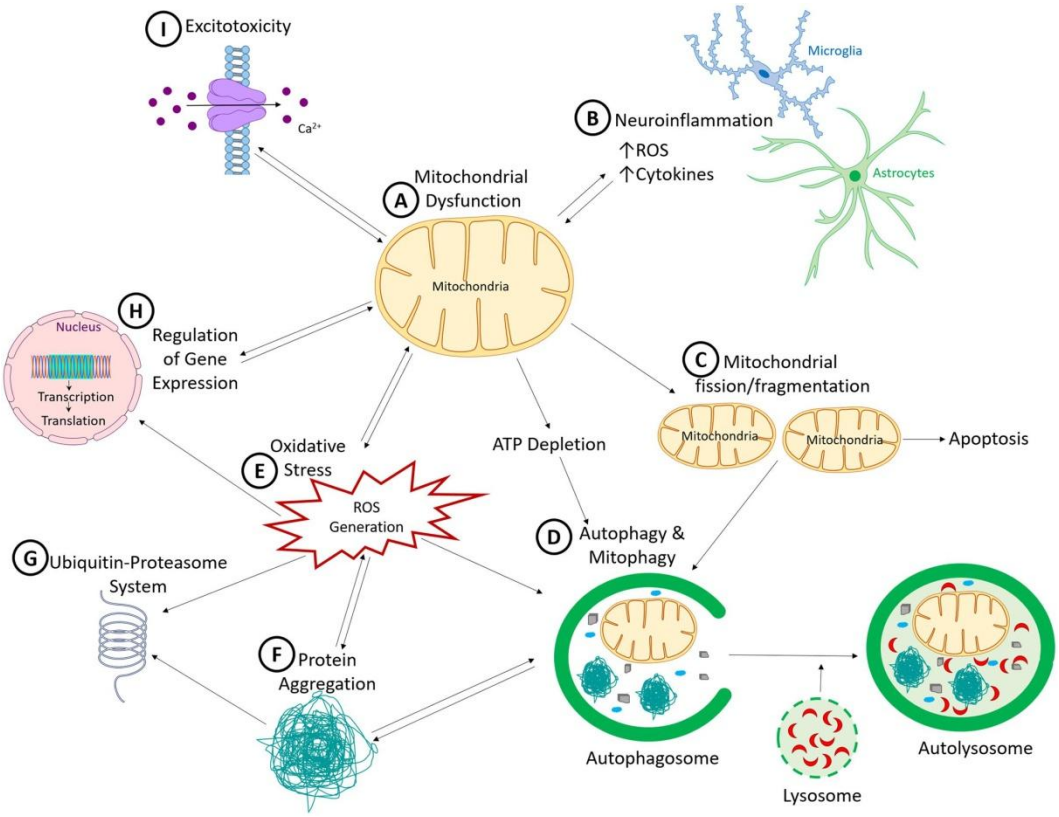

Figure 2: Common pathogenic mechanism in PD. (A) Mitochondrial dysfunction, (B) Neuroinflammation, (C) Increased mitochondrial fission and fragmentation,. (D) Autophagy, (E) Generation of ROS, (F) Impair ubiquitin proteasomal system function, (G) DNA damage, (H) Nuclear DNA encodes mitochondrial proteins, (I) Increased cellular Ca^{2+} and excitotoxicity. Adapted from (Helley et al. 2017)

3. MITOCHONDRIAL DYSFUNCTION IN PD

PD is now widely accepted as a complex, multifactorial disease that can have diverse genetic, biological and environmental influences (Polito, Greco and Seripa 2016). Sporadic PD patients, who lack evidential family history and a definitive genetic basis, account for > 90% of disease cases. However, the familial forms of PD involve mutations in a number of genes that allowed to infer cellular pathways central to PD pathophysiology (Singleton, Farrer and Bonifati 2013). Many lines of evidence implicate that oxidative stress, neuroinflammation and environmental factors are increasingly appreciated as key determinants of DA neuronal susceptibility in PD, and are a feature of both familial and sporadic forms of the disease (Ryan et al. 2015). In both cases, mitochondrial dysfunction is thought to be the common underlying mechanism that leads to cellular dysfunction and, eventual neuronal death.

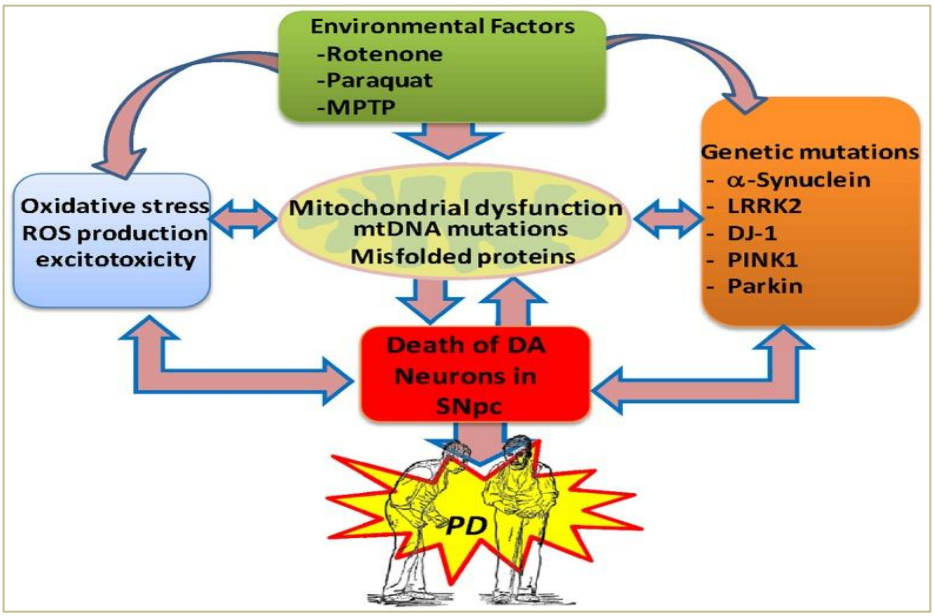

Figure 3: Central role of mitochondrial dysfunction in etiology of PD. Recent evidence suggests that environmental and genetic risk factors induces oxidative stress, excitotoxicity and mitochondrial dysfunction determine the degeneration of midbrain DA system, resulting in PD. Adapted from (Barreto, Iarkov and Moran 2014)

3.1 Mitochondrial Dysfunction in Sporadic PD

Sporadic PD occurs as a seemingly random occurrence due to undetermined genetic or environmental bases in the absence of an obvious family history.

Mitochondrial dysfunction plays a major role in the pathogenesis of PD, and in particular, defects of mitochondrial complex-I of the respiratory chain may be the most appropriate cause degeneration of neurons in PD by reducing the synthesis of ATP. Several epidemiological studies have shown that pesticides and other toxins from the environment that inhibits complex-I is involved in the pathogenesis of sporadic PD.

Rotenone, MPTP, paraquat, nitric oxide, the dopamine metabolite aminochrome are endogenous and exogenous inhibitors of mitochondrial function with an increase generation of ROS. In particular, rotenone is a widely used pesticide. Chronic systemic exposure to rotenone in rats causes many features of PD, and also including nigrostriatal DA degeneration. In fact, it is highly lipophilic and readily enter in all neuronal cells and intracellular organelles, such as mitochondria, without the aid of transporters. Once inside them, it binds and inhibits mitochondrial complex I, causing formation of ROS and inhibiting proteasome activity. Rotenone administration has been shown to oxidatively modify DJ-1 and cause α-synuclein aggregation, which are effects linked to PD and localised to the DA neurons of the SNpc (Betarbet et al. 2006). Paraquat has very similar structure to MPTP and MPP^+, suggesting a similar toxic mechanism. However, unlike rotenone and MPP^+, paraquat does not inhibit Complex I and is not taken up by DAT, suggesting an alternative mechanism of cell death (Richardson et al. 2005). Whichever complex or enzyme is involved, the paraquat radical can react with oxygen to form and cause oxidative stress and mitochondrial dysfunction (Cochemé and Murphy 2008). Furthermore, systemic administration of paraquat to mice leads to SNpc DA neuron degeneration accompanied by a-synuclein containing inclusions, although DA cell loss is moderate. Consistently with these evidences, a significantly younger onset of sporadic PD has been linked to chronic occupational exposure to pesticides and heavy metals (Ratner et al. 2014).

MPTP

The first toxin that linked mitochondrial Complex I inhibition and PD was MPTP. MPTP is a by-product of the synthesis of a meperidine analogue with heroin-like properties (LEE and ZIERING 1947). In 1982, MPTP was accidentally discovered because young drug addicts developed an idiopathic parkinsonian syndrome after intravenous injection of this compound. After investigating the etiology of their condition, in humans and monkeys, it was found that MPTP produces an irreversible and severe parkinsonian syndrome characterized by all of the features of PD, including tremor, rigidity, slowness of movement, postural instability, and freezing. As in PD, monkeys treated with low-dose MPTP exhibit preferential degeneration of putamenal versus caudate dopaminergic nerve terminals (Moratalla et al. 1992).Similarly, MPTP damages the DA pathways in a pattern similar to that seen in PD, including relatively greater cell loss in the SNpc than the VTA and a preferential loss of neurons in the ventral and lateral segments of the SNpc (Varastet et al. 1994) this regional pattern is also found in MPTP-treated mice (Seniuk, Tatton and Greenwood 1990, Muthane et al. 1994).

In MPTP-intoxicated humans and nonhuman primates, the beneficial response to levodopa and development of long-term motor complications to medical therapy are virtually identical to that seen in PD patients. Also similar to PD, the susceptibility to MPTP increases with age in both monkeys and mice (Irwin, DeLanney and Langston 1993, Ovadia, Zhang and Gash 1995, Rose et

al. 1993). For all these reasons, today it represents the most important and most frequently used parkinsonian toxin applied in animal models.

Mechanism of action

MPTP, which is highly lipophilic, crosses the blood-brain barrier within minutes (Markey et al., 1984). Once in the brain, the pro-toxin MPTP is oxidized to 1-methyl-4-phenyl-2,3-dihydropyridinium (MPDP1) by monoamine oxidase B (MAO-B) in glia and serotonergic neurons, the only cells that contain this enzyme. It is then converted to MPP^+ (probably by spontaneous oxidation), the active toxic molecule, released from the astrocytes into the extracellular space via the OCT-3 transporter. Once released, MPP^+ is taken up into the neuron by DAT. Inside neurons, MPP1 can follow at least three routes: (1) it can bind to the vesicular monoamine transporter-2 (VMAT2), which translocates MPP1 into synaptosomal vesicles (Liu, Roghani and Edwards 1992); (2) it can be concentrated within the mitochondria by a mechanism that relies on the mitochondrial transmembrane potential (Ramsay and Singer 1986); and (3) it can remain in the cytosol to interact with cytosolic enzymes, especially those carrying negative charges (Klaidman et al. 1993). Vesicular sequestration of MPP1 appears to protect cells from MPTP-induced neurodegeneration by sequestering the toxin and preventing it from accessing mitochondria, its likely site of action.

The importance of vesicular sequestration has been established by a number of experiments, including those showing that cells transfected to express greater density of VMAT2 are converted from MPP1-sensitive to MPP1-resistant cells (Liu et al. 1992) and that heterozygous VMAT2 null mice display enhanced sensitivity to MPTP-induced neurodegeneration (Takahashi et al. 1997). It appears that the ratio of DAT to VMAT2 expression predicts the likelihood of neuronal degeneration both in PD and the MPTP model. For instance, the putamenal dopaminergic terminals, which are most severely affected by both MPTP and PD, have a higher DAT/VMAT2 ratio than those in the caudate, which are less affected (Miller et al. 1999). Consequently, mice lacking the DAT are protected from MPTP toxicity (Meredith and Rademacher 2011).

Once inside the mitochondria MPP^+ is taken up into via passive transport due to the large mitochondrial transmembrane gradient , where MPP^+ is able to inhibits mitochondrial Complex I (Nicklas et al. 1987). This inhibition of Complex I leads to cell death via energy deficits (Przedborski et al. 2000), free radical and ROS generation, and possibly excitotoxicity (Zhang et al. 2011). Alterations in energy metabolism and generation of ROS peak within hours of MPTP administration, days before overt neuronal death has occurred (Jackson-Lewis et al. 1995). Therefore, these initial events are not likely to directly kill most cells but rather set into play downstream cellular events that ultimately kill most DA neurons (Mandir et al. 1999, Saporito et al. 1999, Vila et al. 2001). Prolonged administration of low to moderate doses of MPTP to mice leads to morphologically defined apoptosis of SNpc DA neurons (Tatton and Kish 1997). Under this regimen of MPTP intoxication, it has been observed an upregulation of Bax, a potent agonist of

programmed cell death (PCD), that trigger the release of cytochrome c and activation of caspases 9 and 3. At the same time, PCD antagonists such as Bcl-2 are downregulated in the SNpc (Vila et al. 2001). Consistent with these observations, Bax null and Bcl-2 transgenic mice are both resistant to MPTP neurotoxicity (Yang et al. 1998, Vila et al. 2001). How MPTP provokes these changes in Bcl-2 family members remains to be elucidated. MPTP causes oxidative damage to DNA (Mandavilli, Ali and Van Houten 2000, Mandir et al. 1999), which may be important in inducing Bax via p53 activation. The tumor suppressor protein p53 is one of the few molecules known to regulate Bax expression and is activated by DNA damage. Furthermore, pharmacological inhibition of p53 attenuates MPTP-induced Bax upregulation and the subsequent SNpc DA neuron death (Duan et al. 2002), and p53 null mice are resistant to MPTP-induced neurodegeneration (Trimmer et al. 1996).

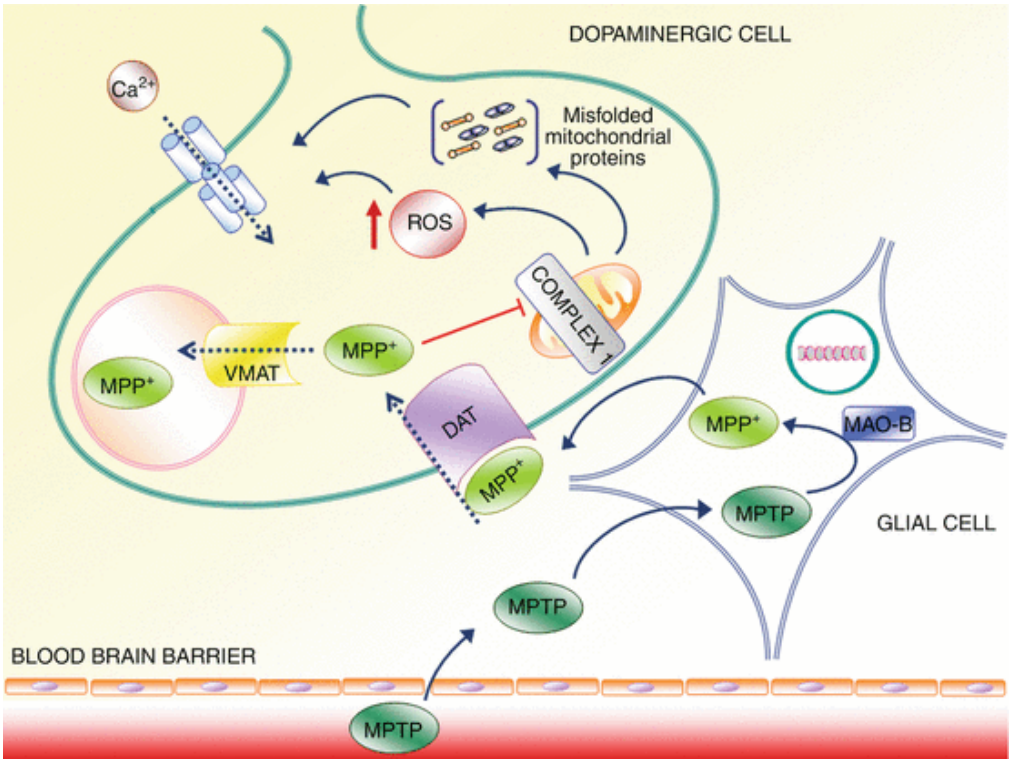

Figure 4: MPTP Neurotoxicity. Mechanism of action of MPTP/MPP^+ in DA neurons. Adapted from Livia Pasquali et al., 2014.

3.2. Mitochondrial Dysfunction in Familial PD

Recent advances in PD genetics have shown the evidence for a vital role of mitochondrial dysfunction in the pathogenesis of the disease. The identification of genes associated with parkinsonism has had a major advance on PD research, showing that most of them can affect or regulate different functional or physiological aspects of mitochondria. Familial PD is caused by

mutations in genes identified by linkage analyses that are inherited in an autosomal recessive or dominant manner. Many of the pathogenic mutations in these genes were directly linked to mitochondrial dysfunction (i.e. autosomal dominant SNCA and LRRK2 mutations and autosomal recessive parkin, PINK1, DJ-1 and ATP13A2 mutations) (Lill 2016). More recently, new roles in the regulation of mitochondrial biology have been determined for these genes, and new PD genes associated with mitochondrial (dys)function, such as VPS35 and CHCHD2, have been identified, further under-pinning the essential role of mitochondrial function to the aetiology of PD. What we know so far about the function and dysfunction of PD genes confirms the relevance of the biochemical alterations found in sporadic PD, i.e., mitochondrial dysfunction, oxidative stress and a dysbalance in protein homeostasis characterized by an increase in protein misfolding and aggregation accompanied by an impaired removal of misfolded proteins. Thus, insight into the function of PD genes can promote our understanding of the molecular causes of PD and help to focus research on key biochemical pathways. The case of α-synuclein provides the first demonstration of a genetic defect leading to PD, and thus has historical and conceptual value. It is a soluble protein that is highly enriched in the presynaptic terminals of neurons. Accumulation of α-synuclein as intracellular filamentous aggregates is a pathological feature of both sporadic and familial PD (Goedert et al. 2013). This evidence was supported by the discovery that aggregates of α-synuclein are the major components of LBs (Spillantini et al. 1998). Although there are many theories on the mechanism by which mutant α-synuclein causes neuronal cell death in PD, it has recently been reported that there is an association between α-synuclein and mitochondrial dysfunction (Hao, Giasson and Bonini 2010, Irrcher et al. 2010). Mutant α-synuclein is targeted to and accumulates in the inner mitochondrial membrane (IMM) and can cause Complex I impairment and an increase in ROS, possibly leading to cell death (Devi et al. 2008). Furthermore, oxidative stress promotes uptake, accumulation, and oligomerization of extracellular α-synuclein in oligodendrocytes (Pukass and Richter-Landsberg 2014) and induces posttranslational modifications of α-synuclein which can increase DA toxicity (Xiang et al. 2013). It has been suggested that the NADPH oxidases, which are responsible for ROS generation, could be major players in synucleinopathies (Cristóvão et al. 2012). Furthermore, mutations in Leucine Rich Repeat Kinase 2 (LRRK2) have been identified as the most common cause of familial PD (Lill 2016). The complex physiological roles of LRRK2 are not fully understood; however, it is associated with many cellular functions, particularly those involving membrane dynamics, including autophagy, cytoskeletal dynamics, vesicle dynamics and mitochondrial function. Attempts to better understand how LRRK2 mutations contribute toward PD pathology have been restricted partly due to the difficulty in creating a LRRK2 transgenic model that recapitulates important features of PD. Several proteins are known to interact with LRRK2 and mediate pathological effects on mitochondria. LRRK2 has been shown to impair mitochondrial dynamics by physically interacting with the mitochondrial fission protein, dynamin-related protein 1 (DRP1) and promoting

mitochondrial fragmentation associated with enhanced mitochondrial fission, increased ROS generation and impaired autophagy (Wang et al. 2012). Mitochondrial dysfunction induced by LRRK2 also provides a strong link to the impaired autophagy pathway in multiple models. For example, an accumulation in autophagic and lysosomal structures occur both in vitro and in vivo caused by overexpression of PD-associated mutations (MacLeod et al. 2006, Plowey et al. 2008, Gómez-Suaga et al. 2012). Parkin and PINK1 are localized in the mitochondria and their functions are tightly connected to the normal functioning of the mitochondria itself (Scarffe et al. 2014). PINK1 accumulates on the outer membrane of damaged mitochondria and recruits parkin to the dysfunctional mitochondrion (Pickrell and Youle 2015). In humans with parkin mutations, mitochondrial complex I activity is impaired (Müftüoglu et al. 2004). Overexpression of parkin in mice reduced DA neuronal cell loss induced by MPTP through the protection of mitochondria and the reduction of α-synuclein (Bian et al. 2012). On the other hand, parkin knock-out (KO) mice showed decreased amounts of several proteins that are involved in mitochondrial function and oxidative stress as well as increases in protein oxidation and lipid peroxidation (Palacino et al. 2004). PINK1-KO mouse and human DA neurons have abnormalities in mitochondrial morphology, reduced membrane potential, increased ROS generation and high sensitivity to apoptosis. Mutations in the PINK1 genes result in enlarged or swollen mitochondria. The decrease in mitochondrial membrane potential is not due to a proton leak, but to respiratory chain defects like complex I and complex III deficiency (Amo et al. 2014). These defects can be ameliorated and rescued by the enhanced expression of parkin (Exner et al. 2007, Yang et al. 2006). This last scenario seems to involve PINK1 and parkin in a common pathway that regulates mitochondrial physiology and cell survival in which PINK1 seems to be functioning upstream of parkin, at least as observed in Drosophila disease models (Clark et al. 2006). Furthermore, DJ-1 gene encodes a widely expressed protein found in neurons and glia in all central nervous system (CNS) regions (Bader et al. 2005). It's first identified an association between DJ-1 and autosomal recessive early-onset PD (Oakley et al. 2007, Morgan et al. 2006), with numerous further familial mutations in DJ-1 being identified (van Duijn et al. 2001). Among its functions, DJ-1 is involved in regulating mitochondrial activity (Junn et al. 2009) and protecting against oxidative stress (Taira et al. 2004). DJ-1 can interact with mitochondrial complex I subunits and is translocated to the mitochondria under stress conditions (Hayashi et al. 2009). DJ-1 and its mutant forms could associate with the chaperone protein Hsp70, a link that was further increased under oxidative stress conditions. DJ-1 deficient mice are more susceptible to MPTP (Kim et al. 2005) and DJ-1 knockdown in a neuroblastoma cell line renders the cells vulnerable to oxidative stress (Taira et al. 2004). In fact, loss of DJ-1 leads to mitochondrial impairment and dysfunctional autophagy (Irrcher et al. 2010, Krebiehl et al. 2010) and overexpression of PINK1 and Parkin is protective (Irrcher et al. 2010). These results are consistent with the proposal that DJ-1 may be aiding PINK1/Parkin in the clearance of misfolded proteins and damaged mitochondria (Xiong et al. 2009). In conclusion, DJ-1

protein has been observed to have pleiotropic functions, with an antioxidative role to be the most consistent finding. This may provide a link to PD whereby a loss of function mutation of DJ-1 causes an increase in mitochondrial dysfunction and oxidative damage leading to nigral neuron cell death. At last, mutations in ATP13A2 cause Kufor-Rakeb syndrome (KRS), a rare form of autosomal recessive juvenile-onset PD (Park et al. 2015). ATP13A2 encodes a lysosomal type 5 P-type ATPase. Several studies employing ATP13A2-deficient cell models have comprehensively shown underlying mitochondrial dysfunction, including reduced ATP production, increased mitochondrial fragmentation and increased ROS production (Ramonet et al. 2012, Park et al. 2014). In addition, loss of ATP13A2 was also found to impair glycolysis, which aggravated mitochondrial dysfunction, suggesting a broader impact of ATP13A2 deficiency on cellular bioenergetics (Park et al. 2016). However, it has been observed that functional ATP13A2 can protect against α-synuclein overexpression induced toxicity and that knockdown of ATP13A2, enhances α-synuclein misfolding in neuronal models of PD (Gitler et al. 2009). With α-synuclein shown to be toxic to Complex I (Devi et al. 2008), loss of function mutations in ATP13A2, and therefore impaired α-synuclein clearance, could be a link to mitochondrial dysfunction in PD.

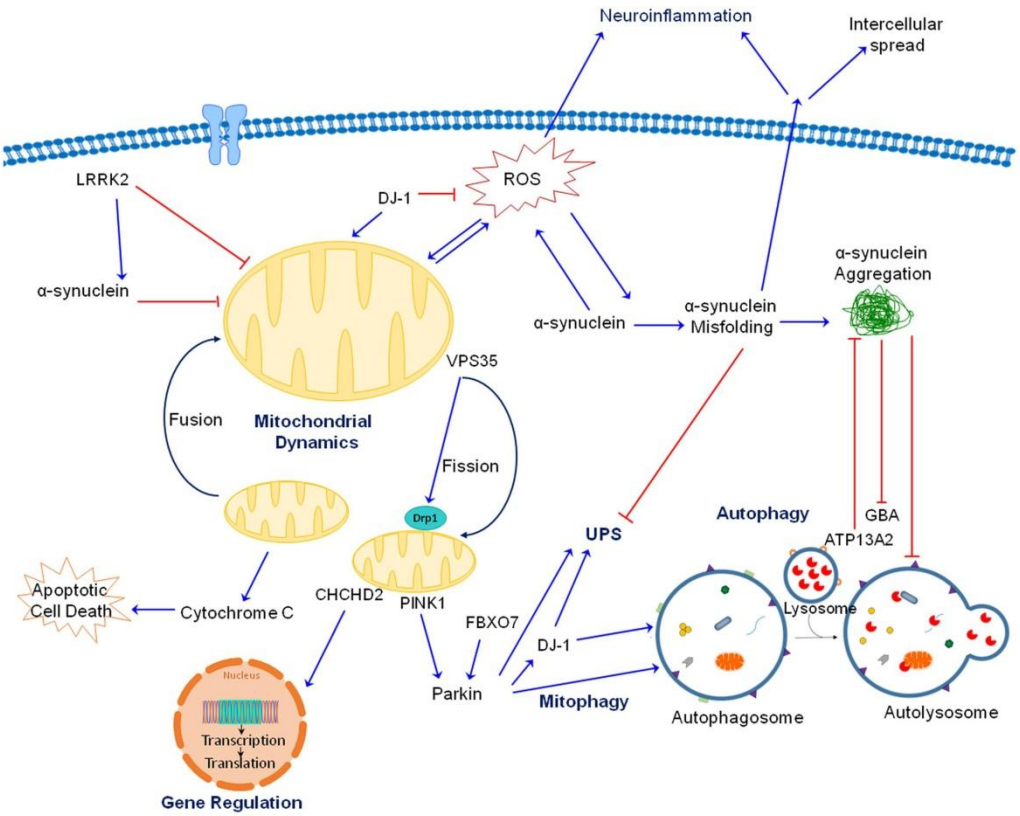

Figure 5: Mitochondrial Dysfunction in Familial PD. Interactions between gene products linked to PD. Adapted from (Helley et al. 2017)

4. PHYSIOLOGICAL BASIS OF NEURONAL VULNERABILITY IN PD

The selective death of distinct neuronal cell populations is the key feature of many disorders of the central nervous system. Not only do neurons secreting particular neurotransmitters appear to exhibit increased vulnerability to specific neurodegenerative diseases but, perhaps more strikingly, even within groups of neurons secreting a single neurotransmitter some groups are vulnerable while others are resistant to neurotoxic stimuli. Importantly, differential vulnerability of neurons is a feature of both sporadic and inherited forms of neurodegeneration, and is also observed in animal models of these diseases. Examples of diseases that are characterized by the selective degeneration of neurons in the CNS include Alzheimer's disease, Amyotrophic Lateral Sclerosis (ALS) autosomal recessive proximal Spinal Muscular Atrophy and PD. It is largely unknown why different groups of neurons are highly vulnerable to degeneration in different diseases. In early Alzheimer's disease, distinct subgroups of neurons in layer II of the entorhinal cortex, the subiculum, and the CA1 region of the hippocampus are particularly vulnerable to degeneration, while many other cortical and hippocampal regions do not show pathological signs at this disease stage (Morrison and Hof 2002, Stranahan and Mattson 2010). Amyotrophic Lateral Sclerosis affects both upper and lower motor neurons (Boillée et al. 2006). However, cortical, spinal and lower cranial nerve motor neurons undergo degeneration early in the disease, while the motor neurons of Onuf's nucleus, as well as the oculomotor, trochlear and abducens nerves remain largely unaffected from cell loss even at late disease stages (Alexianu et al. 1994, von Lewinski and Keller 2005). Autosomal recessive proximal spinal muscular atrophy is characterized by the progressive selective loss in particular of the lower motor neurons in the anterior horns of the spinal cord, while upper motor neurons are spared (Talbot and Davies 2001). In PD, whether sporadic or inherited, the motor manifestations are primarily linked to the selective loss of DA neurons in the SNpc (Brichta, Greengard and Flajolet 2013). In contrast, the very similar DA neurons in the VTA demonstrate a higher degree of resistance to degeneration (Dauer and Przedborski 2003). This pattern is conserved in toxic (6-OHDA, MPTP, rotenone, proteasome inhibition) and genetic (MitoPark) animal models of PD. Even in Drosophila, in which PD is modelled by over expressing wild-type or mutant α-synuclein, one DA neuron group selectively degenerates. It is unclear why, some neurons die and others survive when exposed to the same toxic stimulus. Understanding why, in a particular condition, some neurons are extremely prone to degeneration while others, very similar neurons are spared over the years, would greatly enhance our comprehension of disease pathogenesis and thereby foster the development of more specific therapeutic strategies. For example, one could envisage pharmacologic manipulations targeted to correcting a particular "vulnerability factor" in a susceptible neuronal population. Characterization of these cell types might also allow for more refined stem cell/regenerative approaches in which transplanted cells more closely reflect lost neuronal subtype or in which cells are engineered to be more resistant to toxicity.

4.1. Identifying DA neurons in the midbrain

DA neurons are distributed in three partially overlapping nuclei: the retrorubral area (RRA, A8), substantia nigra (SN, A9), and ventral tegmental area (VTA, A10), located in very close proximity to each other. SNpc and VTA DA neurons represent two of the nine major DA neuron groups in the mammalian brain as identified by staining for tyrosine hydroxylase (TH), the enzyme that catalyzes the rate-limiting step in the synthesis of dopamine (Björklund and Dunnett 2007). In mice and rats there are a considerably comparable numbers of DA neurons SNpc and VTA, while SNpc DA neurons outnumber VTA DA neurons in monkeys and humans. SNpc DA neurons are heavily involved in the control of movement, whereas VTA DA neurons are responsible for the regulation of reward, emotional behavior and addiction. Both groups of neurons are characterized by distinct but overlapping projection patterns. A combination of electrophysiological and basic molecular studies and retrograde tracing in mice demonstrated that distinct subgroups of VTA and SNpc DA neurons in confined midbrain territories project to specific striatal, cortical and limbic target regions, and these neurons can be distinguished by their expression levels of dopamine transporter (DAT), their electrophysiological properties and their capacities for dopamine D2 autoreceptor signaling (Lammel et al. 2008). The majority of projections that originate from SNpc DA neurons innervate the dorsal striatum, and only some nigral fibers project to the ventral striatum and the cortex. In contrast, VTA DA neurons mainly project to the ventral striatum as well as cortical areas, while significantly fewer projections innervate the dorsal striatum. Both SNpc and VTA DA neurons send minor projections to additional brain regions including the globus pallidus, the subthalamic nucleus, and the habenula. Moreover, a minority of DA projections originating in the VTA projects to the amygdala. DA neurons located in the midbrain also sparsely innervate distinct hippocampal regions. The density of the DA innervation of a distinct brain region often varies significantly between different species. Interestingly, anatomic differences in the DA projection sites correlate with several dissimilarities observed in DA neuron function. In the 1980s, functional analysis of individual DA midbrain neurons was boosted by the now classical studies of Grace and Bunney. They were the first to record electrical activity of neurochemically defined DA midbrain neurons intracellularly in vivo (Grace and Bunney 1980, Grace et al. 2007). A robust set of relatively homogeneous features emerged from their observations. In fact, they defined a still valid functional fingerprint of DA midbrain neurons: a distinct action-potential waveform associated with two different discharge patterns that spontaneously occurred in vivo in the anesthetized rodent brain either discharge in an irregular single spike mode with a very narrow frequency band (between 1 and 8 Hz) or alternatively short bursts of action potentials at higher frequencies (Grace and Bunney 1984). Given the nature of their experimental settings, the behavioral significance of these distinct patterns of DA activity had to remain unclear including broad action potential waveforms, inhibition by DA D2 auto-receptor stimulation, and two modes of in vivo discharge pattern, either low-frequency (1-8 Hz) single action potential discharge or transient high-frequency

bursting (15 Hz). This stereotypical "functional finger-print" of DA neurons in rodents was confirmed and extended in the studies in awake behaving primates by Schultz and co-workers, which has allowed them in a string of landmark studies to define the behavioral significance of the distinct discharge patterns of DA midbrain neurons in an unprecedented fashion (Schultz 2007). It is mainly due to their research efforts over the last 20 years that we now possess a sophisticated and quantitative theory of the behavioral roles of the distinct DA discharge patterns, which prominently appear to signal reward prediction errors in context of temporal-difference learning paradigms (Schultz 2007). In parallel, the development of reduced brain preparations and patch-clamp techniques enabled the study of biophysical mechanisms and ion channels that generate and control electrical activity in DA neurons (Puopolo, Raviola and Bean 2007). More recently, the combined analysis of function and gene-expression at the level of individual DA midbrain neurons enabled their distinct molecular definition (Liss and Roeper 2004). In addition to dopaminergic diversity according to their distinct anatomical or functional identities under physiological control conditions, other functional differences might only become apparent during disease-related challenges thereby revealing distinct "pathophysiological identities" among DA midbrain neurons (Liss et al. 2005). Indeed, the phenomenon of differential vulnerability of DA neurons in PD is well documented and reflects the fact that some of the DA cell groups in the midbrain are particularly affected by the neurodegenerative process while others are relatively spared (Damier et al. 1999).

4.1.1. Distinct identities of DA midbrain neurons

DA midbrain neurons have been defined as those nerve cells positioned in the mesencephalon, which possess the ability for synthesis, packaging, release, and reuptake of the neurotransmitter dopamine. These key features are easily captured by qualitatively probing for the expression of a number of marker genes like TH, AADC (aromatic amino acid decarboxylase) or the vesicular monoamine transporter (VMAT2) (Björklund and Dunnett 2007). The absence of other catecholamine-containing neurons in the midbrain allows using TH expression as a consistent and sufficient marker for demonstrating DA identity. Despite the fact that SNpc and VTA DA neurons generate, store and release the same neurotransmitter, that their cell bodies in the midbrain are localized in close proximity to each other, and that significant overlap exists in the brain areas that are innervated by the projections of these neurons, SNpc and VTA DA neurons exhibit a different susceptibility to degeneration.

This differential vulnerability of the DA system is found in drug abuse (Belin et al. 2013, Lüscher and Malenka 2011, Volman et al. 2013) in schizophrenia (Modinos et al. 2015), and has recently been highlighted in depression models affecting distinct DA neuron subpopulations (Chaudhury et al. 2013, Friedman et al. 2014, Krishnan et al. 2007, Russo et al. 2012). However, this phenomenon is most prominent in PD.

The DA neurons in the SNpc are highly vulnerable to the fatal molecular mechanisms associated with the disease. Along with the formation of Lewy Bodies in various brain regions (Spillantini et

al. 1997, Braak et al. 2003), the progressive loss of pigmented SNpc DA neurons is a pathological hallmark of PD (Brichta et al. 2013). Calculations of the number of DA neurons (as identified by the expression of TH) in post-mortem tissue from patients with advanced idiopathic (non-genetic) PD and control subjects revealed that, on average, almost 80% of all SNpc DA neurons undergo degeneration in PD (Damier et al. 1999). DA cell loss is most severe in the ventrolateral part of the SNpc (Damier et al. 1999, Braak et al. 2003). This was also unequivocally demonstrated in a more current study that investigated a large set of post-mortem brain samples obtained from patients with PD (Kordower et al. 2013). These data show that DA cell loss in the SNpc follows a specific pattern and suggest that subtle molecular differences exist among subgroups of SNpc DA neurons.

In contrast to SNpc DA neurons, the very similar DA neurons in the VTA are more resistant to degeneration. In their studies, Damier and Hirsch analyzed the number of both SNpc and VTA DA neurons, providing cell counts that can be directly compared with each other due to the investigation of the same midbrain tissue samples and the application of the same statistical methods. The average loss of VTA DA neurons observed in patients with advanced idiopathic PD as compared to unaffected controls was estimated to be only about 50% which is a much lower percentage of DA neuron loss than in the SNpc (Damier et al. 1999). These data strongly suggest that specific modifiers partially protect VTA DA neurons from degeneration as compared to SNpc DA neurons, and/or that specific modifiers increase the vulnerability of SNpc DA neurons to PD-associated cell loss as compared to VTA DA neurons.

4.2. Patterns of electrical activity of midbrain DA neurons

The general problem of defining neuronal subtypes, might also be discussed in the light of homeostatic neuronal plasticity present in DA midbrain neurons (Davis 2006). Studies suggest that neurons, when perturbed, possess an astonishing flexibility to regain their cell-specific functional properties even in the absence of key components of their biophysical machinery. This homeostatic plasticity might argue for a conceptional preference of “functional identity” rather than the use of a rigid set of molecular markers defining a “molecular identity”, when aiming to define neuronal subtypes (Schulz, Goaillard and Marder 2006). A cardinal feature of neurons that separates them from nearly all other cell types is excitability.

Thus, one alternative approach for functional and molecular definition of DA subtypes is to focus on their intrinsic excitability in addition to the expression of basic marker-gene-sets (phenotype–genotype correlation). Intrinsic excitability defines the input–output relations of specific neurons within synaptic networks thus endowing it with a specific functional identity (Schulz et al. 2006). However, this functional identity is not simply fixed by the co-expression of a certain set of marker genes and ion channels but it actively adapts (functionally as well as molecularly) during perturbations to defend a specific type of intrinsic excitability that gives rise to their typical cell-specific neuronal activity.

So, electrical activity and calcium-dependent homeostatic mechanisms (Salthun-Lassalle et al. 2005, Toulorge et al. 2011) are reasonable candidates to be involved in stabilizing DA neuron subtype identities.

Adult SNpc DA neurons are autonomous pacemakers exhibiting slow broad spikes and lacking significant intrinsic Ca^{2+} -buffering capacity. In these neurons, sustained pacemaking must come with a significant metabolic price tag. The ionic gradients underlying excitability are under constant assault. Although most neurons rely exclusively on channels permeable to Na to drive pacemaking, the slow pacemakers with broad action potentials use Ca^{2+} channels to help push the plasma membrane toward spike threshold.

However, the differences in electrical activity and its related ion fluxes have also been proposed to contribute to differential vulnerability between vulnerable SNpc DA and resistant VTA DA neurons.

In this view, two different classes of ion channels have emerged to be particularly relevant for SN DA neuron activity, related calcium and metabolic homeostasis, as well as for PD-pathophysiology: voltage-gated calcium channels (VGCCs), and metabolically gated ATP-sensitive potassium (K-ATP) channels.

Surmeier and colleagues have shown the important role of voltage-gated L-type calcium channels for creating the basic subthreshold membrane potential oscillations that underlie pacemaker activity (Puopolo et al. 2007). However, the calcium dependence of the spontaneous pacemaker is not a homogenous property of all DA midbrain neurons (Puopolo et al. 2007, Chan et al. 2007).

In particular, they have shown that in vitro pacemaker activity is associated with dendritic calcium oscillations mediated by L-type calcium channels in SNpc DA but not VTA DA neurons (Chan et al. 2007, Guzman et al. 2009, Sulzer and Surmeier 2013)

Another study points to a key role of L-type calcium channel Cav1.3, which is activated at more negative potentials compared to other members of the L-type calcium channel family, also expressed in DA midbrain neurons (Chan et al. 2007).

SNpc DA neurons engage L-type channels with a Cav1.3 pore-forming subunit, leading to elevated intracellular concentrations Ca^{2+} must be pumped across the plasma membrane against a very steep potential gradient. In adult SNpc DA neurons, the currents that flow through these channels are of sufficient magnitude to sustain a membrane potential oscillation when voltage-dependent Na channels are blocked with tetrodotoxin (TTX) VTA DA neurons, which also are slow pacemakers, diverge from SNpc DA neurons in two potentially important respects. First, the Cav1.3 Ca^{2+} channel density is dramatically lower than in SNpc DA neurons (Guzman et al. 2010, Chan et al. 2007). Second, the expression of the Ca^{2+}-buffering protein calbindin is much higher in VTA DA neurons than it is in SNpc DA neurons (German et al. 1992).

This calcium component is far more dominant in SN DA neurons compared to those of other pacemaker neurons in the brain, which mainly rely on interspike sodium influx by TTX-sensitive sodium channels or HCN channels (Bean 2007).

Mitochondrial dysfunction, might lead to tonic activation of K-ATP channels and consequently to chronic membrane hyperpolarization (Liss, Bruns and Roeper 1999a). These channels, composed of discrete pore-forming (Kir6.1/Kir6.2) and regulatory subunits (SUR1/ SUR2), are called 'metabolic sensors', as their open probability depends on the metabolic state of a cell (Seino and Miki 2004, Ashcroft and Rorsman 2004).

K-ATP channels in DA neurons have been shown to open in response to partial complex I inhibition as well as in response to ATP depletion and increased oxidative stress (Liss, Neu and Roeper 1999b, Avshalumov et al. 2005). Thus, cell type specific K-ATP channel activation would provide a convergent downstream target that could integrate energy depletion and oxidative stress, offering a candidate mechanism for the differential vulnerability of DA neurons in PD.

Liss and collaborators suggest that differential degrees of uncoupling of the mitochondrial respiratory chain are critical for the control of K-ATP channel activity in DA midbrain neurons. Although extensive uncoupling in vitro activates K-ATP channels in all DA neurons, they have found that mild uncoupling has opposite effects on K-ATP channel activity in response to complex I inhibition: it causes decreased K-ATP conductances in SNpc DA neurons but increased K-ATP channel conductances in VTA DA neurons.

K-ATP channels are selectively activated in response to complex I inhibition in SNpc DA neurons but not in VTA DA neurons; this is unexpected, as adult VTA DA neurons have functional K-ATP channels with the same molecular make-up (Duda, Pötschke and Liss 2016).

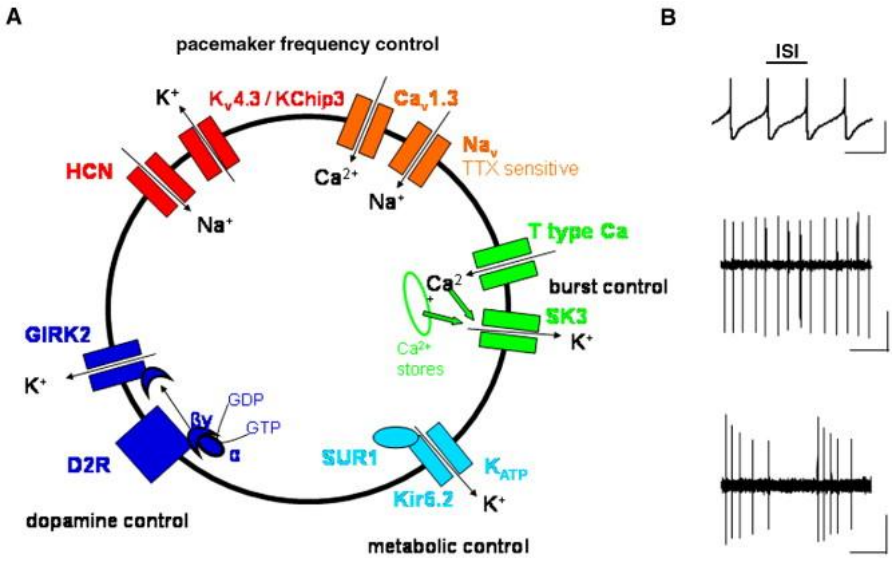

Figure 6: Spontaneous activity patterns and related ion channels expressed in DA midbrain neurons. (A) Schematic illustration of distinct ion channels expressed in DA midbrain neurons, modulating their spontaneous activity (pacemaker, burst as well as metabolic and dopamine control) (B) Examples of activity

patterns of three individual DA midbrain neurons from adult mouse: In vitro (upper, current-clamp, perforated-patch recording) and in vivo (middle, extracellular recording, sampling rate 12.5 kHz) pacemaker activity, as well as in vivo burst activity (lower panel). Scale bars: upper 0.5 s, 25 mV, middle/lower 1 s, 0.5 mV. Adapeted from (Liss and Roeper 2008)

Considering the preferential degeneration of SNpc DA neurons in PD, acute and chronic K-ATP channel activity has also bidirectional protective but also detrimental effects on SNpc DA survival. Chronic K-ATP channel activity in SN DA neurons in vivo in response to metabolic stress situations is not beneficial anymore, but seems to trigger degeneration in this neurons of K-ATP channel-deficient mice [Kir6.2KO] (Minami et al. 2004) displaying a significantly higher vulnerability in two different PD mouse models (Liss et al. 2005) in the chronic neurotoxic MPTP/probenecid PD-model (Jackson-Lewis and Przedborski 2007, Meredith and Rademacher 2011), as well as the homozygous weaver GIRK2 mutant mouse, a chronic genetic model of PD (Slesinger et al. 1997, Navarro et al. 1996). In the latter, a missense mutation (G953A) in the Girk2 gene (KCNJ6), which codes for a subunit of a G-protein-activated inwardly rectifiying K 1 channel, has been identified (Patil et al. 1995) causing degeneration of DA neurons in the SNpc. So, there is clear evidence that physiological LTCC (in particular of the Cav1.3 type) as well as K-ATP channel (made up by Kir6.2/SUR1 subunits) function contribute to metabolic stress and the selective high vulnerability of SNpc DA neurons to degeneration in PD and its animal models.

Nevertheless, these channels in SNpc DA but not in VTA DA neurons seem to be crucial for their distinct electrical activity patterns, their physiological signaling (e.g. calcium-dependent enzyme activation and regulation of gene expression), and their related complex functions within the basal ganglia network (e.g. novelty-related behavior).

Another example of genetic PD model in which mitochondrial dysfunction leads to differential DA vulnerability is the MitoPark mouse. In this model, a transgenically induced defeact in the respiratory chain in midbrain DA neurons leads to the progressive development of key PD features: adult onset of neurodegeneration; slowly progressive clinical course; formation of intraneuronal inclusions; earlier onset of cell death and more extensive cell death in SNpc than in VTA, and responsiveness to L-DOPA therapy with a differential response depending on disease stage (Ekstrand et al. 2007). The MitoPark mice provides another instance of selective SNpc vs VTA differential degeneration , which is hardly explained by the main hypotheses on PD pathogenesis. For this reason in spite of the general consensus over the relevance of mitochondrial function in nigrostriatal degeneration underlying PD, it is reasonable to hypothesize that additional, yet unversed mechanism underlie differential DA vulnerability in PD.

4.3. Alteration of neuronal electrophysiological properties caused by mitochondrial dysfunction in animal models

The elucidation of the molecular determinants that increase the susceptibility of SNpc DA neurons or decrease the susceptibility of VTA DA neurons to degeneration in PD is a very exciting but challenging research area that holds great potential for the development of novel therapeutic strategies for PD (Brichta and Greengard 2014). Despite the evidence suggesting an important role for mitochondrial dysfunction among loss of different midbrain DA populations, considerable uncertainty remains about the mechanism involved and alternative targets could explain the selectivity of toxic action. Generic complex I inhibitors, such as MPTP or rotenone, can induce parkinsonian syndromes in humans and animal models, however, it is not clear whether their mode of action is restricted to complex I inhibition. The role of complex I inhibition in PD has been challenged by a study using mice that lack functional Ndufs4, a gene encoding a subunit implicated in assembly and function of complex I. (Exner et al. 2012) In fact, it was demonstrated that in primary mesencefalic cultures obtained from mice Ndufs4$^{-/-}$, basal death of DA neurons was unaffected (Choi et al. 2008). Moreover, such cells still retained vulnerability to paraquat and MPP^+ toxic action. Surpresingly, these DA neurons were more sensitive to rotenone, whereas an already compromised complex I would make these cell resistent accordingly to its toxic mechanism of action. In this respect, given the importance of the topic, my research group focused the attention on acute effects carried by the parkinsonian toxin MPP^+ by analyzing neurophysiological properties of SNpc DA neurons in acute midbrain slices. To this aim, they challenged rat SNpc DA neurons with relevant concentrations of MPP^+ and performed whole-cell/cell-attached recordings. They found that MPP^+, at concentrations approaching those used to induce nigrostriatal degeneration in mice (Jackson-Lewis and Przedborski 2007) and rats (Lin et al. 2012), induce a rapid hyperpolarization along with a reduction of spontaneous firing activity of SNpc DA neurons. These effect were already seen in perforated patch in the same region (Liss et al., 2005) and linked to the opening of K-ATP channels due to a decrease of cellular ATP levels after mithocondrial failure. But in our case, this effect occurs under blockade of K-ATP channels and in the presence of ATP (in whole-cell solution). And it solely dependent on the hyperpolarization-activated inward current (Ih) inhibition. Pharmacological experiments indicate that cAMP pathway are not involved (Masi et al. 2013). Furthermore, the acute inhibition of Ih by MPP^+ leads to hyperpolarization, reduction of spontaneous firing activity and increased temporal summation of excitatory inputs in SNpc DA neurons. Firing activity of these neurons is very regular in vitro, whereas it shows a bursting pattern in vivo or in organotypic cultures (Rohrbacher, Ichinohe and Kitai 2000). Given this marked difference, one cannot assume that Ih inhibition by MPP^+ reduces discharge frequency of SNpc DA neurons in vivo. Moreover, a reduction in excitability can hardly be considered noxious in general. On the other hand, the finding that MPP^+ enhances synaptic summation of excitatory inputs in SNpc DA neurons may have high-potential pathogenic relevance. As reported by studies in many

neuronal cells, excessive depolarization due to massive glutamate release (as during ischemia or seizure) results in somatic calcium overload, a major death signal triggering a host of apoptotic pathways (Szydlowska and Tymianski 2010). In PD, the involvement of glutamate NMDA receptor is controversial, with some studies showing that NMDA antagonist do not protect from MPTP toxicity (Sonsalla et al. 1992), and others reporting that impairment of glutamate homeostasis plays a role in this model (Meredith et al. 2009). Regardless of NMDA glutamate receptor involvement, temporal summation leads to greater and more sustained depolarization epochs at the soma and, likely, in dendrites. This may, in turn, result in increased calcium entry through voltage-gated calcium channels. In keeping with this, Surmeir and co-workers have shown that isradipine, a Cav 1.3 blocker, is able to stop dendritic calcium oscillations and accumulation and to protect from MPTP-induced degeneration in vitro and in vivo (Chan et al. 2007, Meredith et al. 2008). Interestingly, it has been reported that Ih is more abundant in calbindin-negative SNpc DA neurons and that this subpopulation is more vulnerable in weaver and MPTP-lesioned mice (German et al. 1996, Neuhoff et al. 2002). Clearly, none of the current hypotheses can sufficiently explain the selective vulnerability of SNpc DA neurons, rather, a combination of the phenomena described above as well as some yet unknown factors are responsible for the preferential susceptibility of this neuronal population. In agreement with this findings, early electrophysiological alterations, including Ih loss of function (LOF), where observed in SNpc DA neurons in acute midbrain slices from MitoPark mice (Branch et al. 2016).

5. THE HYPERPOLARIZATION-ACTIVATED CURRENT AND HCN CHANNELS

The hyperpolarization-activated current (Ih), was first described in sino-atrial node tissue in 1976 and later identified in rod photoreceptors and hippocampal pyramidal neurons (Halliwell and Adams 1982, Noma and Irisawa 1976). Due to its unique properties, particularly the activation upon hyperpolarization of the membrane potential, Ih has been also termed If (f for funny) or Iq (q for queer). The ion channels underlying Ih were identified in the late 1990s and with reference to their complex dual gating mode (Altomare et al. 2001, Craven and Zagotta 2006, DiFrancesco 1999), these proteins were termed hyperpolarization-activated cyclic nucleotide-gated (HCN) channels. In mammals, the HCN channel family comprises four distinct members (HCN1-4), with different physiological properties. Many physiological roles have been attributed to Ih, including the setting of resting membrane potential (RMP), generation of neuronal oscillation, and regulation of dendritic integration and synaptic transmission. Ih is implicated in major higher order brain functions such as sleep and arousal, learning and memory, sensation and perception. In the nervous system, the functional properties and expression of HCN channels are diversified to adapt to the corresponding physiological roles. The regulation of HCN channels involves short-term regulation through cellular metabolites that directly interact with these channels or protein kinases that induce phosphorylation of channel proteins, and long-term regulation via the regulation of channel expression, heteromerization or subcellular redistribution.

5.1. Biophysical Properties of Ih

Native Ih as well as currents induced by heterologously expressed HCN channels are characterized by some hallmark properties. Ih is a mixed cationic current carried by permeation of Na^+ and K^+ in ranges from 1:3 to 1:5, but recent evidence supports the presence of a small but significant Ca^{2+} permeability (Michels et al. 2008). Since its reversal potential is around -20 mV at physiological ionic conditions (DiFrancesco 1993), Ih is inwardly directed at rest and, hence, depolarizes the membrane potential. However, unlike the vast majority of cellular conductance, that are activated upon membrane depolarization, Ih is activated by hyperpolarizing voltage steps to potentials negative to -55 mV, and does not display voltage-dependent inactivation. In addition, activation of Ih is controlled through dually interdependent membrane potentials and cAMP binding (Kusch et al. 2010, Wu et al. 2012). Furthermore, Ih has a distinctive pharmacological profile which includes sensitivity to external Cs concurred and relative insensitivity to Ba^{2+}. Typically, two kinetic components can be distinguished upon activation of Ih: a minor instantaneous current (IINS) (Proenza et al. 2002, Macri and Accili 2004),which is fully activated within a few milliseconds, and a major slowly developing component (ISS) that reaches its steady-state level within a range of tens of milliseconds to several seconds under fully activating conditions. While there is no doubt that ISS is generated by cations passing the well-characterized pore of HCN channels, the ionic nature of IINS is a matter of current dispute. IINS is not consistently observed in all measurements

of Ih and, if so its amplitude is usually small. Generally, IINS is considered as a leak conductance or an experimental artefact (Macri and Accili 2004) .Depending on the cell type, the activation of ISS can be empirically described by either a single (Erickson, Ronnekleiv and Kelly 1993, Kamondi and Reiner 1991, McCormick and Pape 1990, Mercuri et al. 1995, Santoro, Wainger and Siegelbaum 2004) or double exponential function (Attwell and Wilson 1980, Edman, Gestrelius and Grampp 1987, van Ginneken and Giles 1991). The kinetics of ISS are quite variable (DiFrancesco 1991). While most HCN channels activate quite slowly with time constants (tact) ranging between hundreds of milliseconds and seconds, there are also currents with profoundly faster activation (Halliwell and Adams 1982, Maccaferri et al. 1993), for example, in hippocampal CA1 neurons, where tact values in the range of 30 –50 ms have been found (Pape 1996, Robinson and Siegelbaum 2003) The diversity of tact probably results from an interplay of several factors. First of all, the differences reflect the diverse intrinsic activation properties of distinct HCN channel isoforms underlying the Ih in a given cell type. Second, there is growing evidence that the cellular microenvironment that fine tunes HCN channel activity (e.g., auxiliary subunits, concentration of cellular factors, etc.) can profoundly vary from cell type to cell type. Third, Ih measurements are highly sensitive to experimental conditions (e.g., pH, temperature, patch configuration, expression system, ionic composition of solutions, etc.). Since Ih activates at around resting membrane potential. The voltage dependence of activation shows a typical S-shaped dependence that can be fit using a Boltzmann function (Bader and Bertrand 1984, Travagli and Gillis 1994). Such fits reveal half-maximal activation ("midpoint") potentials (V0.5) of around 70 to 100 mV in most cell types. Another key feature of Ih is its regulation by cyclic nucleotides. Hormones and neurotransmitters that elevate cAMP levels facilitate activation of Ih and by accelerating the opening kinetics (Banks, Pearce and Smith 1993, Tokimasa and Akasu 1990). It has been shown that the acceleration of the opening kinetics with cAMP can be attributed to the shift in voltage dependence of activation (Wainger et al. 2001). Thus, in the presence of high cAMP concentrations, Ih channel opening is faster and more complete than at low cAMP levels. Conversely, neurotransmitters that downregulate cAMP inhibit Ih activation by shifting its activation curve to more hyperpolarized voltages (DiFrancesco and Tromba 1988). The range of V0.5 shift induced by saturating cAMP concentrations is quite large (0 –20 mV), depending on the cell type (Erickson et al. 1993, Tokimasa and Akasu 1990) and the expressed Ih channel isoform (Ishii et al. 1999, Ludwig et al. 1998, Santoro et al. 1998). Most notably, the cAMP-mediated modulation of Ih channel activity is considered to play a major role in the up- or downregulation of the heart rate during sympathetic stimulation and muscarinic regulation of heart rate at low vagal tone (Brown, DiFrancesco and Noble 1979). There is also good evidence that cAMP-dependent modulation of Ih is of crucial significance in some neuronal circuits, e.g., in sleep-related thalamocortical circuits (Lüthi and McCormick 1999). There are a few studies showing that Ih can also be regulated by nitric oxide (NO)-mediated increase of cGMP levels in brain (Pape and Mager

1992) and heart (Musialek et al. 1997). However, so far the physiological role of this modulation remains unclear. The principal mechanism by which cyclic nucleotides regulate Ih channel gating was uncovered by DiFrancesco and Tortora in the early 1990s using current recordings in excised patches of sinoatrial node cells. It came as a big surprise that in contrast to many other ion channels that are regulated by cAMP via protein kinase A (PKA)-mediated serine or threonine phosphorylation (Park et al. 2008, Schulz et al. 2008, Yao, Kwan and Huang 2005), Ih channels are activated by cAMP through direct interaction with a cyclic nucleotide-binding domain (CNBD), located at the COOH terminus of the channel and not through phosphorylation by PKA (DiFrancesco and Tortora 1991).

5.1.1. Pharmacological Profile

One of the most remarkable features of Ih and HCN channels is their pharmacological properties. HCN channels distinguish themselves from other K^+ currents for the sensitivity to low millimolar concentrations of external Cs^+ ions. Unlike most K^+ conductances, Ih is insensitive to millimolar concentrations of external Ba2 and tetraethylammonium (TEA) (Ludwig et al. 1998). Ih is also insensitive to 4-aminopyridine, a blocker of voltage-gated K channels (Ludwig et al. 1998). A number of organic blockers have been developed to inhibit HCN channels. Among them, the most widely used is a bradycardic one termed ZD7288. ZD7288 blocks Ih at concentrations between 10 to 100 μM (Gasparini and DiFrancesco 1997) and exhibits slow kinetics (5-10 minutes). In addition ZD7288 block is poorly reversible and not use dependent in moderate voltage ranges. These properties suggest that the localization of ZD7288 binding site near the intracellular portion of the HCN channels pore, as confirmed by a specific analysis carried on HCN1-expressing HEK293 cells, where it was demonstrated that, to exert its action, ZD7288 requires to enter through the pore and become trapped in the closed state (Shin, Rothberg and Yellen 2001). In addition, Ih block by ZD7288 is significantly relieved by hyperpolarization, therefore the reduced affinity of the binding site for the blocker can be the result of a conformational change that occurs during membrane hyperpolarization (Harris and Constanti 1995). Ivabradine is the only Ih blocker used in therapy to manage chronic stable angina pectoris. It reduces heart rate via inhibition of HCN4 channels, whose role in regulating pacemaker activity in the sinoatrial node cells is crucial. Ivabradine blocks HCN channels in a use-dependent manner by occupying a cavity below the channel pore and shows an IC50 between 2 and 3 μM (Bucchi et al. 2013). Finally, QX-314, the quaternary derivative of lidocaine normally employed to abolish voltage-activeted Na channels, completely blocks Ih in CA1 pyramidal cells (Perkins and Wong 1995).

5.2. The HCN Channel Family

HCN channels together with cyclic nucleotide-gated (CNG) channels and the Eag-like K channels belong to the superfamily of voltage–gated pore loop channels (Craven and Zagotta 2006, Yu et al.

2005, Kaupp and Seifert 2002). HCN channels have been cloned from both Vertebrates and Invertebrates, but have not been found in C. elegans and yeast nor in a prokaryotic genome. In mammals, four isoforms (HCN 1-4) have been identified (Robinson and Siegelbaum 2003). These isoforms differ by patterns of gene expression and tissue distribution (Ludwig et al. 1998, Santoro et al. 1998).

5.2.1. Structure of HCN channels

Each HCN channel subunit consists of three principal structural modules: the transmembrane core and the cytosolic NH2-terminal and COOH-terminal domain. Each subunit has six transmembrane helices (S1–S6), forming the trasmembrane channel core. The region forming the ion-conducting pore loop is between S5 and S6, while the ion selectivity filter is constituted by the pore region carrying the GYG motif between S5 and S6. The positively charged voltage sensor (S4) , carries nine arginine or lysine regularly spaced at every third position (Chen et al. 2005), its resulting positive charge confers to this domain the voltage sensitivity. All the voltage-dependent members of the pore-loop cation channel superfamily present positively charged S4 segment (Yu and Catterall 2004), but while inward movement of S4 charges leads to the closure of depolarization-activated channels, in HCN channel it triggers their opening. Following S6 is the 80-residue C-linker comprising six a-helices (A0–F0) and the cyclic nucleotide-binding domain (CNBD). The transmembrane core harbours the gating machinery and the ion-conducting pore while the proximal part of the cytosolic COOH-terminal domain consisting of the CNBD and the peptide that connects the CNBD with the transmembrane core (the “C-linker”) permits modulation by cyclic nucleotides. Together, the C-linker and CBND can be referred to as the ‘cAMP-sensing domain’ (CSD) because they are of functional importance for the cAMP-induced positive shift of the voltage-dependent activation of HCN channels. The transmembrane core and the proximal COOH terminus allosterically interact with each other during channel gating and reveal a high degree of sequence homology within the HCN channel family (sequence identity of 80 –90% between HCN1-4) (Kaupp and Seifert 2001). In contrast, cytosolic NH2 termini and the sequence downstream of the CNBD vary considerably in their length and share only modest to low homology between various HCN channels (Baruscotti, Bucchi and Difrancesco 2005). HCN channels commonly exist in homomeric tetramer configurations in vivo and form four subtypes of homotetramers. The assembly of heteromeric complexes increases the diversity of HCN channels, facilitating the adaptation of HCN channels to multiple functions in the nervous system. The four subtypes of HCN channels exhibit distinct cAMP-sensitivity with strong HCN2 and HCN4 regulation and weak HCN1 and HCN3 regulation. The HCN channel subtypes also have different activation kinetics. The activation of HCN1 is the fastest, while the activation of HCN4 is the slowest. The activation time constants of HCN2 and HCN3 are intermediate.

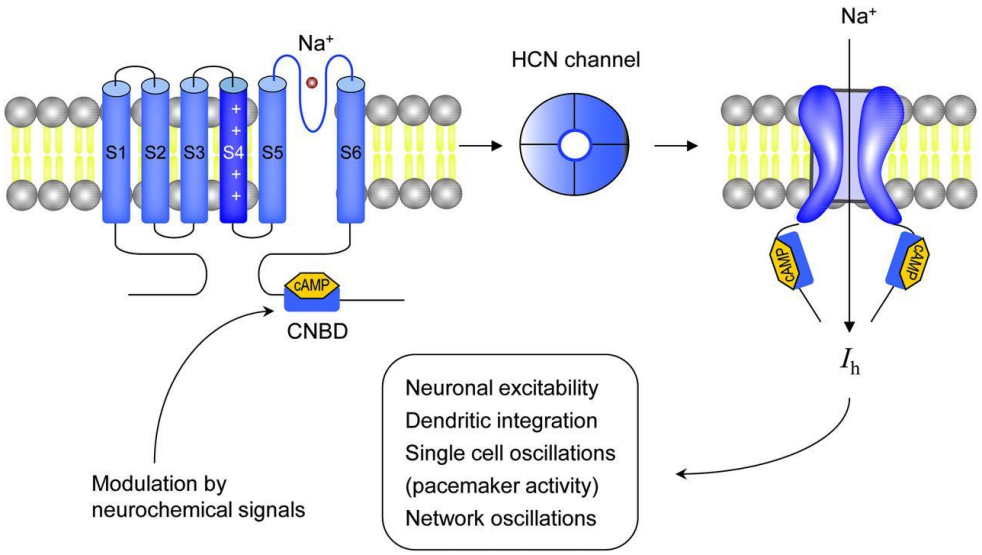

Figure 7: Generic structure of HCN channels. One subunit is composed of six transmembrane segments (S1–S6), with the positive charged voltage sensor (S4) and the pore region carrying the GYG motif between S5 and S6. The C-terminal of HCN channels is composed of the C-linker and the cyclic nucleotide-binding domain (CNBD) which mediates their responses to cAMP. Ih current flows through the HCN channel. Adapted from (Benarroch 2013)

5.2.2. Distributions of HCN channels

The expression pattern of HCN channels has been studied in several species, both at the tissue and single-cell level. HCN subunits are strongly expressed in the Central and Peripheral Nervous System (CNS, PNS), with subunit-specific pattern (Doan et al. 2004, Santoro et al. 2000). In the CNS, HCN1 is highly expressed in the neocortex, hyppocampus, cerebellar cortex, brainstem and spinal cord. HCN2 is nearly ubiquitous across the CNS but especially abundant in thalamic and brainstem nuclei. Conversely, HCN4 is expressed strongly but in a limited number of areas such as the olfactory bulb and the thalamus, with a distribution pattern that appears complementary to that of HCN1. The expression of HCN3 is scattered throughout the brain and modest. All isoforms, except HCN3, are present in the retina (Fyk-Kolodziej and Pourcho 2007). In the PNS, all HCN subunits are expressed. HCN1 is the most abundant in dorsal root ganglia (Chaplan et al. 2003) although a prominent function of HCN2 in the transmission of painful stimuli has also been reported (Emery, Young and McNaughton 2012). The expression of HCN channels has been found also in enteric neurons (Galligan et al. 1990), and in the spiral (Chen 1997) and trigeminal ganglion neurons (Janigro, Martenson and Baumann 1997) with HCN1 exhibiting the highest expression (Chaplan et al. 2003, Kouranova et al. 2008, Mayer and Westbrook 1983, Moosmang et al. 2001, Scroggs et al. 1994), and the majority of trigeminal ganglion neurons were immune-positive for HCN1, HCN2 and HCN3 (Wells, Rowland and Proctor 2007).

5.3. Physiological role of Ih in neuronal function

In the nervous system, Ih displays a set of unique biophysical features that is essential to control excitability and electrical responsiveness of cells. Ih are involved in the regulation of resting membrane potential and membrane input resistance, normalization of synaptic inputs and selective filtering for coincident inputs. Moreover, these functions are classified into three groups: excitatory, inhibitory and modulatory functions.

5.3.1. Regulation of resting membrane potential and intrinsic excitability

The influence exerted by Ih current on the intrinsic excitability of the neuron has a complex nature. At -65 mV, a fraction of HCN channels are tonically open (Kase and Imoto 2012). This results in persistent sodium inflow, which depolarizes the membrane and counteracts hyperpolarizing inputs. However, depolarization causes channel deactivation, and the resulting pause in the inward cationic current has a hyperpolarizing effect. Therefore, by opposing negative and positive perturbations, Ih current stabilizes the membrane potential in the subthreshold range. Although inactivation of Ih current hyperpolarizes the neuron and reduces its intrinsic excitability, the resulting increase in input resistance at subthreshold potentials makes the neuron becomes more responsive toward depolarizing synaptic inputs. This dual action exerted by Ih current on overall neuronal excitability has been clearly established in many neurons and brain areas, including the thalamus, the hippocampus and the cerebellum, and has important repercussions on higher-order brain functions such as learning and memory, control of circadian rhythm and sleep/wakefulness state (McCormick and Pape 1990, Maccaferri et al. 1993, Gasparini and DiFrancesco 1997).

In the axon initial segment of medial superior olive principal neurons, HCN1-mediated current reduces spike probability by elevating the firing threshold. 5-HT1A receptor signaling shifts HCN channel activation curve in the hyperpolarizing direction thereby relieving the brake on spike probability (Ko et al. 2016). Serotonin-dependent modulation of Ih current is also involved in the control of respiratory rhythm in the retrotrapezoid nucleus (RTN). Activation of the 5-HT7 receptor causes a cAMP-dependent depolarizing shift in the activation curve of HCN current, increasing the firing rate of RTN neurons in vitro and respiratory rhythm in vivo (Hawkins et al. 2015)

5.3.2. Rhythmogenesis

In a functional interplay with other membrane ionic mechanisms, the activation-deactivation cycle of HCN channels helps setting the pace of subthreshold membrane oscillations, which eventually determines AP discharge rate and neuronal output. Ih current cooperates with a persistent, subthreshold Na^+ current in setting a 4 to 10 Hz (theta-like) rhythm pyramidal and stellate cells of the entorhinal cortex (EC) layer II (Alonso and Llinás 1989). Both cell types in this area are

critically involved in a special spatial navigation task and thus named “grid cells”. Entorhinal grid cells show periodic, hexagon-shaped firing locations that scale up progressively along the dorsal-ventral axis of medial entorhinal cortex (Moser, Rowland and Moser 2015). Relative HCN1/HCN2 expression ratio, and oscillation frequency, goes down in this structure following a dorsal-ventral gradient (Notomi and Shigemoto 2004). Such dorsal-ventral frequency gradient correlates with the distinct time constants of HCN1 and HCN2 isoforms. In HCN1 KO mice, the dorsal-ventral gradient of the grid pattern is preserved, but the size and spacing of the grid fields, as well as the period of the accompanying theta modulation, is expanded (Giocomo and Hasselmo 2009, Giocomo et al. 2011).

In thalamocortical neurons, Ih current is mainly sustained by HCN2 isoform. Adrenergic and serotonergic stimulation causes a cAMP-mediated modulation of Ih current, which in turn govern the firing pattern of thalamocortical neurons. During wakefulness and REM sleep, thalamocortical neurons fire in a single-spike, or “transmission”, mode. In this state, information is effectively transmitted to the cortex. During non-REM sleep and absence seizures, thalamocortical neurons fire in “burst” mode, and transfer of signals to the cortex is believed not to be as effective (McCormick and Pape 1990). In agreement, global HCN2 deletion causes absence epilepsy with typical “spike-and-wave” discharges in EEG recordings (Ludwig et al. 2003).

A similar role for HCN3 has been described in the intergeniculate leaflet neurons, a retino-recipient thalamic structure implicated in orchestrating circadian rhythm. Here, HCN3-mediated current drives low-threshold burst firing and spontaneous oscillations and is bi-directionally modulated by PI(4,5)P2. Depletion of PI(4,5)P2 or pharmacologic block of HCN current results in a profound inhibition of excitability (Ying et al. 2011).

5.3.3. Role of Ih in synaptic excitability and plasticity

By the properties described previously, Ih current shapes the temporal dynamics of synaptic potentials. This deeply affects the integrative properties of the somatodendritic compartment and the ability of the neuron to express different forms of plasticity.

Functional HCN channels are strongly expressed along the dendritic arborisation of neocortical and hippocampal neurons with a soma-to-dendrites expression gradient (Bender et al. 2001, Lörincz et al. 2002, Harnett, Magee and Williams 2015). Here, Ih current constitutes a shunt conductance accelerating the decay of Excitatory Post-Synaptic Potentials (EPSPs). As a result, temporal summation during EPSP sequences is minimal and the ability of the neuron to resolve individual inputs at somatic level is maximal. This function, first discovered and characterized in pyramidal neurons of the hippocampal CA1 region and somatosensory cortex (Magee 1998, Magee 1999, Williams and Stuart 2000, Berger, Senn and Lüscher 2003), has then been described in subcortical structures (Ying et al. 2007, Engel and Seutin 2015). In the dendritic compartment of CA1 pyramidal neurons, the shunting effect exerted by Ih current limits the activation of voltage-

dependent calcium entry, with important consequences on synaptic excitability (Tsay, Dudman and Siegelbaum 2007). The non-uniform distribution of Ih current is also responsible for a phenomenon termed "site independence" of synaptic potentials, whereby the decay time of distally-generated EPSPs is similar to that of proximally-generated EPSPs (Williams and Stuart 2000).

Ih current accelerates the decay time of both forward- and backward-propagating depolarization waves, thus increasing the precision with which the dendrite detects the concurrence of salient electrical events. These include temporal coincidence of EPSPs and APs, an event leading to neuronal plasticity (Pavlov et al. 2011). In several brain areas, HCN function constrains long-term potentiation (LTP) and associated cognitive functions in basal conditions. Indeed, HCN1 KO mice show improved hippocampal dependent learning and memory performance. In these mice, proximal CA3-CA1 synapses function normally, whereas distal EC Layer III-CA1 contacts are potentiated, as predicted by stronger expression of HCN channels in this compartment (Nolan et al. 2004).

It has been suggested that Ih current affects cortical functions such as cognition, movement planning and execution by setting the strength of connectivity within local cortical microcircuits. Ih current is abundantly expressed in dorsal-lateral Prefrontal Cortex (PFC) layer III neurons, a population crucially involved in spatial working memory. Here, HCN channels are modulated by the opposite action of α2-adrenergic (α2-AR) and type-1 dopaminergic (D1) receptor stimulation on cAMP signalling. When α2-AR stimulation inhibits cAMP-HCN channel signalling, neurons are more tightly connected to recurring microcircuit activity and performance is optimal. In contrast, exposure to stress causes a D1 receptor-mediated enhancement of cAMP-HCN activity leading to a functional disconnection from the local network and impairment of spatial working memory (Wang et al. 2007, Arnsten and Jin 2014).

In the mouse primary motor cortex, HCN expression is specifically elevated in corticospinal neurons of the layer V. Ih current confers these neurons a 4 Hz-resonance preference and gates synaptic inputs from layer II/III pyramidal neurons, determining the efficacy of signal transmission between the two layers. In this context as well, α2-AR stimulation modulates HCN function (Sheets et al. 2011).

5.4. Resonance properties

Dendritic Ih current confers the neuron specific "resonance" properties, i.e., the ability to respond preferentially to inputs at a certain frequency, and thus determines to what extent the neuron responds to synchronous network activity. Due to its slow gating kinetics, Ih current has high-pass filtering properties which, combined to the low-pass filtering action exerted by membrane time constant (Bédard, Kröger and Destexhe 2006), results in a resonance frequency of 1-10 Hz (Hutcheon, Miura and Puil 1996). The power of theta oscillation and the strength of Perforant Path-CA1 pyramidal neuron synapses, which are both under the influence of HCN1 function, have been

proposed as the physiological background of hippocampal-dependent learning and memory storage (Nolan et al. 2004). The ability to resonate in an Ih-dependent manner has been reported for other areas (Ulrich 2002, Wang et al. 2006, Xue et al. 2012, Borel et al. 2013). Although the role of Ih current in oscillating activity and resonance have been clearly established at single cell or local network level, the significance on higher-order functions remains undetermined.

5.5. Neurotransmitter release

Ih current at synaptic terminals has been reported to control the efficacy of vesicle release. HCN1 and HCN2 isoforms are present at GABAergic terminals of pallidal axon collaterals (Boyes et al., 2007) as well as glutamatergic terminals making contacts onto Entorhinal Cortex (EC) layer III pyramidal neurons (Huang et al. 2011). In both cases, pharmacological or genetic knock out of HCN function leads to elevation of spontaneous synaptic release. Huang et al. (2011) have suggested that Ih current exerts this inhibitory action by setting the potential to values where N-type Cav3.2 channels are in a partially inactivated state. HCN- KO hyperpolarizes the terminal and removes calcium channel inactivation. Thus, when an AP invades the terminal, more calcium flows in through calcium channels. A follow-up study from the same authors shows that HCN1 channels restrict the rate of exocytosis from a subset of cortical synaptic terminals within the EC and constrain spontaneous as well as evoked release (Huang et al. 2017).

Despite a large mass of information on the cellular effects of HCN channels, our knowledge of their role in more integrate CNS functions and behaviour is rather indirect and derived from pathophysiological studies as described below. An interesting insight comes from recent evidence in Aplysia californica, whose neuroanatomy and physiology are by far less complex than the mammalian brain (Yang et al. 2015). Aplysia c. motor neurons possess only one HCN isoform, acHCN; Ih current appears to be involved in classical conditioning upon stimulation by nitric oxide/cGMP signalling and subsequent enhancement of a NMDA-like current pathway, similarly to the mammalian hippocampal neurons (Neitz et al. 2014).

6. AIM OF THE THESIS

The aim of this PhD project was to investigate the contribution of Ih LOF to the selective degeneration of SNpc DA neurons in PD. To achieve this goal, in vitro (1) and in vivo (2) experiments were pursued.

(1) The impact of Ih inhibition at the cellular and molecular level was initially studied, focusing on the electrical properties discriminating among differentially vulnerable subsets of midbrain DA neurons in TH-GFP mice. Then, the participation of VGCC-dependent calcium entry during evoked synaptic activity was investigated by combined electrophysiological and calcium fluorometry experiments in the SNpc and VTA DA neuron in wild-type rats.

(2) Evaluation the effect of Ih suppression on DA cell viability in vivo. To this aim, we performed stereotaxic, intracerebral injections of Ih specific blockers (ZD7288 and Ivabradine) followed by behavioral motor tests and immunodetection of tyrosine hydroxylase (TH) in striatal cryosections midbrain.

(2b) Assessment of the neuroprotective efficacy of Ih LOF rescue in vivo To this aim, pharmacological reactivation of Ih was be attempted in presymptomatic MitoPark mice, by injection of Lamotrigine (LTG), an anticonvulsant drug, recently reported to increase the functional regulation of Ih in DA neurons (Friedman et al. 2014). Functional rescue of Ih in MitoPark mice was evaluated for neuroprotective efficacy by behavioral motor tests.

7. METHODS

7.1. Animals

All procedures required for ex vivo experiments were conducted in compliance with the Council Directive of the European Community (2010/63/EU), Decreto Legislativo Italiano 26 (13/03/2014) and approved by the Animal Care Committee of the Department of Neurofarba, University of Florence. B6.Cg-Tg (TH-GFP) mice (Matsushita et al. 2002) were obtained from Riken BioResource Center, Japan. In these mice, green-fluorescent protein (GFP) expression is driven by TH promoter. Wistar rats were purchased from Charles River Italia (Lecco, Italy) and were used of either sex at postnatal day 20–30 in this study. MitoPark mice (Ekstrand et al. 2007) were obtained from Dr. Nils-Göran Larsson (Karolinska Institutet, Stockholm, Sweden Laboratories) now at Max Planck Institute for Biology of Aging, Cologne, Germany, and were used of either sex from 6 to 18 weeks old.

7.2. Midbrain slice preparation

Animals were anaesthetized with isoflurane and decapitated. Brains were removed and mounted in the slicing chamber of a vibroslicer (Leica VT 1000S, Leica Microsystem, Wetzlar, Germany). Midbrain horizontal slices (250 µm) were cut in chilled artificial cerebral spinal fluid (a CSF), composed of (in mM) 130 NaCl, 3.5 KCl, 1.25 NaH_2PO_4, 25 $NaHCO_3$, 10 glucose, 2 $CaCl_2$ and 1 $MgSO_4$; and saturated with a 95% O_2 + 5% CO_2 gas mixture. Slices were allowed to recover in the same solution maintained at 34°C with constant oxygenation for 1h prior to experiments.

7.3. The patch-clamp technique

The patch-clamp technique, invented by Erwin Neher and Bert Sakmann in 1976, consists of sealing the tip of a pipette filled with a physiological solution to the membrane of a cell, maintaining it at a specific voltage to measure currents flowing through ion channels. Alternatively the experimenter can control the current injected into the cell through the recording electrode, measuring its potential. There are five different configurations of patch-clamping: “whole-cell”, “cell-attached”, “inside-out”, “outside-out” and “perforated”. Amoung them the less invasive is the cell-attached configuration, where the patch electrode is sealed to the membrane (reaching an electrical resistance in the order of a GΩ), leaving the cell intact and allowing the recording of currents through single ion channels. The whole-cell configuration is obtained with the rupture of the seal, allowing the pipette to become continuous with the membrane. If alter the formation of gigaseal the pipette is quickly withdrawn from the cell, the piece of membrane inside of it will be exposed to the extracellular media (inside-out configuration). Pulling the membrane from both sides of a whole-cell configured patch in order to let the external faces being in contact with the external solution will result in the outside-out configuration. During whole-cell recordings an

irreversible washout of diffusible intracellular constitutes (e.g. ATP, phosphorylating moleculs ect) into the relatively larger volume of the pipette through dialysis can occur. As a consequence, properties and functions of ion channels can be impaired, leading to a decrease of ionic currents over time. The permeabilized-patch whole cell configuration overcomes this problem by accessing the intracellular space not by seal rupture but buy forming pores thanks to a pipette solution containing antibiotics. In this way the dialysis is much slower and the intracellular environment is preserved for a long recordings.

7.4. Electrophysiology

Patch pipettes were made from thin-walled borosilicate capillaries (Harvard Apparatus, London, UK) with a vertical puller (Narishige PP830, Narishire International Ltd, London, UK) and back-filled with an intracellular solution containing solution (in mM): K^+ Methanesulfonate (120), KCl (15), HEPES (10), EGTA (0.1), $MgCl_2$, (2), Na_2PhosphoCreatine (5), Na_2GTP (0.3), MgATP (2), resulting in a bath resistance of 2–3 MΩ in the bath. This solution was used for both cell-attached and whole-cell recordings. Access resistance was monitored during voltage-clamp recordings throughout experiments with 100-ms, –10-mV steps. Recordings were performed at 34 °C. Membrane potential values were corrected offline for measured junction potential (8 mV). Recordings undergoing a drift in access resistance ≥ 10% were discarded. No whole-cell compensation was used. Signals were sampled at 10 kHz and low-pass filtered at 3 kHz with an Axon Multiclamp 700B (Molecular Devices, Sunnyvale, CA, USA). For coupled recordings of electrical and optical signals, 0.1 mM of Fluo 4 pentapotassium salt was added. SNpc and VTA DA neurons were identified with infrared or fluorescence microscopy based on GFP expression and position relative to the medial terminal nucleus of the accessory optic tract (MT; (Neuhoff et al. 2002, Margolis et al. 2006) in slices at dv –4.2 to dv –4.8 (Paxinos & Franklin, 2007). In current clamp, Ih-mediated VS was elicited with 500-ms, –100-pA current steps and measured as the difference between the voltage at the bottom of the sag and that at the end of the pulse. Ih was blocked with the specific organic blocker ZD7288 (Tocris Bioscience, Bristol, UK,10 µM) applied by bath perfusion or included in whole-cell pipette solution. Single or multiple EPSPs were elicited with single or multiple (five) pulses (frequency, 20 Hz; amplitude, 5–15 mV) and in the second part of experiments the single or multiple EPSPs were elicited every 15 s (10 pulses at 10 Hz or 40 pulses at 20 Hz; 5–15 V amplitude), delivered with a bipolar tungsten electrode (FHC, Bowdoin, ME, USA) placed at ~200 µm from the soma of recorded neuron or in the SNr for recordings of evoked GABA-mediated Inhibitory. During current-clamp recordings, neurons were moderately hyperpolarized (~ -2 / -3 mV) in order to minimize membrane oscillations and hamper the generation of spontaneous or synaptically-induced action potentials. Ih block was monitored with 500 ms, –100-pA pulses at the end of each sweep. Paired-pulse ratio (PPR) was determined measuring the amplitude of two consecutive (50 ms apart) evoked EPSCs. Spontaneous excitatory

activity was stimulated with the voltage-dependent potassium channel blocker 4-aminopyridine (4-AP; Sigma-Aldrich, Saint-Louis, MO, USA 50µM). Excitatory synaptic activity during recordings of spontaneous EPSCs (sEPSCs) was isolated by using the $GABA_A$ receptor blocker gabazine (Tocris Bioscience, Bristol, UK 10µM). Post-Synaptic Potentials (IPSPs). During EPSP recordings, neurons were moderately hyperpolarized (~ -2/ -3 mV) in order to stabilize the membrane potential and hamper the generation of spontaneous or synaptic-driven action potentials (APs). To monitor pharmacological block, Ih-mediated sag potential was elicited by imposing short current pulses (-100 pA, 500 ms) at the end of the sweep. MultiEPSP summation was expressed as the ratio of 10th/1st EPSP amplitude and multiEPSP area was reported as mV x ms. In voltage clamp recordings, access resistance was monitored for the entire duration of the experiment with brief test pulses (-10 mV, 500 ms). Recordings undergoing a drift in access resistance ≥ 10% were discarded. No whole-cell compensation was used. Ih activation curves were obtained by measuring the amplitude of tail currents at -115 mV following a sequence of 4 s-long test pulses from -45 mV to -125 mV. Electrophysiological and optical traces shown in figures are obtained by averaging five consecutive traces and represent typical observations.

7.5. Microfluorometric determination of calcium responses

Fluorescence signal was collected from a square-shaped window comprising the cell body of the neuron under investigation loaded with 100 µM of the high-affinity, non-ratiometric calcium dye Fluo4 pentapotassium salt (Molecular Probes). Two to three minutes were usually sufficient for complete loading. No differences in major electrophysiological parameters were observed between dye-filled and control neurons. Fluorescence was elicited with a 488 nm LED and collected with a photomultiplier tube (PMT; Cairns Research) with a 10 kHz sampling rate. LED excitation was triggered with the electrophysiological protocol and the PMT signal was acquired and processed as described for voltage signal. SCRs are reported as $\Delta F/F_0$, where F_0 signal was the baseline emission of the loaded neuron at rest, and ΔF was defined as F_{peak}- F_0. Background fluorescence was obtained by measuring the emission of a Fluo 4-free area of the slice and subtracting the obtained value from F_0. Off-line analysis was performed with Clampfit 10 (Molecular Devices) and Origin 9.1. For the analysis of SCRs kinetics, rise and decay time are intended as the time required to reach 50% of peak. Recordings showing F_0 decay exceeding 0.5%/s within a single trial, or undergoing irreversible F_0 rise during consecutive trials were discarded.

7.6. Single-cell labeling and TH immunostaining

For the post hoc identification of recorded neurons, Alexa 350 hydrazide (Life Technologies, Carlsbad, CA, USA) was added to whole-cell pipette solution (5 mM). Cell loading was facilitated by passing negative current (-50 pA) and membrane reseal was allowed by gentle removal of the patch pipette at the end of the experiment. Slices were fixed with 4% paraformaldehyde, incubated

overnight with a monoclonal anti-TH (1 : 500; Boster, Pleasanton, CA, USA) and labeled with a Cy3-conjugated anti-mouse IgG (1 : 500). Images were acquired with an Olympus BX63 microscope equipped with CellSense Dimension Software (Olympus, MI, Italy).

7.7. In Vivo Procedures

All in vivo procedures were conducted in compliance with the Council Directive of the European Community (2010/63/EU), Decreto Legislativo Italiano 26 (13/03/2014) and approved by the Animal Care Committee of the University of Florence. Male Wistar rats (200–220 g) were purchased from Charles River Laboratories Italia (Lecco, Italy). Animals were housed in humidity- and temperature-controlled room (22–24 ºC), allowed free access to food (4RF21; Mucedola s.r.l., Milan, Italy) and water, and kept on a 12-h light/dark cycle (lights start at 7:00 AM). Procedures were performed according to a previous report (Provensi et al. 2017), with modifications due to the different brain areas involved. One week after arrival, animals were anesthetized with an intraperitoneal (i.p.) injection of 80 mg/kg zoletil plus 15 mg/kg xylazine and placed on a stereotaxic frame (Stellar, Stoelting Co., Wood Dale, IL, USA). A stainless steel cannula (22 gauge) was implanted bilaterally above the SNpc-VTA boundary (anterior, -5.3 mm; lateral, ± 2 mm; ventral, -6.6 mm from Bregma) and fixed to the skull by using dental cement. Correct cannula placement was verified postmortem. Animals were allowed 3 days to recover from surgery before microinjection procedure. For microinfusions, animals were gently restrained by hand, and an injection needle (30 gauge) was inserted tightly into the guide to 1 mm beyond the end of the guide cannulas. The injection needle was connected to a 1 mL Hamilton microsyringe, and the infusions were performed at a rate of 1 µl/60 s. The injection needle was left in place for an additional 60 s to minimize backflow. It was then withdrawn and placed on the other side, where the procedure was repeated. The drugs used were ZD7288 (5 µg/µl) and Ivabradine (5 µg/µl) dissolved in saline. The volume of the drugs infused was 2 µl per side for four consecutive days. Control groups received equal volumes of sterile saline (0.9%). Correct cannula placement was verified by infusing a 4% (weight/volume) methylene blue solution over 30 s (2 µl). Brains were fixed by transcardiac perfusion 24 h after the last injection with cold physiological saline followed by 4% (volume/volume) paraformaldehyde in 0.1 M phosphate buffer (PB; pH 7.4). Brains were postfixed in the same solution overnight (4º C) and cryoprotected in 30% (weight/volume) sucrose in PB. Cannula placements were considered correct when the spread was 1 mm^3 or less from the intended infusion sites. Only data from animals confirmed for correct cannula placement were analyzed.

7.8. Behavioral Tests

Twenty-four hours after the last injection, animals were tested for general motor activity with a standard open field test (OFT). Animals were positioned in a corner of an open-field arena (w = 60 cm; h = 30 cm; d = 70 cm) and the general motor activity was assessed in 10-min sessions.

Animals were monitored with a camera and the covered distance (in cm) measured using a Smart 2.5 software. Animals were then tested for the expression of motor symptoms associated to monolateral DA degeneration, by measuring the number of apomorphine-induced rotations. Briefly, animals received an i.p. injection of apomorphine (0.5 mg/kg), then placed in a transparent Perspex cylinder. Animals were video recorded for 30 min. An operator unaware of pharmacological treatments counted the number of rotations. The Rotarod test were used to test MitoPark mice. Mice were tested by being placed on a rotating rod that starts at 5 revolutions per minute (rpm) and then accelerates to 20 rpm in 10 seconds and remains at that velocity for 180 seconds (constant velocity testing) with evaluation of numbers of falls.

7.9. Histological Evaluation of DA Degeneration

After paraformaldehyde fixation, brains were cut with a cryostate (Leica Microsystems, Buffalo Grove, IL, USA) to obtain 50-µm thick coronal sections of the mesencephalon (~15 sections/brain). Sections were then probed with a mouse monoclonal anti-Tyrosine Hydroxylase (anti-TH) antibody (1:500; Boster Bio, CA, USA) and revealed with an Alexa 488-conjugated secondary antibody (1:500; Abcam, Cambridge, UK). Images were taken with the 10x objective of an epifluorescence microscope (Olympus BX63, Milan, Italy), then digitally reconstructed with the CellSens Dimension software. Quantitative analysis was performed on images of to the ventral half of whole sections according to a previously published method (Gerace et al. 2014). In brief, mean pixel intensity was measured in same-size square regions of interest from the drug-injected and the saline-injected area of each brain. This value was then normalized to the total intensity of the entire TH positive area of the drug-injected side and compared to corresponding value of the controlateral saline-injected side (x5 sections; each brain).

7.10. Reagents

Unless otherwise specified, reagents were purchased from Sigma-Aldrich (Saint-Louis, MO, USA). AMPA, NMDA and type 1 metabotropic glutamate receptors (mGluRs) were blocked with, respectively, NBQX, D-APV and CPCOOEt (10 µM, 50 µM, 1 µM; Tocris bioscience, Bristol, UK). $GABA_{A-B}$ receptors were blocked with SR95531 and CGP55845, (10 µM, 1 µM; Tocris). T-type and L-type Voltage-Gated calcium channels (VGCCs) were blocked with mibefradil and isradipine (5 µM each; Tocris). Pharmacological suppression of Ih was obtained with ZD7288 (10 µM; Tocris). Fluo 4 was purchased from Thermo Fisher Scientific (Waltham, MA, USA). $GABA_B$ agonist baclofen was used at 1 µM. The K-ATP channel blocker glybenclamide was used at 10 µM. Ih enhancer Lamotrigine was used 15 mg/kg ip.

7.11. Data analysis and statistics

Pooled data are presented as mean standard error (SEM) of ‘‘n’’ neurons/animals unless otherwise specified, statistical significance was assessed with Student’s t-test for paired samples (Microcal Origin 9.1; Northampton, MA, USA). Graphs and representative traces were generated with Microcal Origin 9.1.Significance at the $p < 0.05$, 0.01, 0.001 and 0.0001 level is indicated, when achieved, with *, ** and ****, respectively, in figures .Example traces represent typical observations. EPSP decay time is defined as the time required for peak amplitude to decrease by 30%. Temporal summation is expressed as EPSP5/EPSP1 ratio. Representative current-clamp recordings of single or multiple EPSPs before and after ZD7288 application were baseline-adjusted to allow comparison. The mean frequency and amplitude of sEPSCs was calculated on the basis of 1-min bins before and at the end of ZD7288 bath application with Clampfit 10.3 (Molecular Devices, Sunnyvale, CA, USA).In the second part examples of electrical and optical recordings are averages of five traces for each condition and intend to represent typical observations. Temporal summation is expressed as 10th EPSP/1st EPSP ratio. Ih activation curves, normalized I/V plot, fitting and determination of $V_{1/2}$ were generated with Origin 9.1 as described previously.

7.12. Genetic model of PD

The Mitopark mouse: breeding and genotyping

The MitoPark mouse model of PD was designed to directly test the hypothesis that mitochondrial dysfunction in DA neurons can cause a progressive parkinsonian phenotype. The model is based on the specific inactivation of mitochondrial transcription factor A, (Tfam), a protein essential for mitochondrial DNA (mtDNA) expression and maintenance. In the absence of Tfam a progressive deficiency in mitochondrial respiratory chain is observed followed by cell death.

To generate the MitoPark mouse model, knock-in mice, expressing Cre recombinase under the control of the dopaminergic transporter (DAT) were crossed with mice in the the loxP recombination sites flank the Tfam gene. In this way Tfam deletion is directed only in cells expressing DAT. MitoPark mouse breeding pairs were obtained from Dr. Nils-Göran Larsson (Karolinska Institutet, Stockholm, Sweden; now at Max Planck Institute for Biology of Aging, Cologne, Germany).

To generate experimental MitoPark mice and littermate controls, the $DAT^{cre}$and $Tfam^{loxP}$ mouse strains were first backcrossed to C57BL/6 J mice (The Jackson Laboratory, Bar Harbor, ME), and offspring were selectively mated to generate double heterozygous males ($DAT^{+/cre}$; $Tfam^{+/loxP}$) and homozygous floxed Tfam females ($DAT^{+/+}$; $Tfam^{loxP/loxP}$). The double heterozygous males were then crossed to homozygous $Tfam^{loxP/loxP}$ females, resulting in an ~25% yield of MitoPark mice ($DAT^{+/cre}$; $Tfam^{loxP/loxP}$), and littermate controls ($DAT^{+/+}$; $Tfam^{loxP/loxP}$). Mice were group-housed in same-sex, standard shoebox cages with ad libitum access to food and water. The room was maintained at 22 °C on a 12 hours light/12 hours dark light cycle.

DNA was prepared from mouse tail and used for PCR according to the extraction kit manufacturer's instructions (MyTaq Extract-PCR Kit, Bioline Reagents Ltd, UK). To identify the $DAT^{+/cre}$ genotype, a multiplex PCR setting with two primer pairs was used. Forward primer sequence was 5′-CATGGAATTTCAGGTGCTTGG, and the reverse primer sequences were 5′-CATGAGGGTGGAGTTGGTCAG and 5′-CGCGAACATCTTCAGGTTCT, which enabled identification of heterozygous mice. For the $Tfam^{loxp/loxp}$ genotype, two primer pairs were also used. The forward primer sequence was 5′-CTGCCTTCCTCTAGCCCGGG, and the two reverse primer sequences were 5′-GTAACAGCAGACAACTTGTG and 5′-CTCTGAAGCACATGGTCAAT, which distinguished between heterozygous and homozygous mice. Thirty-eight cycles were run at 95°C for 30 seconds, 58°C for 30 seconds and 72°C for 45 seconds. The PCR products were separated using electrophoresis on 2% agarose gels and were visualized with UV after ethidium bromide staining.

Two bands at 310 and 470 base pairs for $DAT^{+/cre}$ and one band at 437 base pairs for $Tfam^{loxp/loxp}$ should be detected from MitoPark mice. One band at 310 base pairs for $DAT^{+/+}$ (wildtype) and one band at 437 base pairs for $Tfam^{+/loxp\ or loxp/loxp}$ should be detected from control littermates.

MitoPark mice colony has recently been established in the animal facility in our Department.

MitoPark mice recapitulate several features of PD in humans such as adult-onset of neurodegeneration; progressive clinical course; earlier onset and more severe and extensive cell death in SNpc than in VTA; responsiveness to L-DOPA administration with a differential response depending on disease stage.

8. RESULTS

8.1. Ventral to dorsal gradient of Ih-mediated VS magnitude in midbrain DA neurons

Electrophysiological investigation was restricted to GFP-positive putative DA neurons in SNpc or VTA in horizontal midbrain slices from TH-GFP mice (Matsushita et al. 2002). A total of 110 neurons were recorded. We found that Ih-dependent VS varies in magnitude within midbrain DA neurons according to a ventral-to-dorsal gradient (Fig. 8, see also Fig. 10 for a quantitative analysis). DA neurons in dorsal midbrain (Fig. 8A; -4.25 mm) show the highest percentage of Ih-positivity (SNpc = 35/38, 92.10%; Fig. 8A (1) and C1; VTA = 41/46, 89.1%; Fig. 8A (2) and C2). Within this group, SNpc DA neurons have, on average, larger VS than do VTA DA neurons. Strikingly, the great majority of GFP-positive neurons in ventral slices (Fig. 8B; -4.75 mm) have signatures characterized by the absence of VS and by higher firing frequency in response to depolarization (24/26, 92.3%; Fig. 8B (3) and C3). This is consistent with the previously reported existence of DA neurons with 'unconventional' electrical properties in the VTA (Lammel, Lim and Malenka 2014). The percentage of Ih-negative, GFP-positive neurons we recorded from largely outnumbers the reported ratio of GFP-positive, TH-negative neurons for these mice (VTA, 8.3%; SNpc, 7.5%; (Matsushita et al. 2002), suggesting the existence of a large number of Ih-negative DA neurons in this district. Recently, however, substantial ectopic GFP expression has been reported in VTA neurons of this transgenic animal (Lammel et al. 2015). To analyze the specificity of GFP labeling in our TH-GFP mice, Ih-negative, GFP-positive neurons from the ventral VTA were labeled with Alexa 350 hydrazide via patch pipette-mediated diffusion (n = 16). Subsequent immunostaining confirmed TH expression in 13 of 16 neurons recorded, indicating a specificity of ~ 80% (Fig. 8D). In conclusion, our results are in agreement with previous studies reporting diverse Ih current densities among subpopulations of midbrain DA neurons (Neuhoff et al. 2002). In addition, we report a very high percentage of neurochemically identified DA neurons, mainly located in ventral portions of the VTA, with Ih-negative signatures.

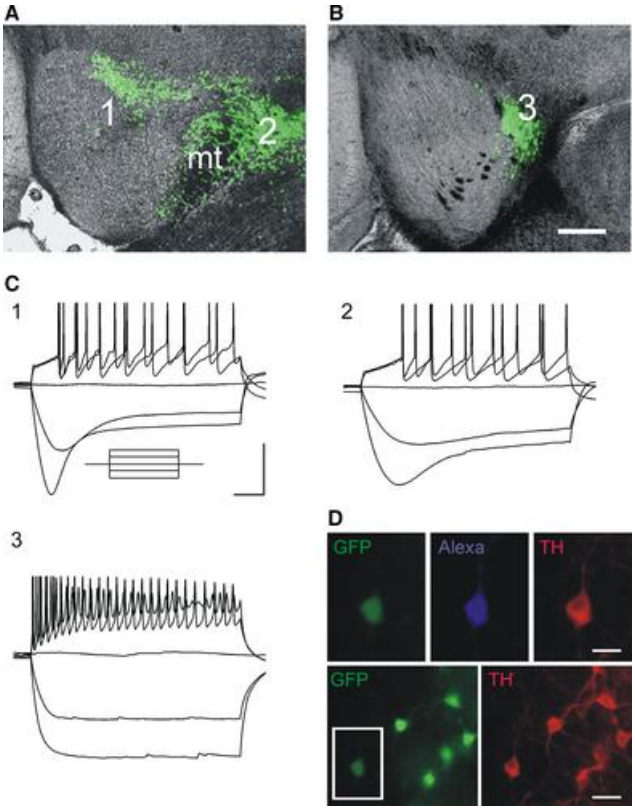

Figure 8: Ventral-to-dorsal gradient of Ih-mediated VS magnitude in midbrain DA neurons. Top, overlay of fluorescence and infrared images of (A) dorsal (−4.25 mm) and (B) ventral (−75 mm) acute horizontal midbrain slices from TH-GFP mice. (C) Typical current-clamp signatures obtained from GFP-positive neurons in (1) the SNpc and (2) dorsal and (3) ventral VTA (corresponding recording sites are indicated in A and B; protocol, −200/+200 pA, 500 ms). Note the absence of Ih-dependent VS in C3. (D) TH immunoreactivity in a GFP-positive, Ih-negative neuron recorded in the ventral VTA and labeled with Alexa 350 hydrazide. On the bottom, lower magnification image of the same field to show positive TH immunoreactivity in GFP-expressing cells surrounding the recorded neuron (box). Scale bars, 250 μm (A and B), 70 ms, 40 mV (C), 20 μm (D top), 40 μm (D, bottom).

8.1.1. Ih limits EPSP amplitude and decay time

Pharmacological suppression of Ih with. ZD7288 10μM was induced while recording locally evoked EPSPs from DA neurons in SNpc or VTA. Block of GABAergic transmission was deliberately omitted in these experiments in order to assess the overall contribution of Ih on synaptic excitability of midbrain DA neurons. Moreover, block of GABAergic transmission did not affect EPSP kinetics in control conditions or after Ih suppression in rat SNpc DA neuron (Masi et al. 2013). As shown in Fig. 9A, ZD7288 10 μM modified single EPSP kinetics. VS was also nearly abolished on the same time scale (~ 10 min). Quantitatively, peak amplitude was modestly raised in both areas by ZD7288 (SNpc – 4.88 ± 0.49 mV vs 6.49 ± 0.66 mV, n = 20, p = 0.009; VTA – 7.37 ±0.69 mV vs 8.61 ±0.77 mV, n = 20, p= 0.02) whereas decay time increased in both SNpc and VTA by 214 and 169%, respectively (SNpc – 18.37 ± 3.01 ms vs 38.43 ± 5.19 ms, n = 20, p = 1.74E-6; VTA – 24.56 ±3.11 ms vs 38.49 ± 3.70 ms, n = 20, p= 0.00021), indicating reduced repolarizing capability in the occurrence of an EPSP (Fig. 9B).

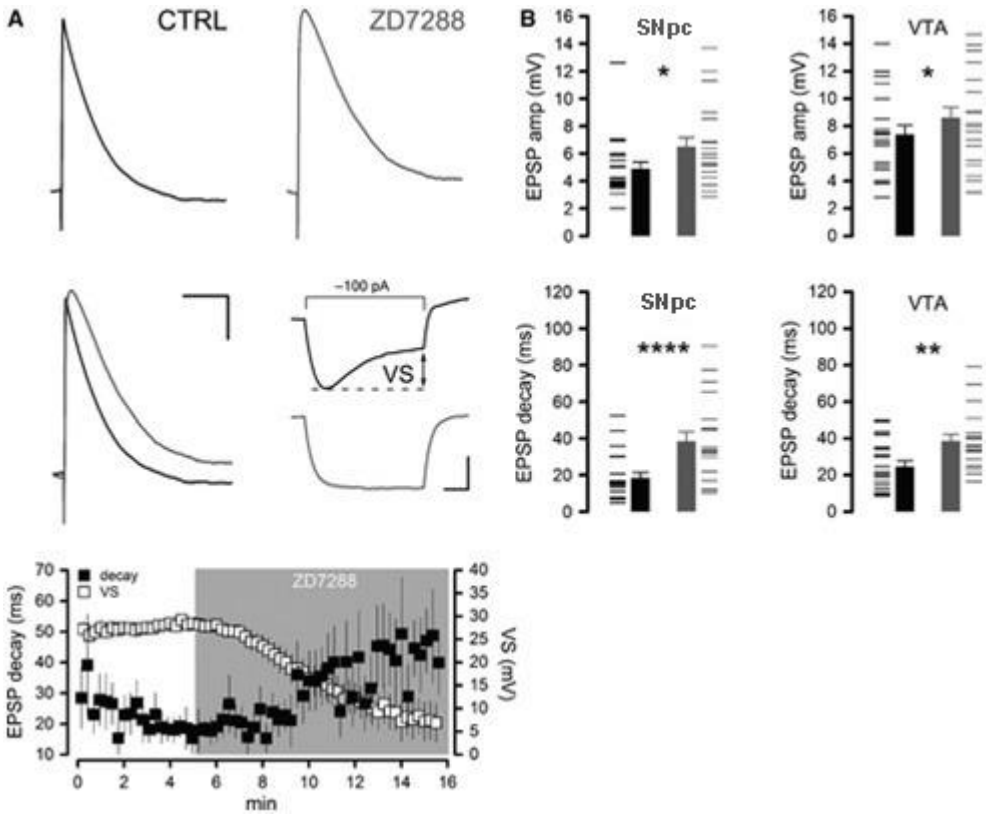

Figure 9: Ih limits EPSP amplitude and decay time. (A) Representative EPSP recorded before (black) and after (gray) pharmacological suppression of Ih with ZD7288 10μM. The action of ZD7288 on VS elicited with a negative current pulse (−100 pA) is also shown (middle, right). Bottom, time course of the effect of Ih blockade on EPSP decay and VS in SNpc DA neurons (n = 7). (B) Cumulative analysis of ZD7288-induced changes in EPSP amplitude (top), and decay time (bottom) in SNpc and VTA DA neurons (*, **, **** = $p < 0.05$, 0.01, 0.0001, respectively). Scale bars, 250ms, 2 mV (A, left), 100 ms, 10 mV (A, right).

8.1.2. Ih suppression affects EPSP kinetics based on VS amplitude, thus differentially in SNpc and VTA DA neurons

A quantitative comparison of the effects of Ih suppression on EPSP decay in SNpc vs. VTA DA neurons is presented in Fig. 10A. Baseline VS is significantly larger in SNpc DA neurons (28.15 ± 1.06 mV vs 15.79 ± 2.57 mV, n = 19–21, p = 0.0015, Mann–Whitney). Consistently, ZD7288-induced increase in EPSP decay time was significantly greater in SNpc DA neurons (SNpc – 214 ± 0.15%; VTA – 169± 0.12%, n = 19–21, p = 0.048, Mann–Whitney). This effect is linearly correlated with baseline VS (y = a + bx; a = 1.38; b = 0.02; Pearson's r-value = 0.41, p= 0.004; Fig. 10B). Furthermore, the graph highlights the different properties of the two populations, with VTA DA neurons showing higher degree of heterogeneity. As mentioned, VS is absent in a large fraction of VTA DA neurons in ventral slices. Consistently, application of ZD7288 did not change EPSP peak amplitude (9.62 ± 1.59 mV vs 9.37 ± 2.86 mV, n = 4, p= 0.91) or decay (42.97± 4.41 ms vs 41.17 ± 3.76 ms, n = 4, p= 0.77) in these neurons (Fig. 10C). In conclusion, the action of Ih on

EPSP kinetics was qualitatively similar in the two populations. Quantitatively, SNpc DA neurons were significantly more sensitive to Ih block due to higher mean current availability at EPSP-relevant potentials.

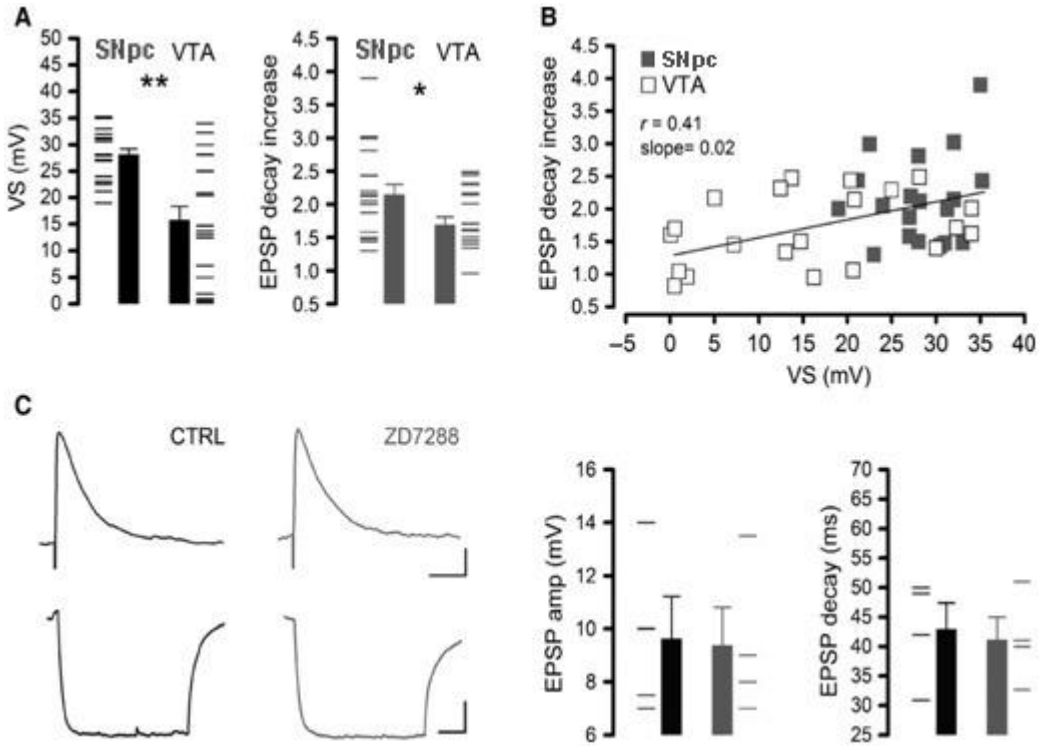

Figure 10: Ih suppression affects EPSP kinetics based on VS amplitude, thus differentially in SNpc and VTA DA neurons. (A) Baseline VS amplitude and ZD7288-induced EPSP changes in SNpc and VTA DA neurons comparatively. (B) ZD7288-induced increase in decay time correlates linearly with baseline VS amplitude and reveals a differential distribution of the two populations. (C) ZD7288 does not affect EPSP properties in VS-negative VTA DA neurons (*, ** = $p < 0.05, 0.01$, respectively). Scale bars, 100 ms, 3 mV (upper); 200 ms, 10 mV (lower).

8.1.3. Ih limits temporal summation of excitatory synaptic inputs

We evoked multiple EPSPs in identified SNpc and VTA DA neurons and measured the increase in EPSP5/EPSP1 ratio brought about by 10-min bath application of ZD7288 10μM. This experiment was performed on neurons with a VS ≥ 15 mV, in which ZD7288 leads to a ≥ 50% mean increase in EPSP decay time. As shown in Fig.11, temporal summation was increased in SNpc and VTA DA neurons by 223 and 142% (SNpc – 0.94 ± 0.11 mV vs 1.95 ± 0.17 mV, n = 10, p = 0.00065; VTA – 1.64 ± 0.19 mV vs 2.32 ± 0.28 mV, n = 10, p= 0.00583). ZD7288-induced increase in summation ratio was significantly more evident in SNpc DA neurons (SNpc – 223 ± 0.41%; VTA – 142± 0.06%; n = 10; p= 0.01, Mann–Whitney). These results indicate that ZD7288-induced

alteration of EPSP kinetics causes reduced capability to resolve individual EPSPs during sustained synaptic stimulation, thus promoting temporal summation. This effect is quantitatively more pronounced in SNpc DA neurons.

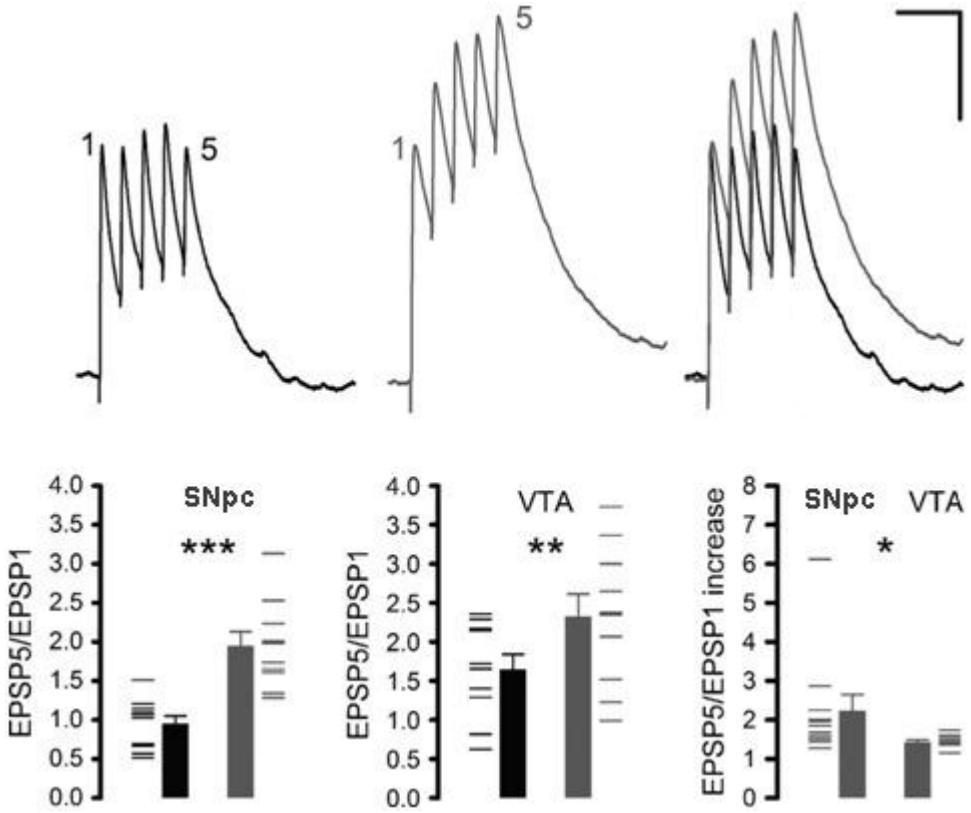

Figure 11: Ih limits temporal summation of excitatory synaptic inputs. (Top) Example traces of multiple EPSPs in CTRL (black) and after ZD7288 (gray). (Bottom) ZD7288 significantly increases EPSP5/EPSP1 in SNpc (left) and VTA (center) DA neurons. Comparatively, the effect is significantly more evident in SNpc DA neurons (right) (*, **, *** = $p < 0.05, 0.01, 0.001$, respectively). Scale bars, 150 ms, 4 mV.

8.1.4. The contribution of Ih in the integration of excitatory synaptic activity depends on postsynaptic HCN channels

Changes in EPSP kinetics are normally indicative of modifications in postsynaptic ionic mechanisms. However, a role for Ih in release probability at presynaptic terminals has been reported (Huang and Trussell 2014, Klar, Surges and Feuerstein 2003). We investigated this possibility in our experimental model by testing the effect of intracellular Ih block on single EPSP kinetics. As shown in the time course in Fig. 12A, membrane rupture with a pipette containing 10

μM ZD7288 (t = 0 min), triggers a progressive increase in EPSP decay time which fully occludes the action of subsequent bath application of the drug. As no difference between SNpc and VTA DA neurons were found, datasets from the two fields were pooled (19.46 ± 2.14 ms vs 18.45 ± 2.17 ms, n = 8, p = 0.51, SNpc + VTA). We then tested whether Ih suppression might determine presynaptic short term changes in release probability, by studying the effect of ZD7288 on PPR (Fig. 12B). Although this experiment was performed in voltage-clamp configuration (Vhold = -55 mV), ZD7288 was included in the whole-cell pipette solution to eliminate the possible contribution of postsynaptic Ih. ZD7288 10 μM did not change PPR in either area (1.01 ± 0.05 vs 1.04 ± 0.05, n = 14, p= 0.28, SNpc + VTA). Finally, we determined whether Ih suppression could alter local excitatory synaptic activity with a presynaptic mechanism (Fig. 12C). In voltage clamp, spontaneous excitatory synaptic activity was stimulated with the potassium channel blocker 4-AP (100 μM) and isolated with gabazine (10 μM). The administration of ZD7288, in agreement with previous data on PPR, did not change the amplitude (-87.69 ± 21.19 pA vs -100.9 ± 18.19 pA, n = 12, p= 0.24; SNpc + VTA) or frequency (9.88 ±3.54 Hz vs 9.38 ± 5.56 Hz, n = 12, p= 0.11; SNpc + VTA) of sEPSCs. Overall, these results indicate that the effects induced by ZD7288 are mediated by postsynaptic HCN channels, whereas HCN channels at presynaptic terminals do not exert a significant control over synaptic activity in this experimental setting.

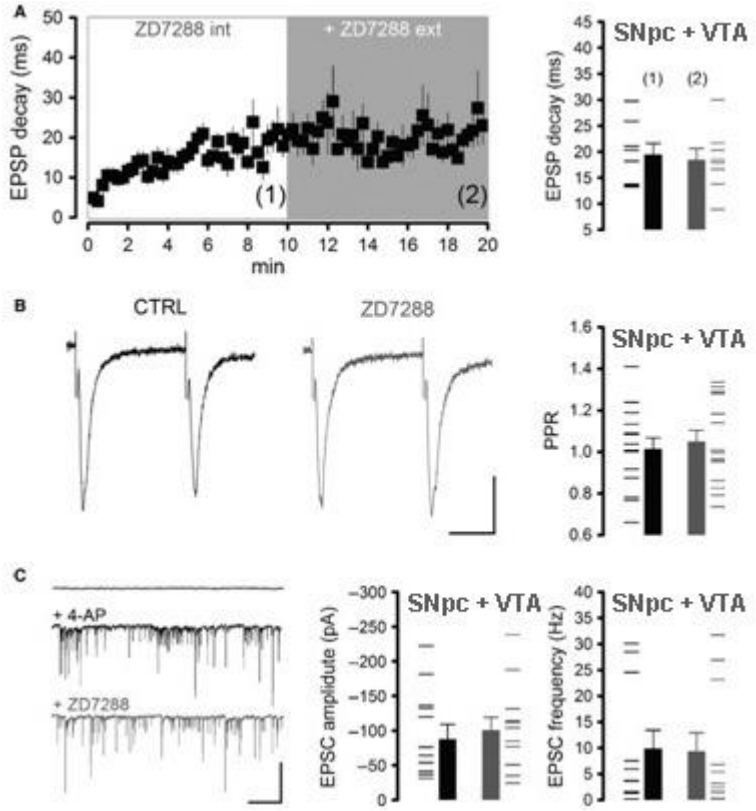

Figure 12: The contribution of Ih in the integration of excitatory synaptic activity depends on postsynaptic HCN channels. (A, left) Time course of the increase in EPSP decay time triggered by intracellular ZD7288 (10 μM). The effect of subsequent application of external ZD7288 is fully occluded (right). (B, left) Paired evoked EPSCs recorded in CTRL (black) and after ZD7288 (gray). PPR is not affected by Ih block (right). (C, left) sEPCS recorded in the presence of 100 μM 4-AP and 10 μM gabazine. ZD7288 does not affect the frequency or amplitude of 4-AP-stimulated sEPSCs (center, right). Scale bars, 200 ms, 200 pA (B), 1.5 s, 150 pA (C).

8.2. Properties of spontaneous SCRs in DA neurons *in vitro*

In this first part, we showed that pharmacological suppression of Ih increases the amplitude and decay time of excitatory postsynaptic potentials, leading to temporal summation of multiple excitatory potentials at somatic level. Importantly, these effects are quantitatively more evident in SNpc DA neurons. In this regard, we present the hypothesis that Ih LOF may be linked to PD trigger mechanisms, such as mitochondrial failure and ATP depletion, and act in concert with SNpc-specific synaptic connectivity to promote selective vulnerability. In the second part, we searched for more subtle elusive elements of diversity. We combined the electrophysiological investigation with the involvement of specific ion channels in PD-related failure of mitochondrial or calcium homeostasis. This study was restricted to neurons of the SNpc or VTA with typical DA morphology and electrical properties: a large, polygonal and fusiform cell body, with Ih ≥ 200 pA. In DA neurons, calcium elevations may arise from the opening of membrane conductances as well as the mobilization of intracellular calcium pools following activation of inositol 1-4-5 trisphosphate (IP3)-coupled receptors. mGluRs are major mobilizers of calcium from internal stores in DA neurons (Cui et al. 2007, Lüscher and Huber 2010). In addition, external calcium may flow in through calcium-permeable glutamate receptors (Morikawa and Paladini 2011) or L- and T-type VGCCs (Dufour, Woodhouse and Goaillard 2014, Philippart et al. 2016) Initial calcium elevation may, in turn, trigger Calcium-Induced Calcium Release from specific intracellular reservoirs (Morikawa et al. 2000). We tested the sensitivity of our experimental setting by measuring AP-dependent or subthreshold SCRs (Fig 13). During spontaneous discharge of APs (Fig 13B, black trace), SCRs appeared as AP-locked positive spikes (green trace, 2.967 ± 0.59%), with distinct rise and decay kinetics (rise, 97.99 ± 8.64 ms; decay, 153.88 ± 11.08 ms, *n*= 7). During spontaneous subthreshold oscillations (Fig 13C), SCRs had comparable amplitude (2.78 ± 0.13%), but slower kinetics (rise, 333.29 ± 19.37 ms; decay, 438.52 ± 16.43 ms, *n* = 5) compared to the previous. In response to pipette-stimulated AP bursts, fluorescence signal showed sustained elevation, due to transient SCR summation. In contrast, somatic hyperpolarization elicited a modest downward deflection of calcium signal followed by a positive rebound at the end of negative current step (Fig 13D).

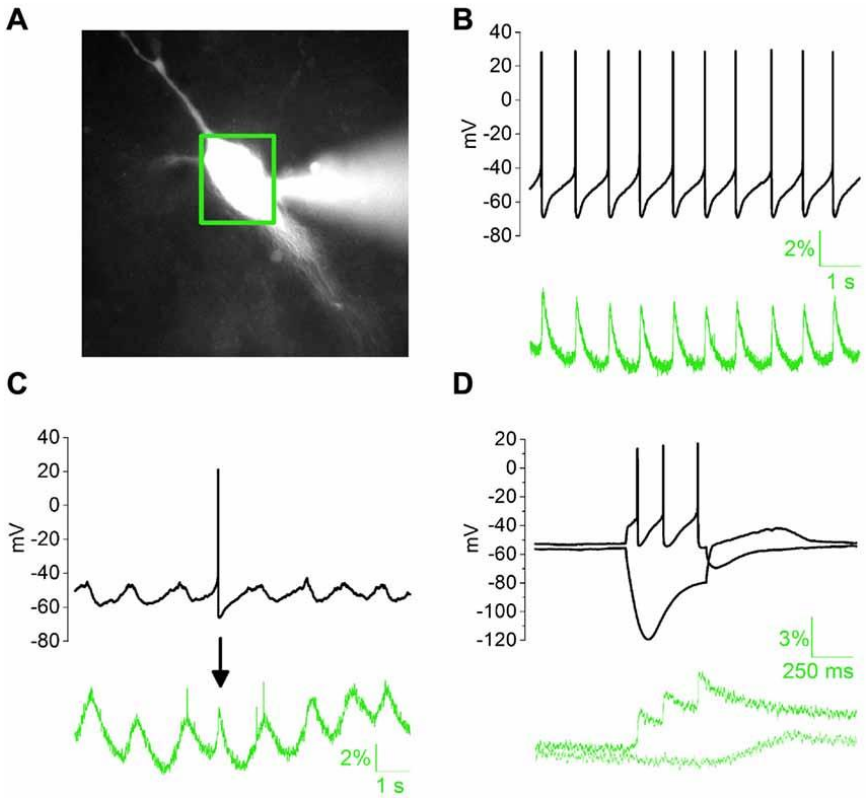

Figure 13: Properties of somatic calcium responses (SCRs) in whole-cell patch clamped DA neurons in acute midbrain slices. (A) SNpc DA neuron loaded with 100 µM Fluo 4 pentapotassium salt with a whole-cell pipette (right-hand side) 5 min after patch rupture. Green box indicates the area selected for optical signal collection. (B) Typical regular spiking (top) is associated with stereotyped, phase-locked SCRs (bottom). (C) Subthreshold oscillatory activity and corresponding slow SCRs. The single action potential (AP)-driven SCR (arrow) in the example trace has faster kinetics but similar amplitude. (D) SCRs elicited by somatic square current injection (-100/+100 pA).

8.2.1. Voltage-Dependent component of evoked EPSP-induced SCRs

Simultaneous recordings of evoked synaptic activity and SCRs were obtained in DA neurons of the SNpc or the VTA in acute horizontal slices prepared from P20 to P30 Wistar rats (Fig 14). The study was restricted to neurons with typical DA morphology and physiological properties (large, polygonal or fusiform cell body, broad AP, Ih ≥ 200 pA). Morphological and electrophysiological properties are good predictors of DA phenotype in the SNpc. In the VTA, DA neurons were selected on the basis of the specified electrophysiological phenotype and their position relative to the medial terminal nucleus of the accessory optic tract (MT; (Neuhoff et al. 2002, Margolis et al. 2006). In addition, because in the VTA standard DA markers are less specific (Margolis et al. 2010), a separate group of DA-like VTA neurons were challenged with the $GABA_B$ agonist baclofen (1 µM). The activation of an outward potassium current following baclofen administration is a good predictor of DA phenotype (Margolis et al. 2012). Eight out of nine neurons showing a

presumed DA phenotype (morphology, Ih ≥ 200 pA) responded to baclofen (Fig 14B) thus confirming the reliability of the selection criteria described above. It has been demonstrated that HCN channels reduce synaptic excitability in many neuronal types by dampening the amplitude and duration of EPSPs (He et al. 2014). Consistently, Ih inactivation enhances dendritic calcium spikes in CA1 pyramidal neurons due to increased EPSP temporal summation and T-/N-Type VGCC recruitment (Tsay et al. 2007). However, it has not been tested whether this phenomenon occurs in midbrain DA neurons, or whether it has any significance in DA pathologies. To address this question, we optimized a stimulation paradigm producing subthreshold EPSPs and simultaneously measured the changes in emission intensity of the high-sensitive, non-ratiometric dye Fluo 4. Stimulation conditions such as frequency, amplitude and duration of stimuli, and baseline potential were adjusted as not to determine plasticity of synaptic responses or irreversible calcium accumulation (Jones and Bonci 2005, Kauer and Malenka 2007, Harnett et al. 2009). Preliminary studies of EPSP-driven calcium signal properties were carried out in SNpc DA neurons. (Fig 14A) shows representative single and multiple EPSPs and associated calcium signals elicited with protocols of increasing duration and frequency, designed to assess the input-output properties of our synaptic stimulation protocol. Single EPSPs (peak amplitude: 4.43 ± 0.53 mV, baseline potential: -62.75 ± 1.06 mV, *n* = 9) failed to elicit measurable SCRs in all neurons tested (Fig 14A left). Ten stimuli at 10 Hz (10 Hz/1 s) produced multiple subthreshold EPSPs (area, 7836 ± 996 mV x ms, *n* = 23) and corresponding SCRs (2.33 ± 0.53%, *n* = 23; (Fig 14A middle). This response was largely below maximal level, as a train with twice the stimulation intensity (20 Hz/2 s) was still able to produce non-saturating SCRs (6.53 ± 1.43%, *n* = 5; (Fig 14A right), although this protocol occasionally caused progressive F_0 rise, likely due to irreversible calcium accumulation. Therefore, the 10 Hz/1 s stimulation protocol was used for all experiments and referred to as ‘‘multiEPSP’’ henceforth throughout text and legends. In SNpc DA neurons, synaptic activation of type-1 metabotropic glutamate receptors (mGlu1) leads to the release of calcium from intracellular stores with an IP3-mediated, Ryanodine-sensitive mechanism (Fiorillo and Williams 2000, Fiorillo and Williams 1998, Morikawa, Khodakhah and Williams 2003). We pharmacologically eliminated this major voltage-independent calcium response by using the mGlu1 selective antagonist CPCOOEt (10 µM). $GABA_{A–B}$ receptor transmission was also blocked with SR95531 (10 µM) and CGP55845 (1 µM) in order to isolate the AMPA/NMDA receptor-mediated component of the multiEPSP and the corresponding SCR. (Fig 13B shows the effect of $GABA_{A–B}$ and mGlu1 receptor blockers (‘‘control solution’’ henceforth) on multiEPSP and SCR Note that abrogation of the slow mGlu1 receptor-dependent hyperpolarization (Fiorillo and Williams 2000) results in the elevation of multiEPSP area and SCR peak as shown in an example recording (Fig 14B, middle). AMPA/NMDA receptor blockers fully abolished both multiEPSP and SCR, suggesting that calcium transients are sustained by activation of NMDA receptors and VGCCs in these experimental conditions (Fig 14B, right). We verified that the 10 Hz/1 s protocol did not elicit

forms of synaptic plasticity by monitoring the amplitude of the first EPSP while stimulating multiEPSP for 10 min in the control solution (Fig 14C). Fig 14D shows the response to baclofen of 8/9 Ih-positive VTA neurons (black traces). Blue traces refer to an Ih-negative VTA neuron which did not respond to baclofen.

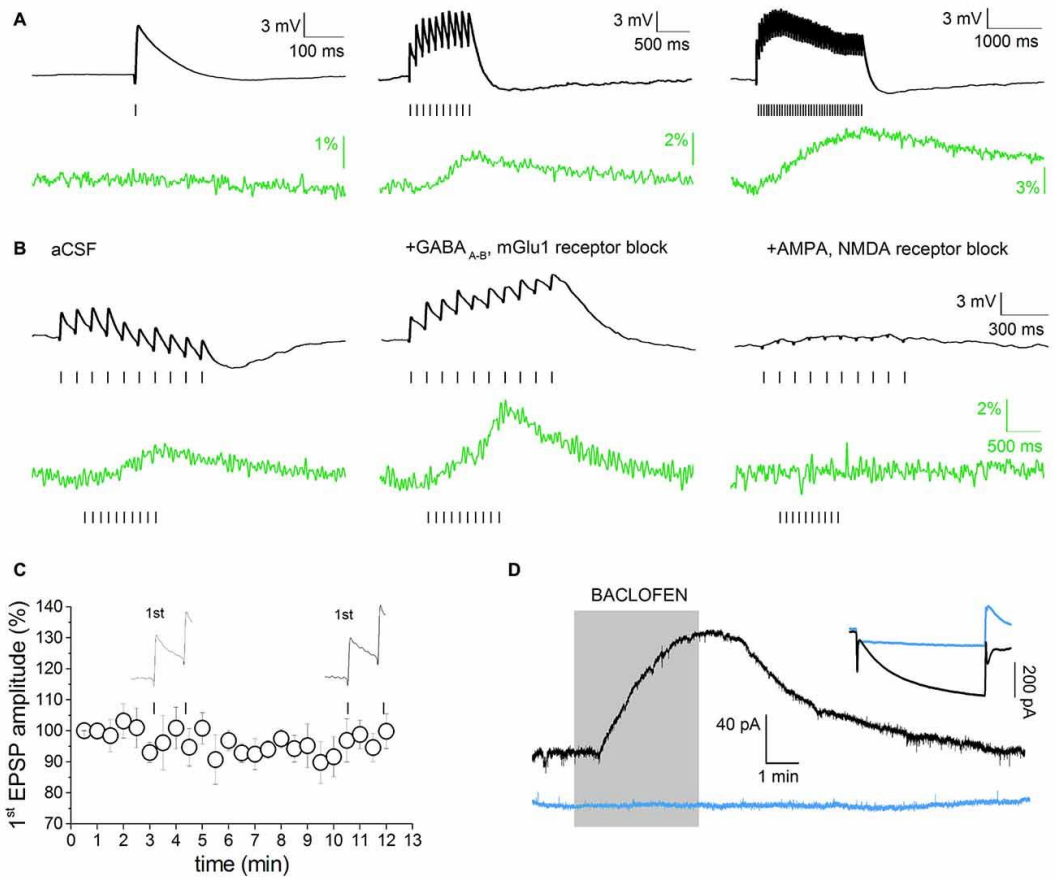

Figure 14: Voltage-dependent component of evoked excitatory post-synaptic potential (EPSP)-induced SCRs. (A) Single or multiple evoked EPSPs (black), in absence of pharmacological isolation, and relative Fluo 4 traces (green). Traces are baseline-adjusted to facilitate comparison. Single EPSPs are not able to elicit detectable SCRs (left). A short EPSP train (10 Hz/1 s) is able to elicit a measurable SCR (middle). Twenty hertz/two seconds stimulation protocols elicit prolonged, slow-decaying, but not saturating, SCRs (right). (B) multiEPSP and relative SCRs recorded before (left) and after superfusion with $GABA_A$, $GABA_B$ and metabotropic glutamate receptors 1 (mGlu1) receptor antagonists (SR95531, 10 µM; CGP55485, 1 µM and CPCCOEt, 1 µM; middle). Subsequent administration of AMPA and NMDA receptor antagonists (NBQX, 10 µM; D-APV, 50 µM) fully abolishes the SCR (right). Note that voltage and optical traces have different time scales. **(C)** The amplitude of first EPSP does not change during 10 min of synaptic stimulation with the 10 Hz/1 s protocol in presence of $GABA_{A–B}$ and mGlu1 antagonists. (D) Characterization of Ih-positive, putative DA neurons in the VTA based on the electrophysiological response to bath application of the $GABA_B$ agonist baclofen (1 µM). The inset shows the whole-cell current in response to a -–95 mV step. Eight/nine neurons showing Ih ≥ 200 pA responded to baclofen. Ih-negative, presumed non-DA neurons do not respond to baclofen (blue traces).

8.2.2. MultiEPSP-Dependent SCRs in SNpc DA neurons are mainly mediated by L-Type calcium channels

We sought to characterize the nature of the calcium rise triggered by multiEPSP in SNpc DA neurons with a pharmacological approach (Fig 15). We did not systematically test the contribution of NMDA receptor activation on SCR because NMDA receptor antagonism negatively affects EPSP kinetics (not shown) and because it was reported that NMDA receptor-mediated calcium transients are modest in the somatodendritic compartment of SNpc DA neurons (Jang et al. 2011). In these neurons, members of the CaV 1 and 2 families have previously been identified as the VGCC pore-forming subunits with activation windows in the subthreshold domain (Chan et al. 2007, Dufour et al. 2014, Poetschke et al. 2015, Philippart et al. 2016), thus most likely involved in calcium inflow associated to subthreshold depolarization episodes such as those triggered by our stimulation protocol. We tested the involvement of T- and L-type VGCCs in multiEPSP-triggered SCRs in SNpc DA neurons by using, respectively, mibefradil (5 µM) and isradipine (5 µM). Mibefradil reduced SCR, but the effect did not reach statistical significance (CTRL, 3.54 ± 1.17%; mibefradil, 2.39 ± 0.75%, $n = 7$, $p = 0.177$). Isradipine, in contrast, caused a near 50%, significant reduction of SCR (CTRL, 2.36 ± 0.48%; isradipine, 1.20 ± 0.24%; $n = 8$, $p = 0.014$). Of note, no alteration of the amplitude or kinetics of the multiEPSP was observed with either blocker (black traces), suggesting a post-synaptic location of drug targets. These results are consistent with the previously mentioned evidence demonstrating the expression of CaV 1.2 and 1.3 L-type calcium channels in the somatodendritic compartment of SNpc DA neurons, and their role at subthreshold potentials.

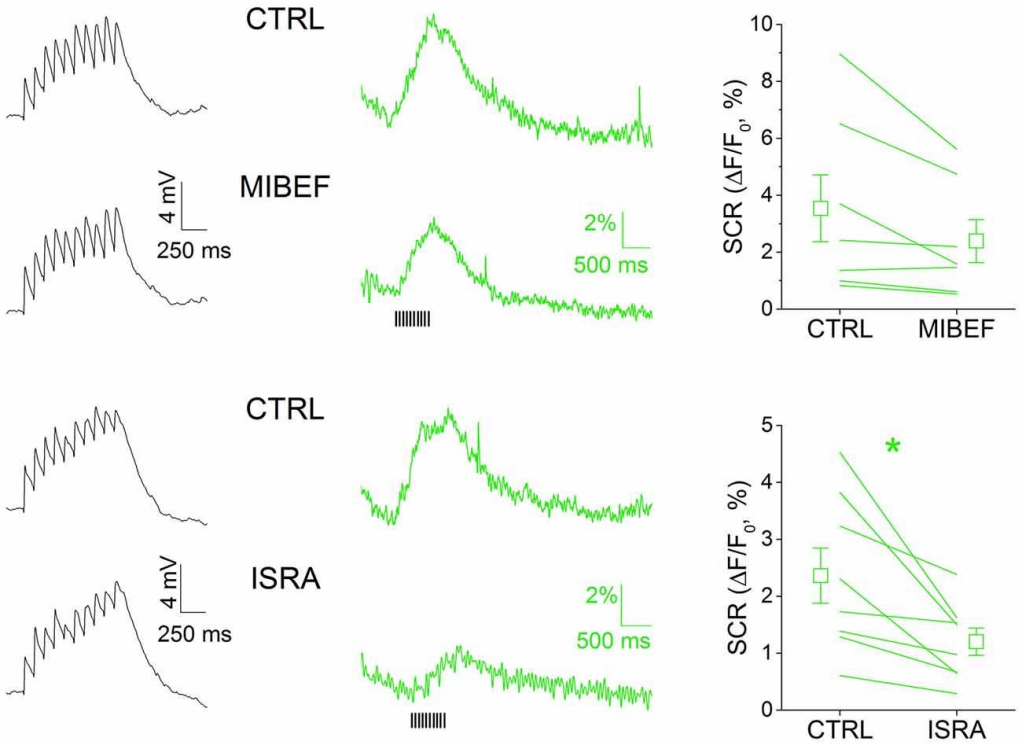

Figure 15 MultiEPSP-dependent SCRs in SNpc DA neurons are mainly mediated by L-type calcium channels. SCRs were tested with the T- and L-type calcium channels' antagonists mibefradil and isradipine (5 µM, each). Both drugs are able to reduce SCRs, but only in the case of isradipine the effect achieved statistical significance. No effect of T- and L-type calcium channels block was seen on multiEPSP (left, black traces).

8.2.3. Ih Block potentiates MultiEPSP and MultiEPSP-dependent SCRs in SNpc DA neurons

The ability of Ih to affect multiEPSP and multiEPSP-driven SCRs was tested using the specific blocker ZD7288 (10 µM, 10 min) in bath application (Fig 15). Prior to drug application, multiEPSP and corresponding SCRs were recorded for 5 min in the control solution to achieve a stable baseline. In SNpc DA neurons (Fig 16A), perfusion with ZD7288 significantly hyperpolarized the neuron (-5.117 ± 0.777 mV; n = 23, p = 1.75 10^{-5}) while increasing multiEPSP temporal summation (CTRL, 2.165 ± 0.374; ZD7288, 3.221 ± 0.688; n = 23, p = 0.0128) and multiEPSP area (CTRL, 7836 ± 996; ZD7288, 14,087 ± 1473; n = 23, p = 1.63 10^{-4}). Of note, multiEPSP-driven SCR increased twofold following HCN block (CTRL, 2.33 ± 0.53%; ZD7288, 4.68 ± 1.32%; n = 23, p = 0.044). In contrast, ZD7288 application did not alter membrane potential (-0.854 ± 1.069 mV, n = 12, p = 0.445), multiEPSP summation (CTRL, 2.819 ± 0.419; ZD7288, 3.648 ± 0.762; n = 12; p = 0.316), and area (CTRL, 7317 ± 675; ZD7288, 8683 ± 1180; n = 12; p = 0.122), or SCR (CTRL, 3.81± 0.85%; ZD7288, 2.94 ± 0.37%, n = 12, p = 0.184) in the VTA. Comparatively, there was no significant difference in mean multiEPSP summation, multiEPSP area

or SCR amplitude between SNpc and VTA DA neurons in control conditions (p = 0.256, p = 0.69 and p = 0.16, respectively; n = 23 and 12, two sample t Test). In presence of ZD7288, the two populations diverged significantly in terms of magnitude of multiEPSP area (SNpc, +110.65 ± 25.68%; VTA, +12.36 ± 13.47%, n = 23 and 12, p = 0.0026, two sample t Test) and SCR (SNpc, +128.25 ± 34.73; VTA,- 3.87± 9.62%, n = 23 and 12, p = 0.0035, two sample t Test), but not of multiEPSP summation (SNpc, 3.222 ± 0.688; VTA, 3.647 ± 0.763, n = 23 and 12, p = 0.682, two sample t Test). Globally, SCR increase was related to multiEPSP area increase by a linear function ($y = a + bx$; a = 0.307; b = 0.835; r = 0.641, $p = 2.35\times10^{-4}$), indicating the strong voltage-dependent nature of SCRs. Overall, these results indicate that Ih inhibition potentiates synaptic excitability and depolarization-dependent somatic calcium entry. Quantitatively, effect magnitude reaches statistical significance only in the SNpc, consistent with the previously reported stronger influence of Ih over synaptic excitability in this subset

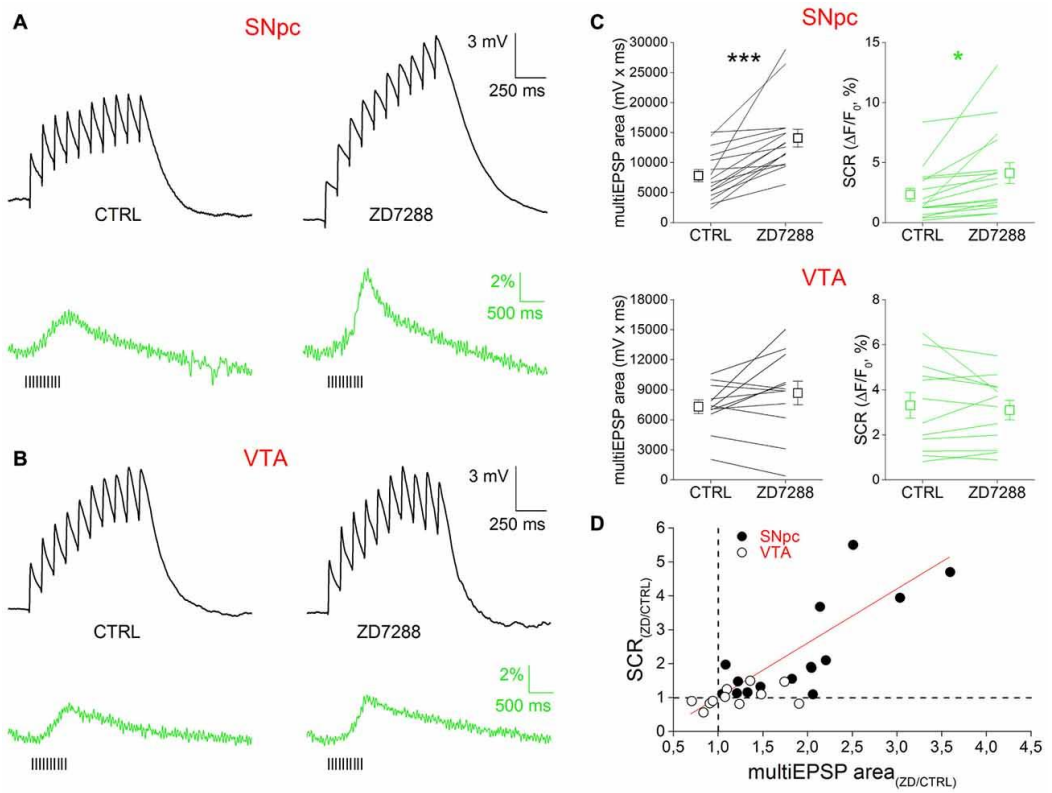

Figure 16: block potentiates multiEPSP and multiEPSP-dependent SCR in SNpc DA neurons. (A) Effect of Ih block in SNpc DA neurons. Example of multiEPSP in presence of $GABA_{A-B}$ and mGluR1 antagonists ("CTRL") and after application of the specific Ih blocker ZD7288 (10 µM, 10 min). The expected membrane hyperpolarization (-5.11 ± 0.77 mV) and multiEPSP area increase (top) is accompanied by potentiation of the SCR (bottom). Voltage traces are baseline-adjusted to facilitate comparison. (B) No hyperpolarization (-0.85 ± 1.07 mV), change in multiEPSP area or SCR peak following Ih blockade in VTA DA neurons. (C) Group data and statistical analysis relative to ZD7288-

induced changes in multiEPSP and SCR in the two areas. (D) SCR and multiEPSP variations caused by ZD7288 have a positive linear correlation.

8.2.4. Ih suppression depresses $GABA_A$ responses in SNpc DA neurons

It has been shown that Ih antagonism reduces the amplitude of $GABA_A$-mediated IPSPs in CA1 pyramidal neurons by hyperpolarizing the membrane potential and thus reducing $GABA_A$ receptor driving force (Pavlov et al. 2011). We tested whether this was also the case in SNpc DA neurons by electrically stimulating GABAergic neurons in the SNr and recording single evoked IPSPs from SNpc DA neurons in presence of glutamatergic synaptic blockers (Fig 17). We found that IPSP amplitude was significantly reduced following bath application of ZD7288 (CTRL,-3.622 ± 0.83; ZD7288,-2.62 ± 0.76, n = 7, p = 0.005). The effect of Ih block on IPSP amplitude depends on the negative shift in membrane potential, as indicated by the recovery of IPSP amplitude obtained by offsetting the ZD7288-induced hyperpolarization. These results indicate that Ih block increases synaptic excitability with a dual mechanism, that is by increasing the response to excitatory inputs and by reducing that to inhibitory inputs.

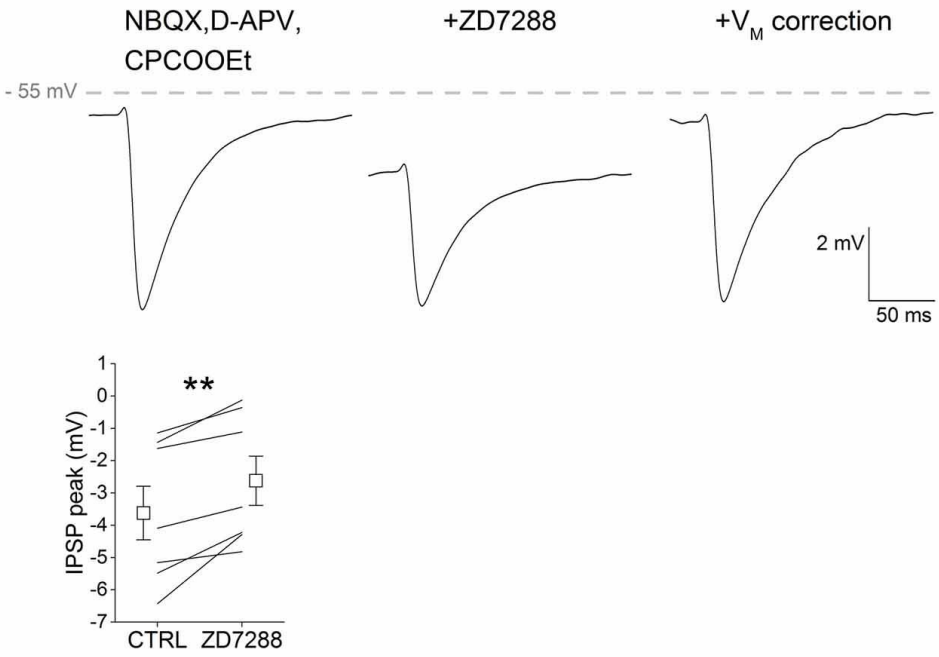

Figure 17: Ih suppression depresses $GABA_A$ responses in SNpc DA neurons. Example of a single, pharmacologically isolated IPSP obtained with extracellular stimulation of the SNr and recorded from a SNpc DA neuron (top). ZD7288 causes membrane hyperpolarization accompanied by a significant reduction of peak amplitude (middle). IPSP amplitude recovers control amplitude when cell membrane is manually held at original potential (right). Bottom, group data and statistical analysis relative to ZD7288-induced change in IPSP amplitude.

8.2.5. Low intracellular ATP causes a negative shift in Ih activation curve

Disruption of mitochondrial homeostasis is increasingly seen as a fundamental pathogenic process involved in both familial and sporadic forms of PD (Schapira and Gegg 2011). Animal models generated by intoxication with mitochondrial poisons, such as MPP^+, or by introduction of DA-targeted mitochondrial defect, as in the case of the MitoPark model, are characterized SNpc-specific DA degeneration (Ekstrand and Galter 2009, Blesa and Przedborski 2014). Both models have been associated to Ih LOF, therefore we asked whether HCN channels in SNpc DA neurons, *in vitro*, respond to block of mitochondrial ATP synthesis and low ATP levels. To this aim, we recorded Ih activation curves using a whole-cell pipette solution containing 0 mM ATP and 10 mM oligomycin, a selective blocker of mitochondrial F_0-F_1 ATP synthase (Fig. 18). Olygomicin causes the block of mitochondrial, but not glycolytic, ATP synthesis, leaving the transmembrane mitochondrial potential unaffected (Nicholls and Budd 2000, Schuchmann et al. 2000). As a control, we used a standard K methanesulfonate-based solution containing 2 mM ATP. Ih activation curves were recorded immediately after patch rupture and 30 min later. Fig 18 shows example traces (left) and activation curves (right) obtained with control (top) and 0 ATP/oligomycin (bottom) pipette solution. No changes in Ih activation curve was observed with control pipette solution ($V_{1/2}$ t_0 = -82.25 ± 0.47 mV; $V_{1/2}$ t_{30} = -82.39 ± 0.73 mV; n = 5, p = 0.269). In contrast, low ATP caused a highly-significant, negative shift in Ih activation curve (t_0, $V_{1/2}$ = -82.85 ± 0.56 mV; t_{30}, $V_{1/2}$ = - 91.48 ± 0.70 mV; n = 7, p = 0.000589). Importantly, the effect occurred in the absence of detectable changes in holding current and membrane resistance. In one case, low ATP solution caused the appearance of an outward current, which was fully reverted by application of 10 µM glybenclamide, a selective K-ATP channel blocker (not shown). The magnitude of the shift in voltage dependence was consistent with the effect exerted by changes in cAMP levels on HCN2 and HCN4 (Biel et al. 2009), the two main Ih pore-forming subunits in SNpc DA neurons (Franz et al. 2000, Dufour et al. 2014), suggesting that impaired cAMP synthesis is the mechanism of action involved here.

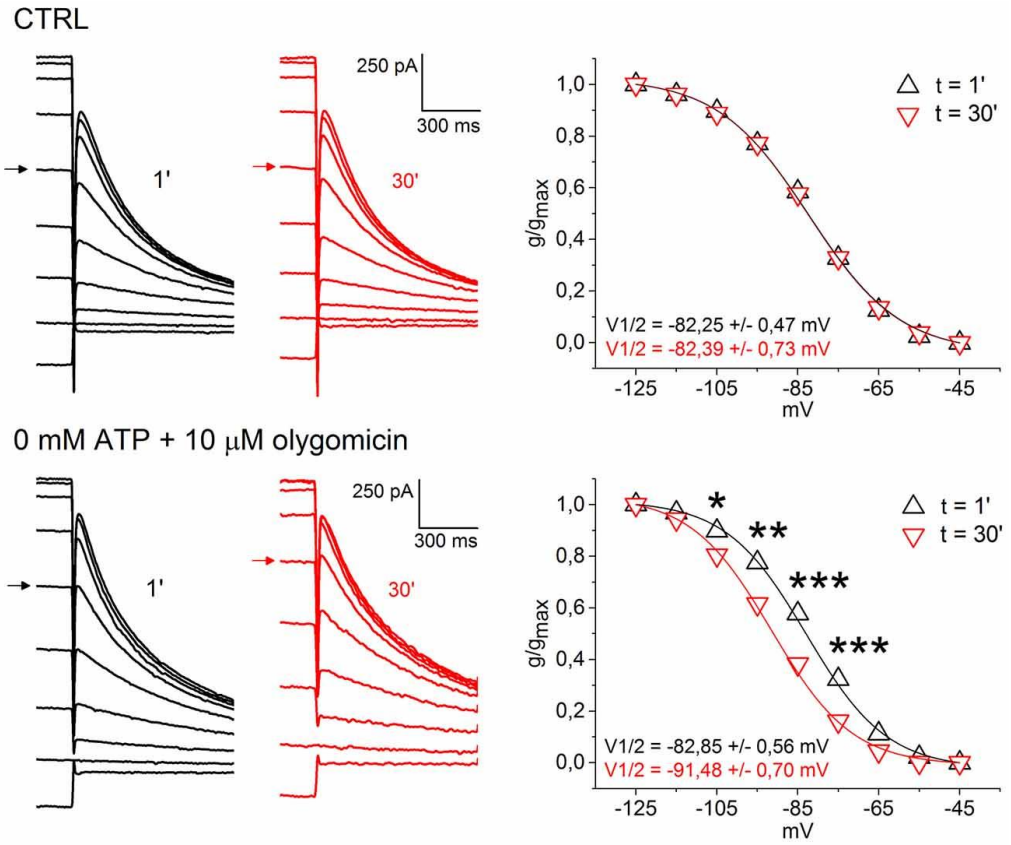

Figure 18: Low intracellular ATP causes a negative shift in Ih activation curve. Top, example of voltage clamp recordings at 1 min (black) and 30 min (red) after patch rupture with control pipette solution. Respective Ih activation curves show perfect overlap (right). Bottom, same experiment, but using a pipette solution with 0 mM ATP and 10 µM oligomycin. Ih activation curve at 30 min is left-shifted by ~9 mV (right). Arrows indicate current traces obtained at the -85 mV test potential to highlight the shift in voltage dependence.

8.2.6. Local Pharmacological Ih suppression causes preferential SNpc DA degeneration and Hemiparkinsonism

We tested the hypothesis that Ih suppression participates in the pathogenic cascade eventually leading to preferential degeneration of nigrostriatal DA neurons. To this aim, we performed intracerebral injections of two distinct Ih blockers following stereotaxic coordinates in adult rats. Injection site was 1 mm above the SNpc-VTA boundary. ZD7288 and Ivabradine (5 µg/µl, 2 µl each) were injected once a day for four consecutive days on one hemisphere, while the contralateral hemisphere was injected with an equal volume of saline. On the fifth day, animals were first tested for spontaneous motility then for the expression of apomorphine-induced rotation behavior, a typical sign of monolateral nigrostriatal degeneration (Hudson et al. 1994). As shown in Fig 19A, ZD7288- or Ivabradine-treated animals did not show changes in spontaneous locomotion compared to controls (ZD7288, 2511 ± 328 cm, n = 8; Ivabradine 2982 ± 303 cm, n = 5; saline 2345± 216 cm, n = 8; one way ANOVA + Newman-Keuls *post hoc* test, $F_{(2,20)} = 1.098$, $p = 0.354$,

for differences among treatments). In contrast, both treatments significantly increased the number of apomorphine-induced rotations (ZD7288, 49 ± 9 turns in 30 min, *n* = 8, Ivabradine, 39 ± 15, *n* = 4, saline, 8 ± 2, *n* = 8, *p* = 0.004, one way ANOVA + Newman-Keuls *post hoc* test, $F._{(2,19)} = 7.671$, *p* < 0.004 for differences among treatments; Fig 19B). Afterwards, DA degeneration was assessed by performing TH immunostaining in coronal sections from the mesencephalon of treated and control animals. As clearly shown by the representative microphotographs (Fig. 19C), the intensity of TH staining is significantly decreased in the SNpc of the drug-injected side compared to saline-injected side (ZD7288, 75.86 ± 4%, n = 8, p = 0.001 vs. control; Ivabradine, 69.51 ± 8.9%, n = 6, p = 0.001 vs. control; Fig. 19D). In contrast, the effect of ZD7288 was much smaller in the VTA, while Ivabradine failed to achieve statistical significance (ZD7288, 86.91± 4%, n = 8, p = 0.01 vs. control; Ivabradine, 94.78 ± 7.9%, n = 6, p = 0.7 vs. control; Fig 19E). Overall, these results suggest that Ih suppression is sufficient to cause degeneration of DA neurons. Furthermore, degeneration is not homogeneous, as SNpc DA neurons are strikingly more sensitive to the effects of Ih suppression compared to VTA DA neurons.

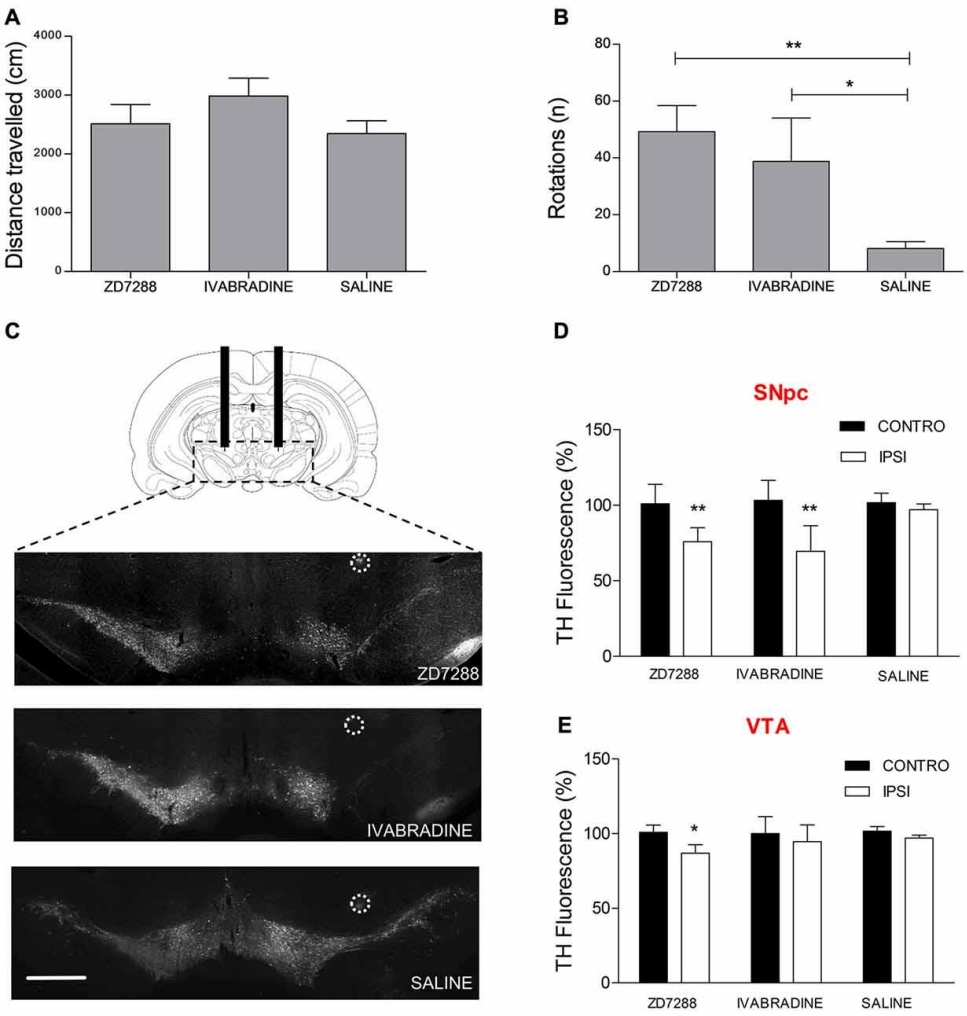

Figure 19 : Local pharmacological Ih suppression causes preferential SNpc DA degeneration and hemiparkinsonism. Spontaneous locomotion **(A)** and apomorphine-induced rotations (B) in rats after repeated monolateral infusions of ZD7288 and Ivabradine (1/day ×4 days). (C) Representative microphotographs showing TH immunofluorescent labeling on midbrain coronal sections. Circles indicate histologically-confirmed injection sites (scale bar = 1 mm). (D,E) Densitometric analysis of ZD7288- and Ivabradine-induced DA degeneration in the SNpc and VTA.

8.3. The anticonvulsant and Ih enhancer Lamotrigine attenuates motor decay in MitoPark mice

In order to investigate the last aim, we tested the hypothesis that pharmacological rescue of HCN LOF may be neuroprotective in PD. To this aim we used The MitoPark mouse, a genetic PD model based on a mitochondrial mutation expressed in DA neurons and featuring HCN LOF at an early disease stage (Ekstrand et al. 2007). Electrophysiological recordings in slices from Mitopark mice at presymptomatic stage (6 weeks) have shown an aberrant activity pattern of SNpc DA neurons, with a concomitant inactivation of the Ih (Good et al. 2011, Branch et al. 2016). We attempted a pharmacological rescue of HCN channels using the anitconvulsant and Ih enhancer LTG (Poolos, Migliore and Johnston 2002) in presymptomatic MitoPark mice (6 weeks). Mitopark mice received daily intraperitoneal injections of LTG (15 mg/kg), or saline, from 6 weeks (presymptomatic stage) to 18 weeks (symptomatic stage) of age. At the end of the treatment, we evaluated locomotion activity using two standar motor tests (Fig 20). The Rotarod test is one of the most widely used tests in mouse models of neurodegeneration as it is very sensitive to motor impairment. The test measures the animal's ability to maintain itself on a rod that spins at growing speed.(Rozas, Guerra and Labandeira-García 1997). The OFT provides a quick assessment of total activity (performance to movement and the distance travelled) and some indication of emotional reactivity to a novel and open environment. The Mitopark mice treated with LTG showed a decrease in the numbers of falls in 3 minutes, that is the index of motor capability for this test (MitoPark saline 51 falls; MitoPark LTG 27 falls; CTRL 7 falls) (Fig 20B). Furthermore we observed reduced decay of locomotor activity in MitoPark mice treated with LTG compared to control littermates, (MitoPark saline 3111.22 cm; MitoPark LTG 3975.64 cm; CTRL 5445.21cm) (Fig 20A).Data were subjected to one-way ANOVA followed by Bonferroni's post hoc test to examine the effect of genotype and LTG treatment. Analysis indicates a significant lower immobility time exposed to OFT and improve the motor capability effects in MitoPark mice treated.

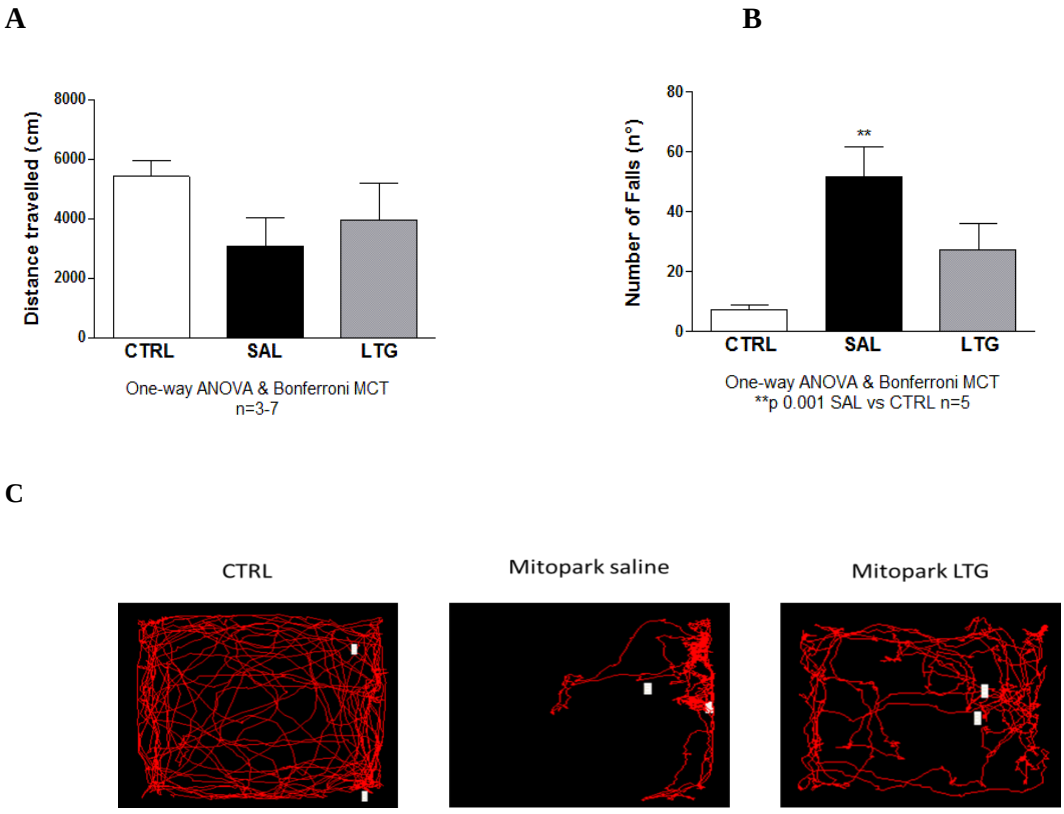

Figure 20: Analysis of spontaneous activity and motor function in 18-week-old MitoPark after treatment with LTG. LTG reduces the decay in locomotor activity of Mitopark mice in terms of distance travelled (fig 20A) during the 10 min time period of the test. Rotarod test demonstrates a significantly lower numbers of falls in the Mitopark treated in comparison to the age-matched littermate during the 3 min time period of the test (fig 20B). Representative movement tracks of mice are shown (Fig 20C). Data represented as the mean ± sem. using one-way ANOVA with Bonferroni post-test comparison and n = 3-7 mice per group (** p <0.001).

9. DISCUSSION

Non-homogeneous degeneration within midbrain DA neurons is a histopathological hallmark of PD. Typically, DA neurons in the SNpc are markedly more vulnerable than in the adjacent VTA (Schapira and Gegg 2011, Brichta and Greengard 2014). Marked differential vulnerability among midbrain DA neurons remains an elusive feature in both of human PD and relative animal models. Experimental and clinical studies suggest that heterogeneous disease-causing factors converge, early on disease progression, in determining a relatively homogeneous pathogenic picture, which includes mitochondrial deficit, increased oxidative stress and impaired protein turnover (Schapira and Gegg 2011). Among the cellular alterations implicated in PD pathogenesis, mitochondrial dysfunction is receiving increasing attention (Schapira and Gegg 2011). Indeed, many PARK loci contain genetic information for proteins involved in the correct mitochondrial maintenance and function. Furthermore, a number of mitochondrial poisons cause experimental parkinsonism in both primates and rodents. MPTP, a blocker of complex I, is extensively used to create animal models of the disease and has provided the initial evidence for the causal link between mitochondrial dysfunction and nigrostriatal degeneration in PD (Blesa and Przedborski 2014). Other molecules capable of antagonizing the mitochondrial complex I were discovered and studied after MPTP (Kotake and Ohta 2003). Many of them are pesticides, and chronic exposure to these molecules dramatically increases the risk of developing PD (Heusinkveld, van den Berg and Westerink 2014). Several transgenic mice have been generated that reproduce human mutations in mitochondria-related PARK loci. Unfortunately, these animals display little or no DA cell loss (Dawson, Ko and Dawson 2010). More recently, a transgenic model was developed which is based on a DA neuron-targeted mutation leading to progressive mitochondrial deficit and cellular degeneration (Ekstrand et al. 2007). This transgenic model, named MitoPark, outperforms all other genetic models in recapitulating the severity and progression of DA loss (Harvey, Wang and Hoffer 2008). This evidence confirms that DA neurons show differential susceptibility, regardless of the nature of the insult (Blesa and Przedborski 2014), implicating that the bases of differential SNpc/VTA vulnerability lie in cell-specific susceptibility factors. Comparative gene expression studies between the two populations have revealed extensive overlap in gene expression signatures, with less than 1-3% of transcripts being differentially represented (Grimm et al. 2004, Greene, Dingledine and Greenamyre 2005). Overall, it is reasonable to suspect that quantitative variations in the expression and/or function of a limited number of cellular factors predispose specific DA neuronal subsets to degeneration (Brichta and Greengard 2014). In this view, some investigators have studied the electrophysiological profile of different DA subsets in search for determinants of differential vulnerability (Neuhoff et al. 2002, Khaliq and Bean 2010). Interestingly, many of the targets implicated in these studies are ion channels with a direct or indirect link to mitochondrial function and ATP production. More specifically, it has been proposed that ATP-gated inward rectifying potassium channels underlie selective SNpc DA degeneration in the MPTP and weaver

mouse models (Liss et al. 2005, Liss et al. 1999a). Likewise, Surmeier and co-workers have shown that CaV 1.3 L-type voltage-gated calcium channels (VGCCs), involved in the generation of SNpc DA autonomous activity, promote chronic metabolic stress and selective nigrostriatal degeneration (Guzman et al. 2009, Surmeier et al. 2010, Ilijic, Guzman and Surmeier 2011). In summary, many reports converge in indicating that intrinsic electrophysiological properties contribute to differential DA vulnerability In this respect, my colleagues have previously demonstrated that MPP^+, the active metabolite of the parkinsonizing toxin MPTP, inhibits Ih at physiological potentials, thus promoting temporal summation of evoked EPSPs in SNpc DA neurons in vitro (Masi et al. 2013). Ih is expressed at different magnitudes among subsets of midbrain DA neurons, thus determining differential subthreshold membrane properties and pacemaking control (Franz et al. 2000, Neuhoff et al. 2002). In the present work, we provide evidence that differential Ih expression between identified DA neurons of the SNpc and VTA underlies differential integrative properties in response to evoked synaptic activity in physiological conditions. Pharmacological suppression of Ih increases EPSP decay time and leads to temporal summation of multiple EPSPs at the somatic level, suggesting that normal Ih function in this context is to promote membrane repolarization after the occurrence of an EPSP, thus enabling the postsynaptic neuron to resolve individual events and limit somatic summation of depolarizing inputs. This phenomenon is quantitatively more evident in SNpc DA neurons, where Ih is expressed by a higher percentage of neurons and at higher levels, than in VTA. Importantly, as both excitatory and inhibitory components of synaptic activity were present during recordings, our findings suggest that the major overall contribution of Ih in the context of synaptic activity is to restrain responsiveness to excitatory inputs. This is consistent with a tonic activation of Ih in these neurons which is able to maintain the membrane potential at relatively depolarized values, thereby limiting the driving force for EPSPs and promoting that for IPSPs. This role of Ih in controlling the balance between excitatory and inhibitory synaptic inputs in midbrain DA neurons is in agreement with previous work in CA1 pyramidal neurons showing that Ih suppression, by hyperpolarizing the cell and increasing the input resistance, elevates the amplitude and duration of EPSPs and reduces the driving force for $GABA_A$-dependent IPSPs (Pavlov et al. 2011). We hypothesize that this discrepancy may represent a physiological background for differential fate in the progression of PD. In the second part of the present work, combining whole-cell patch clamp electrophysiology and microfluorometric calcium measurements in rat brain slices. We demonstrate that Ih not only determines synaptic excitability in DA neurons as we previously showed but also indirectly regulates synaptic-driven, voltage-dependent calcium entry. This function is area-specific, as Ih pharmacological blockade causes significant enhancement of multiEPSP and associated SCR in the SNpc, while neither parameter is significantly affected in the VTA. This is consistent with the differential control exerted by Ih over synaptic excitability between the two areas in TH-GFP mice Of note, functional Ih diversity between SNpc and VTA was quantitative in TH-GFP mice, while it appears to be qualitative in

rats, a discrepancy which presumably results from the species difference. We pharmacologically characterized the source of calcium recruited by multiEPSP in SNpc DA neurons with the L- and T-type VGCCs blockers isradipine and mibefradil. Only isradipine was effective in causing a significant reduction of SCRs. This finding does not allow discrimination between CaV 1.2 and 1.3, as the two pore-forming subunits show comparable affinity for the drug (Zamponi et al. 2015), while the non-significant effect produced by mibefradil indicates a limited contribution of T-type calcium channels to SCRs, in agreement with the relatively hyperpolarized activation window of these channels. The contribution of an NMDA receptor-dependent calcium component to SCRs, although possible in our experiments, was not tested because NDMA receptor blockers alter EPSP kinetics, thus confounding the effect of Ih blockade on dendritic integration. Moreover, it has been shown that NMDA receptor-dependent calcium inflow is relatively modest at proximal dendritic locations, while VGCC-dependent calcium inflow is relatively large, suggesting a limited contribution of the first to SCRs, at least in quantitative terms (Jang et al. 2011). In agreement, another study has reported strong expression of CaV 1.2, 1.3 and CaV 3.1, 3.2, 3.3 pore-forming subunits in the somatodendritic compartment of SNpc DA neurons in rats (Dufour et al. 2014). Our results imply that one physiological function of Ih is to limit synaptic-dependent calcium entry. Ih suppression enhances AMPA/NMDA receptor-mediated response and blunts $GABA_A$ receptor-mediated response, thus increasing synaptic excitability in a dual manner. Moreover, we also show that Ih is functionally regulated by intracellular ATP concentration. Low intracellular ATP, obtained by using a pipette solution containing 0 mM ATP and 10 µM of the F0-F1 ATP synthase blocker oligomycin, causes a ~10 mV negative shift in Ih activation curve. This is compatible with the reported cAMP sensitivity of HCN2 and HCN4 (Biel et al. 2009), the two isoforms sustaining Ih in SNpc DA neurons (Franz et al. 2000, Dufour et al. 2014). As there is no evidence for a direct modulation of HCN channels by ATP, the observed shift in the voltage dependence is likely due to reduced cAMP synthesis. Importantly, this experiment suggests a mechanistic link between ATP levels, Ih-dependent synaptic excitability and calcium dynamics. Moreover, we show that local administration of Ih blockers leads to DA degeneration in adult rats. Like in many established PD models, DA degeneration is most severe in the SNpc, while the VTA appears substantially spared. In view of PD pathogenesis, Ih loss of function may possibly be regarded as an acquired alteration, caused by disruption of mitochondrial metabolism, affecting specifically, or to a larger extent, DA neurons in the SNpc, where Ih is critical in the regulation of synaptic excitability. SNpc DA neurons receive a tonic excitatory input from the STN, which is disinhibited during PD progression as a consequence of striatal dopamine loss. Experimental ablation of this input protects SNpc DA neurons from MPTP and 6-OHDA-induced degeneration (Piallat, Benazzouz and Benabid 1996, Wallace et al. 2007), suggesting the involvement of an excitotoxic pathogenic mechanism in these models. Therefore, it is conceivable that STN disinhibition may add to the excitation/inhibition unbalance caused by Ih loss of function and eventually determine a SNpc-specific pathogenic

pathway involving L-type VGCCs activation. CaV 1.3-mediated dendritic calcium oscillations, characterizing rhythmic activity of SNpc DA neurons, have previously been suggested to determine the vulnerable phenotype of these neurons (Guzman et al. 2009, Ilijic et al. 2011, Surmeier and Schumacker 2013). In agreement, clinical studies and meta-analyses indicate that users of brain-permeable L-type VGCC blockers have a 30% reduced risk of developing PD (Ritz et al. 2010, Lang, Gong and Fan 2015). Our results indicate that L-type calcium channels are activated by normal subthreshold synaptic activity and become hyperactivated in SNpc DA neurons following pharmacological Ih suppression. In vivo, Ih loss of function may result from mitochondrial dysfunction, a key disease mechanism at the basis of extensively studied PD animal models, which is gaining increasing attention in the human pathology too. In this regard, there is increasing evidence linking mitochondrial damage to Ih function. Ih is suppressed by the mitochondrial toxin MPP+ in vitro (Masi et al. 2013) and LTG, a commercial anticonvulsant agent reported to activate Ih (Poolos et al. 2002, Friedman et al. 2014), it is neuroprotective in MPTP-induced DA degeneration models (Archer and Fredriksson 2000, Lagrue et al. 2007). Furthermore, Ih current density is diminished in SNpc DA neurons of MitoPark mice at 6 weeks of age, well before the appearance of neurodegeneration (Good et al. 2011). This evidence supports the proposition that Ih LOF, which may result from mitochondrial failure during PD progression, leads to SNpc-specific DA degeneration through toxic calcium overload. Based on these premises, we tested the hypothesis that Ih LOF is a necessary pathogenic step in relevant PD animal models, and that reversion of this defect is neuroprotective. To test our hypothesis, we used The MitoPark mouse, a model based on a mitochondrial mutation expressed in DA neurons and featuring HCN LOF at an early disease stage (Ekstrand et al. 2007). This model shows late-onset, slow-progressing DA degeneration with differential vulnerability between SNpc and VTA. furthermore, electrophysiological recordings in slices from mice at presymptomatic stage (6 weeks) have shown an aberrant activity pattern of SNc DA neurons, with a concomitant inactivation of the Ih (Branch et al. 2016). In this regard, we performed a pharmacological rescue of HCN channels using LTG in presymptomatic Mitopark mice (6 weeks). LTG, a voltage-gated sodium and calcium channel blocker, used in clinic as a anticonvulsivant, was reported to potentiate Ih (Poolos et al. 2002). LTG has already been used to functionally upregulate HCN function in DA neurons in vivo (Friedman et al. 2014). Based on the above hypothesis, we attempted a pharmacological rescue of Ih function by administering chronic LTG. LTG was administered daily starting from 6 weeks (presymptomatic stage), when Ih LOF has been described, until 18 weeks (the beginning of the symptomatic stage). What we observed is a dramatic reduction of motor decay compared to MitoPark mice treated with vehicle. Pharmacological manipulation of Ih function in vivo suggests a possible link to DA vulnerability during disease progression. MitoPark mice has better face and construct validity compared with major toxin-induced models, the rat 6-OHDA model and the mouse MPTP-model (Terzioglu and Galter 2008). Indeed, MitoPark mice display a very slow progression of the

symptoms, more similarly reflecting the disease progression in PD patients vs. the acute ablation of the DA system manifested in most lesion models. In addition, the slow progression of symptoms in MitoPark mice offers the opportunity to study the effects of chronic treatments for prolonged periods of time (i.e. several months) under conditions of a slow and gradual aggravation of symptoms in line with the situation in PD patients (Galter et al. 2010). Our findings indicate that:

1) HCN loss of function, when pharmacologically induced in healthy animals, is able to drive SNpc-specific DA neurodegeneration;

2) Pharmacological HCN rescue protects from motor decay in a slow-progressing PD model.

This mechanism may be exploited to design a neuroprotective, disease-modifying strategy for the treatment of early-stage PD patients. Unfortunately, no specific pharmacological HCN enhancers are available at present. Furthermore, HCN channels are widely expressed in the central and peripheral nervous system, as well as in the heart, therefore, they are far from being optimal disease-specific targets. However, lack of tissue and disease-specificity could be, in principle, overcome by using a viral delivery approach. This would imply performing bilateral stereotaxic injections of recombinant HCN-carrying viral particles in the substantia nigra of patients with an early diagnosis of PD, when a substantial proportion of nigrostriatal DA neurons are still viable. Brain surgery is already used, as a last resort, for the implantation of electrodes for deep brain stimulation in those patients who have developed levodopa-induced diskynesia, and viral particles are already safely used to achieve gene therapy in certain diseases, such as inherited retinal disease now treated with an adeno-associated viral vector carrying a wild type allele of the mutated gene voretigene neparvovec-rzyl (LUXTURNA) Considering the total lack of neuroprotective medications in PD therapy, and in consideration of the serious side effects associated with long-term levodopa therapy, even an invasive therapeutic approach such as brain surgery could be considered a valid option by a patient otherwise facing the invalidating motor decay resulting from the side effects and the lack of neuroprotective efficacy of existing medications.

10. LIST OF ABBREVIATIONS

ALS	Amyotrophic Lateral Sclerosis
4-AP	4-Aminopyridine
ATP	Adenosine-5'-triphospate
BBB	Blood-brain barrier
cAMP	Cyclic adenosine monophosphate
CN	caudate nucleus
CNBD	Cyclic nucleotide binding domain
CNS	Central nervous system
CSD	cAMP-sensing domanin
D_1R	dopamine 1-type receptor
D_2R	dopamine 2-type receptor
DA	dopamine
DAT	dopamine transporter
EC	Enthorhinal cortex
EPSC	Excitatory postsynaptic current
EPSCs	Excitatory postsynaptic potentials
GABA	γ-aminobutyric acid
GFP	Green fluorescent protein
GP	Globus pallidus
GPe	Globus pallidus externus
GPi	Globus pallidus internus
HCN	Hyperpolarization-activated cyclic nucleotide-gated channel
HD	Huntington disease
IMM	inner mitochondrial membrane
IPSCs	Inhibitory postsynaptic currents
LBs	Lewi's bodies
LTG	Lamotrigine

MAO-A	Monoamine oxidase A
MAO-B	Monoamine oxidase B
$MPDP^+$	1-methyl-4-phenyl-2,3-dihydropyridinium
MPP^+	1-methyl-4-phenylpyridinium
MPTP	n-methyl-4-phenyl-1,2,3,6-tetrahydropyridine
MSNs	Medium spiny neurons
NAc	accumbens nucleus
NMDA	N-methyl-D-aspartate
NOS	nitric oxide synthase
OCT3	organic cation transporter 3
OFT	open field test
PD	Parkinson's disease
PPR	Paired pulse ratio
RMP	Resting membrane potential
ROS	Reactive oxygen species
SCR	Somatic calcium responses
SN	Substancia nigra
SNpc	Substancia nigra pars compacta
SNr	Substancia nigra pars reticulate
SOD2	Superoxide dismutase-2
STN	Subthalamic nucleus
TH	Tyrosine hydroxalse
VGCCs	voltage-gated calcium channels
VMAT	Vescicular monoamine transporter
VMAT1	Vescicular monoamine transporter 1
VMAT2	Vescicular monoamine transporter 2
VTA	Ventral tegmantal area
K-ATP	ATP-sensitive potassium channel

BIBLIOGRAPHY

Albin, R. L. & J. T. Greenamyre (1992) Alternative excitotoxic hypotheses. *Neurology,* 42**,** 733-8.

Alexander, G. E., M. D. Crutcher & M. R. DeLong (1990) Basal ganglia-thalamocortical circuits: parallel substrates for motor, oculomotor, "prefrontal" and "limbic" functions. *Prog Brain Res,* 85**,** 119-46.

Alexianu, M. E., B. K. Ho, A. H. Mohamed, V. La Bella, R. G. Smith & S. H. Appel (1994) The role of calcium-binding proteins in selective motoneuron vulnerability in amyotrophic lateral sclerosis. *Ann Neurol,* 36**,** 846-58.

Alonso, A. & R. R. Llinás (1989) Subthreshold Na+-dependent theta-like rhythmicity in stellate cells of entorhinal cortex layer II. *Nature,* 342**,** 175-7.

Altomare, C., A. Bucchi, E. Camatini, M. Baruscotti, C. Viscomi, A. Moroni & D. DiFrancesco (2001) Integrated allosteric model of voltage gating of HCN channels. *J Gen Physiol,* 117**,** 519-32.

Amo, T., S. Saiki, T. Sawayama, S. Sato & N. Hattori (2014) Detailed analysis of mitochondrial respiratory chain defects caused by loss of PINK1. *Neurosci Lett,* 580**,** 37-40.

Archer, T. & A. Fredriksson (2000) Restoration and putative protection in Parkinsonism. *Neurotox Res,* 2**,** 251-92.

Ares-Santos, S., N. Granado, I. Espadas, R. Martinez-Murillo & R. Moratalla (2014) Methamphetamine causes degeneration of dopamine cell bodies and terminals of the nigrostriatal pathway evidenced by silver staining. *Neuropsychopharmacology,* 39**,** 1066-80.

Arnsten, A. F. & L. E. Jin (2014) Molecular influences on working memory circuits in dorsolateral prefrontal cortex. *Prog Mol Biol Transl Sci,* 122**,** 211-31.

Asanuma, M., I. Miyazaki & N. Ogawa (2003) Dopamine- or L-DOPA-induced neurotoxicity: the role of dopamine quinone formation and tyrosinase in a model of Parkinson's disease. *Neurotox Res,* 5**,** 165-76.

Ashcroft, F. & P. Rorsman (2004) Type 2 diabetes mellitus: not quite exciting enough? *Hum Mol Genet,* 13 Spec No 1**,** R21-31.

Attwell, D. & M. Wilson (1980) Behaviour of the rod network in the tiger salamander retina mediated by membrane properties of individual rods. *J Physiol,* 309**,** 287-315.

Avshalumov, M. V., B. T. Chen, T. Koós, J. M. Tepper & M. E. Rice (2005) Endogenous hydrogen peroxide regulates the excitability of midbrain dopamine neurons via ATP-sensitive potassium channels. *J Neurosci,* 25**,** 4222-31.

Bader, A. G., S. Kang, L. Zhao & P. K. Vogt (2005) Oncogenic PI3K deregulates transcription and translation. *Nat Rev Cancer,* 5**,** 921-9.

Bader, C. R. & D. Bertrand (1984) Effect of changes in intra- and extracellular sodium on the inward (anomalous) rectification in salamander photoreceptors. *J Physiol,* 347**,** 611-31.

Banks, M. I., R. A. Pearce & P. H. Smith (1993) Hyperpolarization-activated cation current (Ih) in neurons of the medial nucleus of the trapezoid body: voltage-clamp analysis and enhancement by norepinephrine and cAMP suggest a modulatory mechanism in the auditory brain stem. *J Neurophysiol,* 70**,** 1420-32.

Barcia, C., A. Fernández Barreiro, M. Poza & M. T. Herrero (2003) Parkinson's disease and inflammatory changes. *Neurotox Res,* 5**,** 411-8.

Barreto, G. E., A. Iarkov & V. E. Moran (2014) Beneficial effects of nicotine, cotinine and its metabolites as potential agents for Parkinson's disease. *Front Aging Neurosci,* 6**,** 340.

Baruscotti, M., A. Bucchi & D. Difrancesco (2005) Physiology and pharmacology of the cardiac pacemaker ("funny") current. *Pharmacol Ther,* 107**,** 59-79.

Bean, B. P. (2007) The action potential in mammalian central neurons. *Nat Rev Neurosci,* 8**,** 451-65.

Beckman, K. B. & B. N. Ames (1998) The free radical theory of aging matures. *Physiol Rev,* 78**,** 547-81.

Belin, D., A. Belin-Rauscent, J. E. Murray & B. J. Everitt (2013) Addiction: failure of control over maladaptive incentive habits. *Curr Opin Neurobiol,* 23**,** 564-72.

Belluzzi, E., M. Bisaglia, E. Lazzarini, L. C. Tabares, M. Beltramini & L. Bubacco (2012) Human SOD2 modification by dopamine quinones affects enzymatic activity by promoting its aggregation: possible implications for Parkinson's disease. *PLoS One,* 7**,** e38026.

Benarroch, E. E. (2013) HCN channels: function and clinical implications. *Neurology,* 80**,** 304-10.

Bender, R. A., A. Brewster, B. Santoro, A. Ludwig, F. Hofmann, M. Biel & T. Z. Baram (2001) Differential and age-dependent expression of hyperpolarization-activated, cyclic nucleotide-gated cation channel isoforms 1-4 suggests evolving roles in the developing rat hippocampus. *Neuroscience,* 106**,** 689-98.

Berardelli, A., J. C. Rothwell, P. D. Thompson & M. Hallett (2001) Pathophysiology of bradykinesia in Parkinson's disease. *Brain,* 124**,** 2131-46.

Berger, T., W. Senn & H. R. Lüscher (2003) Hyperpolarization-activated current Ih disconnects somatic and dendritic spike initiation zones in layer V pyramidal neurons. *J Neurophysiol,* 90**,** 2428-37.

Berman, S. B. & T. G. Hastings (1999) Dopamine oxidation alters mitochondrial respiration and induces permeability transition in brain mitochondria: implications for Parkinson's disease. *J Neurochem,* 73**,** 1127-37.

Bernheimer, H., W. Birkmayer, O. Hornykiewicz, K. Jellinger & F. Seitelberger (1973) Brain dopamine and the syndromes of Parkinson and Huntington. Clinical, morphological and neurochemical correlations. *J Neurol Sci,* 20**,** 415-55.

Betarbet, R., R. M. Canet-Aviles, T. B. Sherer, P. G. Mastroberardino, C. McLendon, J. H. Kim, S. Lund, H. M. Na, G. Taylor, N. F. Bence, R. Kopito, B. B. Seo, T. Yagi, A. Yagi, G. Klinefelter, M. R. Cookson & J. T. Greenamyre (2006) Intersecting pathways to neurodegeneration in Parkinson's disease: effects of the pesticide rotenone on DJ-1, alpha-synuclein, and the ubiquitin-proteasome system. *Neurobiol Dis,* 22**,** 404-20.

Betarbet, R., T. B. Sherer, G. MacKenzie, M. Garcia-Osuna, A. V. Panov & J. T. Greenamyre (2000) Chronic systemic pesticide exposure reproduces features of Parkinson's disease. *Nat Neurosci,* 3**,** 1301-6.

Bian, M., J. Liu, X. Hong, M. Yu, Y. Huang, Z. Sheng, J. Fei & F. Huang (2012) Overexpression of parkin ameliorates dopaminergic neurodegeneration induced by 1- methyl-4-phenyl-1,2,3,6-tetrahydropyridine in mice. *PLoS One,* 7**,** e39953.

Biel, M., C. Wahl-Schott, S. Michalakis & X. Zong (2009) Hyperpolarization-activated cation channels: from genes to function. *Physiol Rev,* 89**,** 847-85.

Björklund, A. & S. B. Dunnett (2007) Dopamine neuron systems in the brain: an update. *Trends Neurosci,* 30**,** 194-202.

Blesa, J., S. Phani, V. Jackson-Lewis & S. Przedborski (2012) Classic and new animal models of Parkinson's disease. *J Biomed Biotechnol,* 2012**,** 845618.

Blesa, J. & S. Przedborski (2014) Parkinson's disease: animal models and dopaminergic cell vulnerability. *Front Neuroanat,* 8**,** 155.

Bloem, B. R., J. M. Hausdorff, J. E. Visser & N. Giladi (2004) Falls and freezing of gait in Parkinson's disease: a review of two interconnected, episodic phenomena. *Mov Disord,* 19**,** 871-84.

Boghen, D. (1997) Apraxia of lid opening: a review. *Neurology,* 48**,** 1491-4.

Boillée, S., K. Yamanaka, C. S. Lobsiger, N. G. Copeland, N. A. Jenkins, G. Kassiotis, G. Kollias & D. W. Cleveland (2006) Onset and progression in inherited ALS determined by motor neurons and microglia. *Science,* 312**,** 1389-92.

Borel, M., S. Guadagna, H. J. Jang, J. Kwag & O. Paulsen (2013) Frequency dependence of CA3 spike phase response arising from h-current properties. *Front Cell Neurosci,* 7**,** 263.

Braak, H., K. Del Tredici, U. Rüb, R. A. de Vos, E. N. Jansen Steur & E. Braak (2003) Staging of brain pathology related to sporadic Parkinson's disease. *Neurobiol Aging,* 24**,** 197-211.

Branch, S. Y., C. Chen, R. Sharma, J. D. Lechleiter, S. Li & M. J. Beckstead (2016) Dopaminergic Neurons Exhibit an Age-Dependent Decline in Electrophysiological Parameters in the MitoPark Mouse Model of Parkinson's Disease. *J Neurosci,* 36**,** 4026-37.

Brichta, L. & P. Greengard (2014) Molecular determinants of selective dopaminergic vulnerability in Parkinson's disease: an update. *Front Neuroanat,* 8**,** 152.

Brichta, L., P. Greengard & M. Flajolet (2013) Advances in the pharmacological treatment of Parkinson's disease: targeting neurotransmitter systems. *Trends Neurosci,* 36**,** 543-54.
Brown, H. F., D. DiFrancesco & S. J. Noble (1979) How does adrenaline accelerate the heart? *Nature,* 280**,** 235-6.
Bucchi, A., M. Baruscotti, M. Nardini, A. Barbuti, S. Micheloni, M. Bolognesi & D. DiFrancesco (2013) Identification of the molecular site of ivabradine binding to HCN4 channels. *PLoS One,* 8**,** e53132.
Bussell, R. & D. Eliezer (2001) Residual structure and dynamics in Parkinson's disease-associated mutants of alpha-synuclein. *J Biol Chem,* 276**,** 45996-6003.
Bédard, C., H. Kröger & A. Destexhe (2006) Model of low-pass filtering of local field potentials in brain tissue. *Phys Rev E Stat Nonlin Soft Matter Phys,* 73**,** 051911.
Caudle, W. M., J. R. Richardson, M. Z. Wang, T. N. Taylor, T. S. Guillot, A. L. McCormack, R. E. Colebrooke, D. A. Di Monte, P. C. Emson & G. W. Miller (2007) Reduced vesicular storage of dopamine causes progressive nigrostriatal neurodegeneration. *J Neurosci,* 27**,** 8138-48.
Chan, C. S., J. N. Guzman, E. Ilijic, J. N. Mercer, C. Rick, T. Tkatch, G. E. Meredith & D. J. Surmeier (2007) 'Rejuvenation' protects neurons in mouse models of Parkinson's disease. *Nature,* 447**,** 1081-6.
Chaplan, S. R., H. Q. Guo, D. H. Lee, L. Luo, C. Liu, C. Kuei, A. A. Velumian, M. P. Butler, S. M. Brown & A. E. Dubin (2003) Neuronal hyperpolarization-activated pacemaker channels drive neuropathic pain. *J Neurosci,* 23**,** 1169-78.
Chaudhury, D., J. J. Walsh, A. K. Friedman, B. Juarez, S. M. Ku, J. W. Koo, D. Ferguson, H. C. Tsai, L. Pomeranz, D. J. Christoffel, A. R. Nectow, M. Ekstrand, A. Domingos, M. S. Mazei-Robison, E. Mouzon, M. K. Lobo, R. L. Neve, J. M. Friedman, S. J. Russo, K. Deisseroth, E. J. Nestler & M. H. Han (2013) Rapid regulation of depression-related behaviours by control of midbrain dopamine neurons. *Nature,* 493**,** 532-6.
Chen, C. (1997) Hyperpolarization-activated current (Ih) in primary auditory neurons. *Hear Res,* 110**,** 179-90.
Chen, X., J. E. Sirois, Q. Lei, E. M. Talley, C. Lynch & D. A. Bayliss (2005) HCN subunit-specific and cAMP-modulated effects of anesthetics on neuronal pacemaker currents. *J Neurosci,* 25**,** 5803-14.
Choi, P. J., L. Cai, K. Frieda & X. S. Xie (2008) A stochastic single-molecule event triggers phenotype switching of a bacterial cell. *Science,* 322**,** 442-6.
Clark, I. E., M. W. Dodson, C. Jiang, J. H. Cao, J. R. Huh, J. H. Seol, S. J. Yoo, B. A. Hay & M. Guo (2006) Drosophila pink1 is required for mitochondrial function and interacts genetically with parkin. *Nature,* 441**,** 1162-6.
Cochemé, H. M. & M. P. Murphy (2008) Complex I is the major site of mitochondrial superoxide production by paraquat. *J Biol Chem,* 283**,** 1786-98.
Cohen, G. (1984) Oxy-radical toxicity in catecholamine neurons. *Neurotoxicology,* 5**,** 77-82.
--- (2000) Oxidative stress, mitochondrial respiration, and Parkinson's disease. *Ann N Y Acad Sci,* 899**,** 112-20.
Cook, C., C. Stetler & L. Petrucelli (2012) Disruption of protein quality control in Parkinson's disease. *Cold Spring Harb Perspect Med,* 2**,** a009423.
Craven, K. B. & W. N. Zagotta (2006) CNG and HCN channels: two peas, one pod. *Annu Rev Physiol,* 68**,** 375-401.
Cristóvão, A. C., S. Guhathakurta, E. Bok, G. Je, S. D. Yoo, D. H. Choi & Y. S. Kim (2012) NADPH oxidase 1 mediates α-synucleinopathy in Parkinson's disease. *J Neurosci,* 32**,** 14465-77.
Crocker, S. J., P. D. Smith, V. Jackson-Lewis, W. R. Lamba, S. P. Hayley, E. Grimm, S. M. Callaghan, R. S. Slack, E. Melloni, S. Przedborski, G. S. Robertson, H. Anisman, Z. Merali & D. S. Park (2003) Inhibition of calpains prevents neuronal and behavioral deficits in an MPTP mouse model of Parkinson's disease. *J Neurosci,* 23**,** 4081-91.
Cui, G., B. E. Bernier, M. T. Harnett & H. Morikawa (2007) Differential regulation of action potential- and metabotropic glutamate receptor-induced Ca2+ signals by inositol 1,4,5-trisphosphate in dopaminergic neurons. *J Neurosci,* 27**,** 4776-85.

Cummings, C. J., E. Reinstein, Y. Sun, B. Antalffy, Y. Jiang, A. Ciechanover, H. T. Orr, A. L. Beaudet & H. Y. Zoghbi (1999) Mutation of the E6-AP ubiquitin ligase reduces nuclear inclusion frequency while accelerating polyglutamine-induced pathology in SCA1 mice. *Neuron,* 24**,** 879-92.

Cummings, C. J., Y. Sun, P. Opal, B. Antalffy, R. Mestril, H. T. Orr, W. H. Dillmann & H. Y. Zoghbi (2001) Over-expression of inducible HSP70 chaperone suppresses neuropathology and improves motor function in SCA1 mice. *Hum Mol Genet,* 10**,** 1511-8.

da Silva, F. L., E. Coelho Cerqueira, M. S. de Freitas, D. L. Gonçalves, L. T. Costa & C. Follmer (2013) Vitamins K interact with N-terminus α-synuclein and modulate the protein fibrillization in vitro. Exploring the interaction between quinones and α-synuclein. *Neurochem Int,* 62**,** 103-12.

Damier, P., E. C. Hirsch, Y. Agid & A. M. Graybiel (1999) The substantia nigra of the human brain. II. Patterns of loss of dopamine-containing neurons in Parkinson's disease. *Brain,* 122 (Pt 8)**,** 1437-48.

Dauer, W. & S. Przedborski (2003) Parkinson's disease: mechanisms and models. *Neuron,* 39**,** 889-909.

Davis, G. W. (2006) Homeostatic control of neural activity: from phenomenology to molecular design. *Annu Rev Neurosci,* 29**,** 307-23.

Dawson, T. M., H. S. Ko & V. L. Dawson (2010) Genetic animal models of Parkinson's disease. *Neuron,* 66**,** 646-61.

Dawson, V. L. & T. M. Dawson (1996) Nitric oxide neurotoxicity. *J Chem Neuroanat,* 10**,** 179-90.

Devi, L., V. Raghavendran, B. M. Prabhu, N. G. Avadhani & H. K. Anandatheerthavarada (2008) Mitochondrial import and accumulation of alpha-synuclein impair complex I in human dopaminergic neuronal cultures and Parkinson disease brain. *J Biol Chem,* 283**,** 9089-100.

DiFrancesco, D. (1991) The contribution of the 'pacemaker' current (if) to generation of spontaneous activity in rabbit sino-atrial node myocytes. *J Physiol,* 434**,** 23-40.

--- (1993) Pacemaker mechanisms in cardiac tissue. *Annu Rev Physiol,* 55**,** 455-72.

--- (1999) Dual allosteric modulation of pacemaker (f) channels by cAMP and voltage in rabbit SA node. *J Physiol,* 515 (Pt 2)**,** 367-76.

DiFrancesco, D. & P. Tortora (1991) Direct activation of cardiac pacemaker channels by intracellular cyclic AMP. *Nature,* 351**,** 145-7.

DiFrancesco, D. & C. Tromba (1988) Inhibition of the hyperpolarization-activated current (if) induced by acetylcholine in rabbit sino-atrial node myocytes. *J Physiol,* 405**,** 477-91.

Doan, T. N., K. Stephans, A. N. Ramirez, P. A. Glazebrook, M. C. Andresen & D. L. Kunze (2004) Differential distribution and function of hyperpolarization-activated channels in sensory neurons and mechanosensitive fibers. *J Neurosci,* 24**,** 3335-43.

Duan, W., X. Zhu, B. Ladenheim, Q. S. Yu, Z. Guo, J. Oyler, R. G. Cutler, J. L. Cadet, N. H. Greig & M. P. Mattson (2002) p53 inhibitors preserve dopamine neurons and motor function in experimental parkinsonism. *Ann Neurol,* 52**,** 597-606.

Duda, J., C. Pötschke & B. Liss (2016) Converging roles of ion channels, calcium, metabolic stress, and activity pattern of Substantia nigra dopaminergic neurons in health and Parkinson's disease. *J Neurochem,* 139 Suppl 1**,** 156-178.

Dufour, M. A., A. Woodhouse & J. M. Goaillard (2014) Somatodendritic ion channel expression in substantia nigra pars compacta dopaminergic neurons across postnatal development. *J Neurosci Res,* 92**,** 981-99.

Dykens, J. A. (1994) Isolated cerebral and cerebellar mitochondria produce free radicals when exposed to elevated CA2+ and Na+: implications for neurodegeneration. *J Neurochem,* 63**,** 584-91.

Edman, A., S. Gestrelius & W. Grampp (1987) Current activation by membrane hyperpolarization in the slowly adapting lobster stretch receptor neurone. *J Physiol,* 384**,** 671-90.

Ekstrand, M. I. & D. Galter (2009) The MitoPark Mouse - an animal model of Parkinson's disease with impaired respiratory chain function in dopamine neurons. *Parkinsonism Relat Disord,* 15 Suppl 3**,** S185-8.

Ekstrand, M. I., M. Terzioglu, D. Galter, S. Zhu, C. Hofstetter, E. Lindqvist, S. Thams, A. Bergstrand, F. S. Hansson, A. Trifunovic, B. Hoffer, S. Cullheim, A. H. Mohammed, L.

Olson & N. G. Larsson (2007) Progressive parkinsonism in mice with respiratory-chain-deficient dopamine neurons. *Proc Natl Acad Sci U S A,* 104**,** 1325-30.
Emery, E. C., G. T. Young & P. A. McNaughton (2012) HCN2 ion channels: an emerging role as the pacemakers of pain. *Trends Pharmacol Sci,* 33**,** 456-63.
Engel, D. & V. Seutin (2015) High dendritic expression of Ih in the proximity of the axon origin controls the integrative properties of nigral dopamine neurons. *J Physiol,* 593**,** 4905-22.
Erickson, K. R., O. K. Ronnekleiv & M. J. Kelly (1993) Electrophysiology of guinea-pig supraoptic neurones: role of a hyperpolarization-activated cation current in phasic firing. *J Physiol,* 460**,** 407-25.
Esteves, A. R., D. M. Arduíno, R. H. Swerdlow, C. R. Oliveira & S. M. Cardoso (2010) Dysfunctional mitochondria uphold calpain activation: contribution to Parkinson's disease pathology. *Neurobiol Dis,* 37**,** 723-30.
Exner, N., A. K. Lutz, C. Haass & K. F. Winklhofer (2012) Mitochondrial dysfunction in Parkinson's disease: molecular mechanisms and pathophysiological consequences. *EMBO J,* 31**,** 3038-62.
Exner, N., B. Treske, D. Paquet, K. Holmström, C. Schiesling, S. Gispert, I. Carballo-Carbajal, D. Berg, H. H. Hoepken, T. Gasser, R. Krüger, K. F. Winklhofer, F. Vogel, A. S. Reichert, G. Auburger, P. J. Kahle, B. Schmid & C. Haass (2007) Loss-of-function of human PINK1 results in mitochondrial pathology and can be rescued by parkin. *J Neurosci,* 27**,** 12413-8.
Finsterer, J. (2006) Central nervous system manifestations of mitochondrial disorders. *Acta Neurol Scand,* 114**,** 217-38.
Fiorillo, C. D. & J. T. Williams (1998) Glutamate mediates an inhibitory postsynaptic potential in dopamine neurons. *Nature,* 394**,** 78-82.
--- (2000) Cholinergic inhibition of ventral midbrain dopamine neurons. *J Neurosci,* 20**,** 7855-60.
Franz, O., B. Liss, A. Neu & J. Roeper (2000) Single-cell mRNA expression of HCN1 correlates with a fast gating phenotype of hyperpolarization-activated cyclic nucleotide-gated ion channels (Ih) in central neurons. *Eur J Neurosci,* 12**,** 2685-93.
Friedman, A. K., J. J. Walsh, B. Juarez, S. M. Ku, D. Chaudhury, J. Wang, X. Li, D. M. Dietz, N. Pan, V. F. Vialou, R. L. Neve, Z. Yue & M. H. Han (2014) Enhancing depression mechanisms in midbrain dopamine neurons achieves homeostatic resilience. *Science,* 344**,** 313-9.
Fyk-Kolodziej, B. & R. G. Pourcho (2007) Differential distribution of hyperpolarization-activated and cyclic nucleotide-gated channels in cone bipolar cells of the rat retina. *J Comp Neurol,* 501**,** 891-903.
Galligan, J. J., H. Tatsumi, K. Z. Shen, A. Surprenant & R. A. North (1990) Cation current activated by hyperpolarization (IH) in guinea pig enteric neurons. *Am J Physiol,* 259**,** G966-72.
Galter, D., K. Pernold, T. Yoshitake, E. Lindqvist, B. Hoffer, J. Kehr, N. G. Larsson & L. Olson (2010) MitoPark mice mirror the slow progression of key symptoms and L-DOPA response in Parkinson's disease. *Genes Brain Behav,* 9**,** 173-81.
Gasparini, S. & D. DiFrancesco (1997) Action of the hyperpolarization-activated current (Ih) blocker ZD 7288 in hippocampal CA1 neurons. *Pflugers Arch,* 435**,** 99-106.
Gerace, E., A. Masi, F. Resta, R. Felici, E. Landucci, T. Mello, D. E. Pellegrini-Giampietro, G. Mannaioni & F. Moroni (2014) PARP-1 activation causes neuronal death in the hippocampal CA1 region by increasing the expression of Ca(2+)-permeable AMPA receptors. *Neurobiol Dis,* 70**,** 43-52.
German, D. C., K. F. Manaye, P. K. Sonsalla & B. A. Brooks (1992) Midbrain dopaminergic cell loss in Parkinson's disease and MPTP-induced parkinsonism: sparing of calbindin-D28k-containing cells. *Ann N Y Acad Sci,* 648**,** 42-62.
German, D. C., E. L. Nelson, C. L. Liang, S. G. Speciale, C. M. Sinton & P. K. Sonsalla (1996) The neurotoxin MPTP causes degeneration of specific nucleus A8, A9 and A10 dopaminergic neurons in the mouse. *Neurodegeneration,* 5**,** 299-312.
Giasson, B. I., J. E. Duda, I. V. Murray, Q. Chen, J. M. Souza, H. I. Hurtig, H. Ischiropoulos, J. Q. Trojanowski & V. M. Lee (2000) Oxidative damage linked to neurodegeneration by selective alpha-synuclein nitration in synucleinopathy lesions. *Science,* 290**,** 985-9.

Gibb, W. R., M. M. Esiri & A. J. Lees (1987) Clinical and pathological features of diffuse cortical Lewy body disease (Lewy body dementia). *Brain,* 110 (Pt 5)**,** 1131-53.

Giladi, N., M. P. McDermott, S. Fahn, S. Przedborski, J. Jankovic, M. Stern, C. Tanner & P. S. Group (2001) Freezing of gait in PD: prospective assessment in the DATATOP cohort. *Neurology,* 56**,** 1712-21.

Giocomo, L. M. & M. E. Hasselmo (2009) Knock-out of HCN1 subunit flattens dorsal-ventral frequency gradient of medial entorhinal neurons in adult mice. *J Neurosci,* 29**,** 7625-30.

Giocomo, L. M., S. A. Hussaini, F. Zheng, E. R. Kandel, M. B. Moser & E. I. Moser (2011) Grid cells use HCN1 channels for spatial scaling. *Cell,* 147**,** 1159-70.

Girotto, S., M. Sturlese, M. Bellanda, I. Tessari, R. Cappellini, M. Bisaglia, L. Bubacco & S. Mammi (2012) Dopamine-derived quinones affect the structure of the redox sensor DJ-1 through modifications at Cys-106 and Cys-53. *J Biol Chem,* 287**,** 18738-49.

Gitler, A. D., A. Chesi, M. L. Geddie, K. E. Strathearn, S. Hamamichi, K. J. Hill, K. A. Caldwell, G. A. Caldwell, A. A. Cooper, J. C. Rochet & S. Lindquist (2009) Alpha-synuclein is part of a diverse and highly conserved interaction network that includes PARK9 and manganese toxicity. *Nat Genet,* 41**,** 308-15.

Gluck, M. R. & G. D. Zeevalk (2004) Inhibition of brain mitochondrial respiration by dopamine and its metabolites: implications for Parkinson's disease and catecholamine-associated diseases. *J Neurochem,* 91**,** 788-95.

Goedert, M., M. G. Spillantini, K. Del Tredici & H. Braak (2013) 100 years of Lewy pathology. *Nat Rev Neurol,* 9**,** 13-24.

Good, C. H., A. F. Hoffman, B. J. Hoffer, V. I. Chefer, T. S. Shippenberg, C. M. Bäckman, N. G. Larsson, L. Olson, S. Gellhaar, D. Galter & C. R. Lupica (2011) Impaired nigrostriatal function precedes behavioral deficits in a genetic mitochondrial model of Parkinson's disease. *FASEB J,* 25**,** 1333-44.

Grace, A. A. & B. S. Bunney (1980) Nigral dopamine neurons: intracellular recording and identification with L-dopa injection and histofluorescence. *Science,* 210**,** 654-6.

--- (1983) Intracellular and extracellular electrophysiology of nigral dopaminergic neurons--1. Identification and characterization. *Neuroscience,* 10**,** 301-15.

--- (1984) The control of firing pattern in nigral dopamine neurons: burst firing. *J Neurosci,* 4**,** 2877-90.

Grace, A. A., S. B. Floresco, Y. Goto & D. J. Lodge (2007) Regulation of firing of dopaminergic neurons and control of goal-directed behaviors. *Trends Neurosci,* 30**,** 220-7.

Greene, J. G., R. Dingledine & J. T. Greenamyre (2005) Gene expression profiling of rat midbrain dopamine neurons: implications for selective vulnerability in parkinsonism. *Neurobiol Dis,* 18**,** 19-31.

Grimm, J., A. Mueller, F. Hefti & A. Rosenthal (2004) Molecular basis for catecholaminergic neuron diversity. *Proc Natl Acad Sci U S A,* 101**,** 13891-6.

Gunter, T. E., L. Buntinas, G. Sparagna, R. Eliseev & K. Gunter (2000) Mitochondrial calcium transport: mechanisms and functions. *Cell Calcium,* 28**,** 285-96.

Guzman, J. N., J. Sanchez-Padilla, D. Wokosin, J. Kondapalli, E. Ilijic, P. T. Schumacker & D. J. Surmeier (2010) Oxidant stress evoked by pacemaking in dopaminergic neurons is attenuated by DJ-1. *Nature,* 468**,** 696-700.

Guzman, J. N., J. Sánchez-Padilla, C. S. Chan & D. J. Surmeier (2009) Robust pacemaking in substantia nigra dopaminergic neurons. *J Neurosci,* 29**,** 11011-9.

Gómez-Suaga, P., B. Luzón-Toro, D. Churamani, L. Zhang, D. Bloor-Young, S. Patel, P. G. Woodman, G. C. Churchill & S. Hilfiker (2012) Leucine-rich repeat kinase 2 regulates autophagy through a calcium-dependent pathway involving NAADP. *Hum Mol Genet,* 21**,** 511-25.

Haas, R. H., F. Nasirian, K. Nakano, D. Ward, M. Pay, R. Hill & C. W. Shults (1995) Low platelet mitochondrial complex I and complex II/III activity in early untreated Parkinson's disease. *Ann Neurol,* 37**,** 714-22.

Halliday, G. M., A. Ophof, M. Broe, P. H. Jensen, E. Kettle, H. Fedorow, M. I. Cartwright, F. M. Griffiths, C. E. Shepherd & K. L. Double (2005) Alpha-synuclein redistributes to neuromelanin lipid in the substantia nigra early in Parkinson's disease. *Brain,* 128**,** 2654-64.

Halliwell, B. (1992) Reactive oxygen species and the central nervous system. *J Neurochem,* 59**,** 1609-23.
Halliwell, J. V. & P. R. Adams (1982) Voltage-clamp analysis of muscarinic excitation in hippocampal neurons. *Brain Res,* 250**,** 71-92.
Hao, L. Y., B. I. Giasson & N. M. Bonini (2010) DJ-1 is critical for mitochondrial function and rescues PINK1 loss of function. *Proc Natl Acad Sci U S A,* 107**,** 9747-52.
Harnett, M. T., B. E. Bernier, K. C. Ahn & H. Morikawa (2009) Burst-timing-dependent plasticity of NMDA receptor-mediated transmission in midbrain dopamine neurons. *Neuron,* 62**,** 826-38.
Harnett, M. T., J. C. Magee & S. R. Williams (2015) Distribution and function of HCN channels in the apical dendritic tuft of neocortical pyramidal neurons. *J Neurosci,* 35**,** 1024-37.
Harris, N. C. & A. Constanti (1995) Mechanism of block by ZD 7288 of the hyperpolarization-activated inward rectifying current in guinea pig substantia nigra neurons in vitro. *J Neurophysiol,* 74**,** 2366-78.
Harvey, B. K., Y. Wang & B. J. Hoffer (2008) Transgenic rodent models of Parkinson's disease. *Acta Neurochir Suppl,* 101**,** 89-92.
Hauser, D. N., A. A. Dukes, A. D. Mortimer & T. G. Hastings (2013) Dopamine quinone modifies and decreases the abundance of the mitochondrial selenoprotein glutathione peroxidase 4. *Free Radic Biol Med,* 65**,** 419-427.
Hawkins, V. E., J. M. Hawryluk, A. C. Takakura, A. V. Tzingounis, T. S. Moreira & D. K. Mulkey (2015) HCN channels contribute to serotonergic modulation of ventral surface chemosensitive neurons and respiratory activity. *J Neurophysiol,* 113**,** 1195-205.
Hayashi, T., C. Ishimori, K. Takahashi-Niki, T. Taira, Y. C. Kim, H. Maita, C. Maita, H. Ariga & S. M. Iguchi-Ariga (2009) DJ-1 binds to mitochondrial complex I and maintains its activity. *Biochem Biophys Res Commun,* 390**,** 667-72.
He, C., F. Chen, B. Li & Z. Hu (2014) Neurophysiology of HCN channels: from cellular functions to multiple regulations. *Prog Neurobiol,* 112**,** 1-23.
Helley, M. P., J. Pinnell, C. Sportelli & K. Tieu (2017) Mitochondria: A Common Target for Genetic Mutations and Environmental Toxicants in Parkinson's Disease. *Front Genet,* 8**,** 177.
Hernán, M. A., B. Takkouche, F. Caamaño-Isorna & J. J. Gestal-Otero (2002) A meta-analysis of coffee drinking, cigarette smoking, and the risk of Parkinson's disease. *Ann Neurol,* 52**,** 276-84.
Heusinkveld, H. J., M. van den Berg & R. H. Westerink (2014) In vitro dopaminergic neurotoxicity of pesticides: a link with neurodegeneration? *Vet Q,* 34**,** 120-31.
Hindle, J. V. (2010) Ageing, neurodegeneration and Parkinson's disease. *Age Ageing,* 39**,** 156-61.
Hornykiewicz, O. & S. J. Kish (1987) Biochemical pathophysiology of Parkinson's disease. *Adv Neurol,* 45**,** 19-34.
Huang, H. & L. O. Trussell (2014) Presynaptic HCN channels regulate vesicular glutamate transport. *Neuron,* 84**,** 340-6.
Huang, P., Y. Y. Tan, D. Q. Liu, M. M. Herzallah, E. Lapidow, Y. Wang, Y. F. Zang, M. A. Gluck & S. D. Chen (2017) Motor-symptom laterality affects acquisition in Parkinson's disease: A cognitive and functional magnetic resonance imaging study. *Mov Disord,* 32**,** 1047-1055.
Huang, Z., R. Lujan, I. Kadurin, V. N. Uebele, J. J. Renger, A. C. Dolphin & M. M. Shah (2011) Presynaptic HCN1 channels regulate Cav3.2 activity and neurotransmission at select cortical synapses. *Nat Neurosci,* 14**,** 478-86.
Hudson, J. L., C. S. Fong, S. J. Boyson & B. J. Hoffer (1994) Conditioned apomorphine-induced turning in 6-OHDA-lesioned rats. *Pharmacol Biochem Behav,* 49**,** 147-54.
Hutcheon, B., R. M. Miura & E. Puil (1996) Models of subthreshold membrane resonance in neocortical neurons. *J Neurophysiol,* 76**,** 698-714.
Ilijic, E., J. N. Guzman & D. J. Surmeier (2011) The L-type channel antagonist isradipine is neuroprotective in a mouse model of Parkinson's disease. *Neurobiol Dis,* 43**,** 364-71.
Irrcher, I., H. Aleyasin, E. L. Seifert, S. J. Hewitt, S. Chhabra, M. Phillips, A. K. Lutz, M. W. Rousseaux, L. Bevilacqua, A. Jahani-Asl, S. Callaghan, J. G. MacLaurin, K. F. Winklhofer, P. Rizzu, P. Rippstein, R. H. Kim, C. X. Chen, E. A. Fon, R. S. Slack, M. E.

Harper, H. M. McBride, T. W. Mak & D. S. Park (2010) Loss of the Parkinson's disease-linked gene DJ-1 perturbs mitochondrial dynamics. *Hum Mol Genet,* 19**,** 3734-46.
Irwin, I., L. E. DeLanney & J. W. Langston (1993) MPTP and aging. Studies in the C57BL/6 mouse. *Adv Neurol,* 60**,** 197-206.
Ishii, T. M., M. Takano, L. H. Xie, A. Noma & H. Ohmori (1999) Molecular characterization of the hyperpolarization-activated cation channel in rabbit heart sinoatrial node. *J Biol Chem,* 274**,** 12835-9.
Jackson-Lewis, V., M. Jakowec, R. E. Burke & S. Przedborski (1995) Time course and morphology of dopaminergic neuronal death caused by the neurotoxin 1-methyl-4-phenyl-1,2,3,6-tetrahydropyridine. *Neurodegeneration,* 4**,** 257-69.
Jackson-Lewis, V. & S. Przedborski (2007) Protocol for the MPTP mouse model of Parkinson's disease. *Nat Protoc,* 2**,** 141-51.
Jana, S., M. Sinha, D. Chanda, T. Roy, K. Banerjee, S. Munshi, B. S. Patro & S. Chakrabarti (2011) Mitochondrial dysfunction mediated by quinone oxidation products of dopamine: Implications in dopamine cytotoxicity and pathogenesis of Parkinson's disease. *Biochim Biophys Acta,* 1812**,** 663-73.
Jang, M., J. Y. Jang, S. H. Kim, K. B. Uhm, Y. K. Kang, H. J. Kim, S. Chung & M. K. Park (2011) Functional organization of dendritic Ca2+ signals in midbrain dopamine neurons. *Cell Calcium,* 50**,** 370-80.
Janigro, D., M. E. Martenson & T. K. Baumann (1997) Preferential inhibition of Ih in rat trigeminal ganglion neurons by an organic blocker. *J Membr Biol,* 160**,** 101-9.
Jankovic, J. (2002) Essential tremor: a heterogenous disorder. *Mov Disord,* 17**,** 638-44.
Jankovic, J., K. S. Schwartz & W. Ondo (1999) Re-emergent tremor of Parkinson's disease. *J Neurol Neurosurg Psychiatry,* 67**,** 646-50.
Jellinger, K. A. (2010) Basic mechanisms of neurodegeneration: a critical update. *J Cell Mol Med,* 14**,** 457-87.
Jones, S. & A. Bonci (2005) Synaptic plasticity and drug addiction. *Curr Opin Pharmacol,* 5**,** 20-5.
Junn, E., K. W. Lee, B. S. Jeong, T. W. Chan, J. Y. Im & M. M. Mouradian (2009) Repression of alpha-synuclein expression and toxicity by microRNA-7. *Proc Natl Acad Sci U S A,* 106**,** 13052-7.
Kamondi, A. & P. B. Reiner (1991) Hyperpolarization-activated inward current in histaminergic tuberomammillary neurons of the rat hypothalamus. *J Neurophysiol,* 66**,** 1902-11.
Kase, D. & K. Imoto (2012) The Role of HCN Channels on Membrane Excitability in the Nervous System. *J Signal Transduct,* 2012**,** 619747.
Kauer, J. A. & R. C. Malenka (2007) Synaptic plasticity and addiction. *Nat Rev Neurosci,* 8**,** 844-58.
Kaupp, U. B. & R. Seifert (2001) Molecular diversity of pacemaker ion channels. *Annu Rev Physiol,* 63**,** 235-57.
--- (2002) Cyclic nucleotide-gated ion channels. *Physiol Rev,* 82**,** 769-824.
Khaliq, Z. M. & B. P. Bean (2010) Pacemaking in dopaminergic ventral tegmental area neurons: depolarizing drive from background and voltage-dependent sodium conductances. *J Neurosci,* 30**,** 7401-13.
Kim, R. H., P. D. Smith, H. Aleyasin, S. Hayley, M. P. Mount, S. Pownall, A. Wakeham, A. J. You-Ten, S. K. Kalia, P. Horne, D. Westaway, A. M. Lozano, H. Anisman, D. S. Park & T. W. Mak (2005) Hypersensitivity of DJ-1-deficient mice to 1-methyl-4-phenyl-1,2,3,6-tetrahydropyrindine (MPTP) and oxidative stress. *Proc Natl Acad Sci U S A,* 102**,** 5215-20.
Klaidman, L. K., J. D. Adams, A. C. Leung, S. S. Kim & E. Cadenas (1993) Redox cycling of MPP+: evidence for a new mechanism involving hydride transfer with xanthine oxidase, aldehyde dehydrogenase, and lipoamide dehydrogenase. *Free Radic Biol Med,* 15**,** 169-79.
Klar, M., R. Surges & T. J. Feuerstein (2003) Ih channels as modulators of presynaptic terminal function: ZD7288 increases NMDA-evoked [3H]-noradrenaline release in rat neocortex slices. *Naunyn Schmiedebergs Arch Pharmacol,* 367**,** 422-5.
Ko, K. W., M. N. Rasband, V. Meseguer, R. H. Kramer & N. L. Golding (2016) Serotonin modulates spike probability in the axon initial segment through HCN channels. *Nat Neurosci,* 19**,** 826-34.

Kopito, R. R. (2000) Aggresomes, inclusion bodies and protein aggregation. *Trends Cell Biol,* 10**,** 524-30.

Kordower, J. H., C. W. Olanow, H. B. Dodiya, Y. Chu, T. G. Beach, C. H. Adler, G. M. Halliday & R. T. Bartus (2013) Disease duration and the integrity of the nigrostriatal system in Parkinson's disease. *Brain,* 136**,** 2419-31.

Kotake, Y. & S. Ohta (2003) MPP+ analogs acting on mitochondria and inducing neuro-degeneration. *Curr Med Chem,* 10**,** 2507-16.

Kouranova, E. V., B. W. Strassle, R. H. Ring, M. R. Bowlby & D. V. Vasilyev (2008) Hyperpolarization-activated cyclic nucleotide-gated channel mRNA and protein expression in large versus small diameter dorsal root ganglion neurons: correlation with hyperpolarization-activated current gating. *Neuroscience,* 153**,** 1008-19.

Krebiehl, G., S. Ruckerbauer, L. F. Burbulla, N. Kieper, B. Maurer, J. Waak, H. Wolburg, Z. Gizatullina, F. N. Gellerich, D. Woitalla, O. Riess, P. J. Kahle, T. Proikas-Cezanne & R. Krüger (2010) Reduced basal autophagy and impaired mitochondrial dynamics due to loss of Parkinson's disease-associated protein DJ-1. *PLoS One,* 5**,** e9367.

Krishnan, V., M. H. Han, D. L. Graham, O. Berton, W. Renthal, S. J. Russo, Q. Laplant, A. Graham, M. Lutter, D. C. Lagace, S. Ghose, R. Reister, P. Tannous, T. A. Green, R. L. Neve, S. Chakravarty, A. Kumar, A. J. Eisch, D. W. Self, F. S. Lee, C. A. Tamminga, D. C. Cooper, H. K. Gershenfeld & E. J. Nestler (2007) Molecular adaptations underlying susceptibility and resistance to social defeat in brain reward regions. *Cell,* 131**,** 391-404.

Krüger, R., W. Kuhn, T. Müller, D. Woitalla, M. Graeber, S. Kösel, H. Przuntek, J. T. Epplen, L. Schöls & O. Riess (1998) Ala30Pro mutation in the gene encoding alpha-synuclein in Parkinson's disease. *Nat Genet,* 18**,** 106-8.

Kuhn, D. M., R. E. Arthur, D. M. Thomas & L. A. Elferink (1999) Tyrosine hydroxylase is inactivated by catechol-quinones and converted to a redox-cycling quinoprotein: possible relevance to Parkinson's disease. *J Neurochem,* 73**,** 1309-17.

Kusch, J., T. Zimmer, J. Holschuh, C. Biskup, E. Schulz, V. Nache & K. Benndorf (2010) Role of the S4-S5 linker in CNG channel activation. *Biophys J,* 99**,** 2488-96.

Lagrue, E., S. Chalon, S. Bodard, E. Saliba, P. Gressens & P. Castelnau (2007) Lamotrigine is neuroprotective in the energy deficiency model of MPTP intoxicated mice. *Pediatr Res,* 62**,** 14-9.

Lammel, S., A. Hetzel, O. Häckel, I. Jones, B. Liss & J. Roeper (2008) Unique properties of mesoprefrontal neurons within a dual mesocorticolimbic dopamine system. *Neuron,* 57**,** 760-73.

Lammel, S., B. K. Lim & R. C. Malenka (2014) Reward and aversion in a heterogeneous midbrain dopamine system. *Neuropharmacology,* 76 Pt B**,** 351-9.

Lammel, S., E. E. Steinberg, C. Földy, N. R. Wall, K. Beier, L. Luo & R. C. Malenka (2015) Diversity of transgenic mouse models for selective targeting of midbrain dopamine neurons. *Neuron,* 85**,** 429-38.

Lanciego, J. L., N. Luquin & J. A. Obeso (2012) Functional neuroanatomy of the basal ganglia. *Cold Spring Harb Perspect Med,* 2**,** a009621.

Lang, Y., D. Gong & Y. Fan (2015) Calcium channel blocker use and risk of Parkinson's disease: a meta-analysis. *Pharmacoepidemiol Drug Saf,* 24**,** 559-66.

Langston, J. W., P. Ballard, J. W. Tetrud & I. Irwin (1983) Chronic Parkinsonism in humans due to a product of meperidine-analog synthesis. *Science,* 219**,** 979-80.

Langston, J. W., L. S. Forno, J. Tetrud, A. G. Reeves, J. A. Kaplan & D. Karluk (1999) Evidence of active nerve cell degeneration in the substantia nigra of humans years after 1-methyl-4-phenyl-1,2,3,6-tetrahydropyridine exposure. *Ann Neurol,* 46**,** 598-605.

Lawson, L. J., V. H. Perry, P. Dri & S. Gordon (1990) Heterogeneity in the distribution and morphology of microglia in the normal adult mouse brain. *Neuroscience,* 39**,** 151-70.

Lee, C. S., E. H. Song, S. Y. Park & E. S. Han (2003) Combined effect of dopamine and MPP+ on membrane permeability in mitochondria and cell viability in PC12 cells. *Neurochem Int,* 43**,** 147-54.

LEE, J. & A. ZIERING (1947) Piperidine derivatives; 2-phenyl- and 2-phenylalkyl-piperidines. *J Org Chem,* 12**,** 885-93.

Lennox, G. G. & J. S. Lowe (1997) Dementia with Lewy bodies. *Baillieres Clin Neurol,* 6**,** 147-66.

Lill, C. M. (2016) Genetics of Parkinson's disease. *Mol Cell Probes,* 30**,** 386-396.
Lin, A. M., L. Y. Wu, K. C. Hung, H. J. Huang, Y. P. Lei, W. C. Lu & L. S. Hwang (2012) Neuroprotective effects of longan (Dimocarpus longan Lour.) flower water extract on MPP+-induced neurotoxicity in rat brain. *J Agric Food Chem,* 60**,** 9188-94.
Lin, M. T. & M. F. Beal (2006) Mitochondrial dysfunction and oxidative stress in neurodegenerative diseases. *Nature,* 443**,** 787-95.
Liss, B., R. Bruns & J. Roeper (1999a) Alternative sulfonylurea receptor expression defines metabolic sensitivity of K-ATP channels in dopaminergic midbrain neurons. *EMBO J,* 18**,** 833-46.
Liss, B., O. Haeckel, J. Wildmann, T. Miki, S. Seino & J. Roeper (2005) K-ATP channels promote the differential degeneration of dopaminergic midbrain neurons. *Nat Neurosci,* 8**,** 1742-51.
Liss, B., A. Neu & J. Roeper (1999b) The weaver mouse gain-of-function phenotype of dopaminergic midbrain neurons is determined by coactivation of wvGirk2 and K-ATP channels. *J Neurosci,* 19**,** 8839-48.
Liss, B. & J. Roeper (2004) Correlating function and gene expression of individual basal ganglia neurons. *Trends Neurosci,* 27**,** 475-81.
--- (2008) Individual dopamine midbrain neurons: functional diversity and flexibility in health and disease. *Brain Res Rev,* 58**,** 314-21.
Liu, Y., A. Roghani & R. H. Edwards (1992) Gene transfer of a reserpine-sensitive mechanism of resistance to N-methyl-4-phenylpyridinium. *Proc Natl Acad Sci U S A,* 89**,** 9074-8.
Ludwig, A., T. Budde, J. Stieber, S. Moosmang, C. Wahl, K. Holthoff, A. Langebartels, C. Wotjak, T. Munsch, X. Zong, S. Feil, R. Feil, M. Lancel, K. R. Chien, A. Konnerth, H. C. Pape, M. Biel & F. Hofmann (2003) Absence epilepsy and sinus dysrhythmia in mice lacking the pacemaker channel HCN2. *EMBO J,* 22**,** 216-24.
Ludwig, A., X. Zong, M. Jeglitsch, F. Hofmann & M. Biel (1998) A family of hyperpolarization-activated mammalian cation channels. *Nature,* 393**,** 587-91.
Lörincz, A., T. Notomi, G. Tamás, R. Shigemoto & Z. Nusser (2002) Polarized and compartment-dependent distribution of HCN1 in pyramidal cell dendrites. *Nat Neurosci,* 5**,** 1185-93.
Lüscher, C. & K. M. Huber (2010) Group 1 mGluR-dependent synaptic long-term depression: mechanisms and implications for circuitry and disease. *Neuron,* 65**,** 445-59.
Lüscher, C. & R. C. Malenka (2011) Drug-evoked synaptic plasticity in addiction: from molecular changes to circuit remodeling. *Neuron,* 69**,** 650-63.
Lüthi, A. & D. A. McCormick (1999) Ca(2+)-mediated up-regulation of Ih in the thalamus. How cell-intrinsic ionic currents may shape network activity. *Ann N Y Acad Sci,* 868**,** 765-9.
Maccaferri, G., M. Mangoni, A. Lazzari & D. DiFrancesco (1993) Properties of the hyperpolarization-activated current in rat hippocampal CA1 pyramidal cells. *J Neurophysiol,* 69**,** 2129-36.
MacLeod, D., J. Dowman, R. Hammond, T. Leete, K. Inoue & A. Abeliovich (2006) The familial Parkinsonism gene LRRK2 regulates neurite process morphology. *Neuron,* 52**,** 587-93.
Macri, V. & E. A. Accili (2004) Structural elements of instantaneous and slow gating in hyperpolarization-activated cyclic nucleotide-gated channels. *J Biol Chem,* 279**,** 16832-46.
Magee, J. C. (1998) Dendritic hyperpolarization-activated currents modify the integrative properties of hippocampal CA1 pyramidal neurons. *J Neurosci,* 18**,** 7613-24.
--- (1999) Dendritic lh normalizes temporal summation in hippocampal CA1 neurons. *Nat Neurosci,* 2**,** 508-14.
Mandavilli, B. S., S. F. Ali & B. Van Houten (2000) DNA damage in brain mitochondria caused by aging and MPTP treatment. *Brain Res,* 885**,** 45-52.
Mandir, A. S., S. Przedborski, V. Jackson-Lewis, Z. Q. Wang, C. M. Simbulan-Rosenthal, M. E. Smulson, B. E. Hoffman, D. B. Guastella, V. L. Dawson & T. M. Dawson (1999) Poly(ADP-ribose) polymerase activation mediates 1-methyl-4-phenyl-1, 2,3,6-tetrahydropyridine (MPTP)-induced parkinsonism. *Proc Natl Acad Sci U S A,* 96**,** 5774-9.
Manning-Bog, A. B., A. L. McCormack, J. Li, V. N. Uversky, A. L. Fink & D. A. Di Monte (2002) The herbicide paraquat causes up-regulation and aggregation of alpha-synuclein in mice: paraquat and alpha-synuclein. *J Biol Chem,* 277**,** 1641-4.
Margolis, E. B., A. R. Coker, J. R. Driscoll, A. I. Lemaître & H. L. Fields (2010) Reliability in the identification of midbrain dopamine neurons. *PLoS One,* 5**,** e15222.

Margolis, E. B., H. Lock, G. O. Hjelmstad & H. L. Fields (2006) The ventral tegmental area revisited: is there an electrophysiological marker for dopaminergic neurons? *J Physiol,* 577**,** 907-24.

Margolis, E. B., B. Toy, P. Himmels, M. Morales & H. L. Fields (2012) Identification of rat ventral tegmental area GABAergic neurons. *PLoS One,* 7**,** e42365.

Marsden, C. D. (1983) Neuromelanin and Parkinson's disease. *J Neural Transm Suppl,* 19**,** 121-41.

Masi, A., R. Narducci, E. Landucci, F. Moroni & G. Mannaioni (2013) MPP(+) -dependent inhibition of Ih reduces spontaneous activity and enhances EPSP summation in nigral dopamine neurons. *Br J Pharmacol,* 169**,** 130-42.

Masoud, S. T., L. M. Vecchio, Y. Bergeron, M. M. Hossain, L. T. Nguyen, M. K. Bermejo, B. Kile, T. D. Sotnikova, W. B. Siesser, R. R. Gainetdinov, R. M. Wightman, M. G. Caron, J. R. Richardson, G. W. Miller, A. J. Ramsey, M. Cyr & A. Salahpour (2015) Increased expression of the dopamine transporter leads to loss of dopamine neurons, oxidative stress and l-DOPA reversible motor deficits. *Neurobiol Dis,* 74**,** 66-75.

Matsushita, N., H. Okada, Y. Yasoshima, K. Takahashi, K. Kiuchi & K. Kobayashi (2002) Dynamics of tyrosine hydroxylase promoter activity during midbrain dopaminergic neuron development. *J Neurochem,* 82**,** 295-304.

Mayer, M. L. & G. L. Westbrook (1983) A voltage-clamp analysis of inward (anomalous) rectification in mouse spinal sensory ganglion neurones. *J Physiol,* 340**,** 19-45.

McCormick, D. A. & H. C. Pape (1990) Properties of a hyperpolarization-activated cation current and its role in rhythmic oscillation in thalamic relay neurones. *J Physiol,* 431**,** 291-318.

McGeer, P. L., S. Itagaki, B. E. Boyes & E. G. McGeer (1988) Reactive microglia are positive for HLA-DR in the substantia nigra of Parkinson's and Alzheimer's disease brains. *Neurology,* 38**,** 1285-91.

Mercuri, N. B., A. Bonci, P. Calabresi, A. Stefani & G. Bernardi (1995) Properties of the hyperpolarization-activated cation current Ih in rat midbrain dopaminergic neurons. *Eur J Neurosci,* 7**,** 462-9.

Meredith, G. E. & D. J. Rademacher (2011) MPTP mouse models of Parkinson's disease: an update. *J Parkinsons Dis,* 1**,** 19-33.

Meredith, G. E., S. Totterdell, M. Beales & C. K. Meshul (2009) Impaired glutamate homeostasis and programmed cell death in a chronic MPTP mouse model of Parkinson's disease. *Exp Neurol,* 219**,** 334-40.

Meredith, G. E., S. Totterdell, J. A. Potashkin & D. J. Surmeier (2008) Modeling PD pathogenesis in mice: advantages of a chronic MPTP protocol. *Parkinsonism Relat Disord,* 14 Suppl 2**,** S112-5.

Michels, G., F. Er, I. F. Khan, J. Endres-Becker, M. C. Brandt, N. Gassanov, D. C. Johns & U. C. Hoppe (2008) K+ channel regulator KCR1 suppresses heart rhythm by modulating the pacemaker current If. *PLoS One,* 3**,** e1511.

Miller, G. W., R. R. Gainetdinov, A. I. Levey & M. G. Caron (1999) Dopamine transporters and neuronal injury. *Trends Pharmacol Sci,* 20**,** 424-9.

Minami, K., T. Miki, T. Kadowaki & S. Seino (2004) Roles of ATP-sensitive K+ channels as metabolic sensors: studies of Kir6.x null mice. *Diabetes,* 53 Suppl 3**,** S176-80.

Mizuno, Y., S. Ohta, M. Tanaka, S. Takamiya, K. Suzuki, T. Sato, H. Oya, T. Ozawa & Y. Kagawa (1989) Deficiencies in complex I subunits of the respiratory chain in Parkinson's disease. *Biochem Biophys Res Commun,* 163**,** 1450-5.

Modinos, G., H. H. Tseng, I. Falkenberg, C. Samson, P. McGuire & P. Allen (2015) Neural correlates of aberrant emotional salience predict psychotic symptoms and global functioning in high-risk and first-episode psychosis. *Soc Cogn Affect Neurosci,* 10**,** 1429-36.

Moosmang, S., J. Stieber, X. Zong, M. Biel, F. Hofmann & A. Ludwig (2001) Cellular expression and functional characterization of four hyperpolarization-activated pacemaker channels in cardiac and neuronal tissues. *Eur J Biochem,* 268**,** 1646-52.

Moratalla, R., B. Quinn, L. E. DeLanney, I. Irwin, J. W. Langston & A. M. Graybiel (1992) Differential vulnerability of primate caudate-putamen and striosome-matrix dopamine systems to the neurotoxic effects of 1-methyl-4-phenyl-1,2,3,6-tetrahydropyridine. *Proc Natl Acad Sci U S A,* 89**,** 3859-63.

Morgan, N. V., S. K. Westaway, J. E. Morton, A. Gregory, P. Gissen, S. Sonek, H. Cangul, J. Coryell, N. Canham, N. Nardocci, G. Zorzi, S. Pasha, D. Rodriguez, I. Desguerre, A. Mubaidin, E. Bertini, R. C. Trembath, A. Simonati, C. Schanen, C. A. Johnson, B. Levinson, C. G. Woods, B. Wilmot, P. Kramer, J. Gitschier, E. R. Maher & S. J. Hayflick (2006) PLA2G6, encoding a phospholipase A2, is mutated in neurodegenerative disorders with high brain iron. *Nat Genet,* 38**,** 752-4.

Morikawa, H., F. Imani, K. Khodakhah & J. T. Williams (2000) Inositol 1,4,5-triphosphate-evoked responses in midbrain dopamine neurons. *J Neurosci,* 20**,** RC103.

Morikawa, H., K. Khodakhah & J. T. Williams (2003) Two intracellular pathways mediate metabotropic glutamate receptor-induced Ca2+ mobilization in dopamine neurons. *J Neurosci,* 23**,** 149-57.

Morikawa, H. & C. A. Paladini (2011) Dynamic regulation of midbrain dopamine neuron activity: intrinsic, synaptic, and plasticity mechanisms. *Neuroscience,* 198**,** 95-111.

Morrison, J. H. & P. R. Hof (2002) Selective vulnerability of corticocortical and hippocampal circuits in aging and Alzheimer's disease. *Prog Brain Res,* 136**,** 467-86.

Moser, M. B., D. C. Rowland & E. I. Moser (2015) Place cells, grid cells, and memory. *Cold Spring Harb Perspect Biol,* 7**,** a021808.

Muchowski, P. J. (2002) Protein misfolding, amyloid formation, and neurodegeneration: a critical role for molecular chaperones? *Neuron,* 35**,** 9-12.

Musialek, P., M. Lei, H. F. Brown, D. J. Paterson & B. Casadei (1997) Nitric oxide can increase heart rate by stimulating the hyperpolarization-activated inward current, I(f). *Circ Res,* 81**,** 60-8.

Muthane, U., K. A. Ramsay, H. Jiang, V. Jackson-Lewis, D. Donaldson, S. Fernando, M. Ferreira & S. Przedborski (1994) Differences in nigral neuron number and sensitivity to 1-methyl-4-phenyl-1,2,3,6-tetrahydropyridine in C57/bl and CD-1 mice. *Exp Neurol,* 126**,** 195-204.

Müftüoglu, M., B. Elibol, O. Dalmizrak, A. Ercan, G. Kulaksiz, H. Ogüs, T. Dalkara & N. Ozer (2004) Mitochondrial complex I and IV activities in leukocytes from patients with parkin mutations. *Mov Disord,* 19**,** 544-8.

Nagatsu, T. (1997) Isoquinoline neurotoxins in the brain and Parkinson's disease. *Neurosci Res,* 29**,** 99-111.

Navarro, B., M. E. Kennedy, B. Velimirovíc, D. Bhat, A. S. Peterson & D. E. Clapham (1996) Nonselective and G betagamma-insensitive weaver K+ channels. *Science,* 272**,** 1950-3.

Neitz, A., E. Mergia, B. Imbrosci, E. Petrasch-Parwez, U. T. Eysel, D. Koesling & T. Mittmann (2014) Postsynaptic NO/cGMP increases NMDA receptor currents via hyperpolarization-activated cyclic nucleotide-gated channels in the hippocampus. *Cereb Cortex,* 24**,** 1923-36.

Neuhoff, H., A. Neu, B. Liss & J. Roeper (2002) I(h) channels contribute to the different functional properties of identified dopaminergic subpopulations in the midbrain. *J Neurosci,* 22**,** 1290-302.

Nicholls, D. G. & S. L. Budd (1998) Mitochondria and neuronal glutamate excitotoxicity. *Biochim Biophys Acta,* 1366**,** 97-112.

--- (2000) Mitochondria and neuronal survival. *Physiol Rev,* 80**,** 315-60.

Nicklas, W. J., S. K. Youngster, M. V. Kindt & R. E. Heikkila (1987) MPTP, MPP+ and mitochondrial function. *Life Sci,* 40**,** 721-9.

Nolan, M. F., G. Malleret, J. T. Dudman, D. L. Buhl, B. Santoro, E. Gibbs, S. Vronskaya, G. Buzsáki, S. A. Siegelbaum, E. R. Kandel & A. Morozov (2004) A behavioral role for dendritic integration: HCN1 channels constrain spatial memory and plasticity at inputs to distal dendrites of CA1 pyramidal neurons. *Cell,* 119**,** 719-32.

Noma, A. & H. Irisawa (1976) Membrane currents in the rabbit sinoatrial node cell as studied by the double microelectrode method. *Pflugers Arch,* 364**,** 45-52.

Norris, K. L., R. Hao, L. F. Chen, C. H. Lai, M. Kapur, P. J. Shaughnessy, D. Chou, J. Yan, J. P. Taylor, S. Engelender, A. E. West, K. L. Lim & T. P. Yao (2015) Convergence of Parkin, PINK1, and α-Synuclein on Stress-induced Mitochondrial Morphological Remodeling. *J Biol Chem,* 290**,** 13862-74.

Notomi, T. & R. Shigemoto (2004) Immunohistochemical localization of Ih channel subunits, HCN1-4, in the rat brain. *J Comp Neurol,* 471**,** 241-76.

Oakley, A. E., J. F. Collingwood, J. Dobson, G. Love, H. R. Perrott, J. A. Edwardson, M. Elstner & C. M. Morris (2007) Individual dopaminergic neurons show raised iron levels in Parkinson disease. *Neurology,* 68**,** 1820-5.

Obeso, J. A., M. C. Rodriguez-Oroz, C. G. Goetz, C. Marin, J. H. Kordower, M. Rodriguez, E. C. Hirsch, M. Farrer, A. H. Schapira & G. Halliday (2010) Missing pieces in the Parkinson's disease puzzle. *Nat Med,* 16**,** 653-61.

Ovadia, A., Z. Zhang & D. M. Gash (1995) Increased susceptibility to MPTP toxicity in middle-aged rhesus monkeys. *Neurobiol Aging,* 16**,** 931-7.

Palacino, J. J., D. Sagi, M. S. Goldberg, S. Krauss, C. Motz, M. Wacker, J. Klose & J. Shen (2004) Mitochondrial dysfunction and oxidative damage in parkin-deficient mice. *J Biol Chem,* 279**,** 18614-22.

Pape, H. C. (1996) Queer current and pacemaker: the hyperpolarization-activated cation current in neurons. *Annu Rev Physiol,* 58**,** 299-327.

Pape, H. C. & R. Mager (1992) Nitric oxide controls oscillatory activity in thalamocortical neurons. *Neuron,* 9**,** 441-8.

Park, J., J. S. Min, B. Kim, U. B. Chae, J. W. Yun, M. S. Choi, I. K. Kong, K. T. Chang & D. S. Lee (2015) Mitochondrial ROS govern the LPS-induced pro-inflammatory response in microglia cells by regulating MAPK and NF-κB pathways. *Neurosci Lett,* 584**,** 191-6.

Park, J. S., B. Koentjoro, D. Veivers, A. Mackay-Sim & C. M. Sue (2014) Parkinson's disease-associated human ATP13A2 (PARK9) deficiency causes zinc dyshomeostasis and mitochondrial dysfunction. *Hum Mol Genet,* 23**,** 2802-15.

Park, J. S., M. K. Thorsness, R. Policastro, L. L. McGoldrick, N. M. Hollingsworth, P. E. Thorsness & A. M. Neiman (2016) Yeast Vps13 promotes mitochondrial function and is localized at membrane contact sites. *Mol Biol Cell,* 27**,** 2435-49.

Park, K. S., J. W. Yang, E. Seikel & J. S. Trimmer (2008) Potassium channel phosphorylation in excitable cells: providing dynamic functional variability to a diverse family of ion channels. *Physiology (Bethesda),* 23**,** 49-57.

Parker, W. D., J. K. Parks & R. H. Swerdlow (2008) Complex I deficiency in Parkinson's disease frontal cortex. *Brain Res,* 1189**,** 215-8.

Patil, N., D. R. Cox, D. Bhat, M. Faham, R. M. Myers & A. S. Peterson (1995) A potassium channel mutation in weaver mice implicates membrane excitability in granule cell differentiation. *Nat Genet,* 11**,** 126-9.

Pavlov, I., A. Scimemi, L. Savtchenko, D. M. Kullmann & M. C. Walker (2011) I(h)-mediated depolarization enhances the temporal precision of neuronal integration. *Nat Commun,* 2**,** 199.

Perkins, K. L. & R. K. Wong (1995) Intracellular QX-314 blocks the hyperpolarization-activated inward current Iq in hippocampal CA1 pyramidal cells. *J Neurophysiol,* 73**,** 911-5.

Perry, V. H. (2012) Innate inflammation in Parkinson's disease. *Cold Spring Harb Perspect Med,* 2**,** a009373.

Philippart, F., G. Destreel, P. Merino-Sepúlveda, P. Henny, D. Engel & V. Seutin (2016) Differential Somatic Ca2+ Channel Profile in Midbrain Dopaminergic Neurons. *J Neurosci,* 36**,** 7234-45.

Piallat, B., A. Benazzouz & A. L. Benabid (1996) Subthalamic nucleus lesion in rats prevents dopaminergic nigral neuron degeneration after striatal 6-OHDA injection: behavioural and immunohistochemical studies. *Eur J Neurosci,* 8**,** 1408-14.

Pickrell, A. M. & R. J. Youle (2015) The roles of PINK1, parkin, and mitochondrial fidelity in Parkinson's disease. *Neuron,* 85**,** 257-73.

Plowey, E. D., S. J. Cherra, Y. J. Liu & C. T. Chu (2008) Role of autophagy in G2019S-LRRK2-associated neurite shortening in differentiated SH-SY5Y cells. *J Neurochem,* 105**,** 1048-56.

Plum, S., S. Helling, C. Theiss, R. E. P. Leite, C. May, W. Jacob-Filho, M. Eisenacher, K. Kuhlmann, H. E. Meyer, P. Riederer, L. T. Grinberg, M. Gerlach & K. Marcus (2013) Combined enrichment of neuromelanin granules and synaptosomes from human substantia nigra pars compacta tissue for proteomic analysis. *J Proteomics,* 94**,** 202-206.

Poetschke, C., E. Dragicevic, J. Duda, J. Benkert, A. Dougalis, R. DeZio, T. P. Snutch, J. Striessnig & B. Liss (2015) Compensatory T-type Ca2+ channel activity alters D2-autoreceptor

responses of Substantia nigra dopamine neurons from Cav1.3 L-type Ca2+ channel KO mice. *Sci Rep,* 5**,** 13688.

Polito, L., A. Greco & D. Seripa (2016) Genetic Profile, Environmental Exposure, and Their Interaction in Parkinson's Disease. *Parkinsons Dis,* 2016**,** 6465793.

Polymeropoulos, M. H., C. Lavedan, E. Leroy, S. E. Ide, A. Dehejia, A. Dutra, B. Pike, H. Root, J. Rubenstein, R. Boyer, E. S. Stenroos, S. Chandrasekharappa, A. Athanassiadou, T. Papapetropoulos, W. G. Johnson, A. M. Lazzarini, R. C. Duvoisin, G. Di Iorio, L. I. Golbe & R. L. Nussbaum (1997) Mutation in the alpha-synuclein gene identified in families with Parkinson's disease. *Science,* 276**,** 2045-7.

Poolos, N. P., M. Migliore & D. Johnston (2002) Pharmacological upregulation of h-channels reduces the excitability of pyramidal neuron dendrites. *Nat Neurosci,* 5**,** 767-74.

Proenza, C., D. Angoli, E. Agranovich, V. Macri & E. A. Accili (2002) Pacemaker channels produce an instantaneous current. *J Biol Chem,* 277**,** 5101-9.

Provensi, G., R. Fabbri, L. Munari, A. Costa, E. Baldi, C. Bucherelli, P. Blandina & M. B. Passani (2017) Histaminergic Neurotransmission as a Gateway for the Cognitive Effect of Oleoylethanolamide in Contextual Fear Conditioning. *Int J Neuropsychopharmacol,* 20**,** 392-399.

Przedborski, S., M. Vila, V. Jackson-Lewis & T. M. Dawson (2000) Reply: a new look at the pathogenesis of Parkinson's disease. *Trends Pharmacol Sci,* 21**,** 165.

Pukass, K. & C. Richter-Landsberg (2014) Oxidative stress promotes uptake, accumulation, and oligomerization of extracellular α-synuclein in oligodendrocytes. *J Mol Neurosci,* 52**,** 339-52.

Puopolo, M., E. Raviola & B. P. Bean (2007) Roles of subthreshold calcium current and sodium current in spontaneous firing of mouse midbrain dopamine neurons. *J Neurosci,* 27**,** 645-56.

Rabinovic, A. D., D. A. Lewis & T. G. Hastings (2000) Role of oxidative changes in the degeneration of dopamine terminals after injection of neurotoxic levels of dopamine. *Neuroscience,* 101**,** 67-76.

Ramonet, D., A. Podhajska, K. Stafa, S. Sonnay, A. Trancikova, E. Tsika, O. Pletnikova, J. C. Troncoso, L. Glauser & D. J. Moore (2012) PARK9-associated ATP13A2 localizes to intracellular acidic vesicles and regulates cation homeostasis and neuronal integrity. *Hum Mol Genet,* 21**,** 1725-43.

Ramsay, R. R. & T. P. Singer (1986) Energy-dependent uptake of N-methyl-4-phenylpyridinium, the neurotoxic metabolite of 1-methyl-4-phenyl-1,2,3,6-tetrahydropyridine, by mitochondria. *J Biol Chem,* 261**,** 7585-7.

Rana, M., I. de Coo, F. Diaz, H. Smeets & C. T. Moraes (2000) An out-of-frame cytochrome b gene deletion from a patient with parkinsonism is associated with impaired complex III assembly and an increase in free radical production. *Ann Neurol,* 48**,** 774-81.

Ratner, M. H., D. H. Farb, J. Ozer, R. G. Feldman & R. Durso (2014) Younger age at onset of sporadic Parkinson's disease among subjects occupationally exposed to metals and pesticides. *Interdiscip Toxicol,* 7**,** 123-33.

Richardson, J. R., Y. Quan, T. B. Sherer, J. T. Greenamyre & G. W. Miller (2005) Paraquat neurotoxicity is distinct from that of MPTP and rotenone. *Toxicol Sci,* 88**,** 193-201.

Riley, D., A. E. Lang, R. D. Blair, A. Birnbaum & B. Reid (1989) Frozen shoulder and other shoulder disturbances in Parkinson's disease. *J Neurol Neurosurg Psychiatry,* 52**,** 63-6.

Ritz, B., S. L. Rhodes, L. Qian, E. Schernhammer, J. H. Olsen & S. Friis (2010) L-type calcium channel blockers and Parkinson disease in Denmark. *Ann Neurol,* 67**,** 600-6.

Robinson, R. B. & S. A. Siegelbaum (2003) Hyperpolarization-activated cation currents: from molecules to physiological function. *Annu Rev Physiol,* 65**,** 453-80.

Rodriguez-Oroz, M. C., M. Jahanshahi, P. Krack, I. Litvan, R. Macias, E. Bezard & J. A. Obeso (2009) Initial clinical manifestations of Parkinson's disease: features and pathophysiological mechanisms. *Lancet Neurol,* 8**,** 1128-39.

Rohrbacher, J., N. Ichinohe & S. T. Kitai (2000) Electrophysiological characteristics of substantia nigra neurons in organotypic cultures: spontaneous and evoked activities. *Neuroscience,* 97**,** 703-14.

Rose, S., M. Nomoto, E. A. Jackson, W. R. Gibb, P. Jaehnig, P. Jenner & C. D. Marsden (1993) Age-related effects of 1-methyl-4-phenyl-1,2,3,6-tetrahydropyridine treatment of common marmosets. *Eur J Pharmacol,* 230**,** 177-85.

Ross, G. W., H. Petrovitch, R. D. Abbott, J. Nelson, W. Markesbery, D. Davis, J. Hardman, L. Launer, K. Masaki, C. M. Tanner & L. R. White (2004) Parkinsonian signs and substantia nigra neuron density in decendents elders without PD. *Ann Neurol,* 56**,** 532-9.

Rozas, G., M. J. Guerra & J. L. Labandeira-García (1997) An automated rotarod method for quantitative drug-free evaluation of overall motor deficits in rat models of parkinsonism. *Brain Res Brain Res Protoc,* 2**,** 75-84.

Russo, S. J., J. W. Murrough, M. H. Han, D. S. Charney & E. J. Nestler (2012) Neurobiology of resilience. *Nat Neurosci,* 15**,** 1475-84.

Ryan, B. J., S. Hoek, E. A. Fon & R. Wade-Martins (2015) Mitochondrial dysfunction and mitophagy in Parkinson's: from familial to sporadic disease. *Trends Biochem Sci,* 40**,** 200-10.

Salthun-Lassalle, B., S. Traver, E. C. Hirsch & P. P. Michel (2005) Substance P, neurokinins A and B, and synthetic tachykinin peptides protect mesencephalic dopaminergic neurons in culture via an activity-dependent mechanism. *Mol Pharmacol,* 68**,** 1214-24.

Santens, P., P. Boon, D. Van Roost & J. Caemaert (2003) The pathophysiology of motor symptoms in Parkinson's disease. *Acta Neurol Belg,* 103**,** 129-34.

Santoro, B., S. Chen, A. Luthi, P. Pavlidis, G. P. Shumyatsky, G. R. Tibbs & S. A. Siegelbaum (2000) Molecular and functional heterogeneity of hyperpolarization-activated pacemaker channels in the mouse CNS. *J Neurosci,* 20**,** 5264-75.

Santoro, B., D. T. Liu, H. Yao, D. Bartsch, E. R. Kandel, S. A. Siegelbaum & G. R. Tibbs (1998) Identification of a gene encoding a hyperpolarization-activated pacemaker channel of brain. *Cell,* 93**,** 717-29.

Santoro, B., B. J. Wainger & S. A. Siegelbaum (2004) Regulation of HCN channel surface expression by a novel C-terminal protein-protein interaction. *J Neurosci,* 24**,** 10750-62.

Saporito, M. S., E. M. Brown, M. S. Miller & S. Carswell (1999) CEP-1347/KT-7515, an inhibitor of c-jun N-terminal kinase activation, attenuates the 1-methyl-4-phenyl tetrahydropyridine-mediated loss of nigrostriatal dopaminergic neurons In vivo. *J Pharmacol Exp Ther,* 288**,** 421-7.

Saudou, F., S. Finkbeiner, D. Devys & M. E. Greenberg (1998) Huntingtin acts in the nucleus to induce apoptosis but death does not correlate with the formation of intranuclear inclusions. *Cell,* 95**,** 55-66.

Scarffe, L. A., D. A. Stevens, V. L. Dawson & T. M. Dawson (2014) Parkin and PINK1: much more than mitophagy. *Trends Neurosci,* 37**,** 315-24.

Schapira, A. H., J. M. Cooper, D. Dexter, J. B. Clark, P. Jenner & C. D. Marsden (1990) Mitochondrial complex I deficiency in Parkinson's disease. *J Neurochem,* 54**,** 823-7.

Schapira, A. H. & M. Gegg (2011) Mitochondrial contribution to Parkinson's disease pathogenesis. *Parkinsons Dis,* 2011**,** 159160.

Schapira, A. H., C. W. Olanow, J. T. Greenamyre & E. Bezard (2014) Slowing of neurodegeneration in Parkinson's disease and Huntington's disease: future therapeutic perspectives. *Lancet,* 384**,** 545-55.

Schuchmann, S., M. Lückermann, A. Kulik, U. Heinemann & K. Ballanyi (2000) Ca(2+)- and metabolism-related changes of mitochondrial potential in voltage-clamped CA1 pyramidal neurons in situ. *J Neurophysiol,* 83**,** 1710-21.

Schultz, W. (2007) Multiple dopamine functions at different time courses. *Annu Rev Neurosci,* 30**,** 259-88.

Schulz, D. J., J. M. Goaillard & E. Marder (2006) Variable channel expression in identified single and electrically coupled neurons in different animals. *Nat Neurosci,* 9**,** 356-62.

Schulz, D. J., S. Temporal, D. M. Barry & M. L. Garcia (2008) Mechanisms of voltage-gated ion channel regulation: from gene expression to localization. *Cell Mol Life Sci,* 65**,** 2215-31.

Scroggs, R. S., S. M. Todorovic, E. G. Anderson & A. P. Fox (1994) Variation in IH, IIR, and ILEAK between acutely isolated adult rat dorsal root ganglion neurons of different size. *J Neurophysiol,* 71**,** 271-9.

Segura-Aguilar, J., I. Paris, P. Muñoz, E. Ferrari, L. Zecca & F. A. Zucca (2014) Protective and toxic roles of dopamine in Parkinson's disease. *J Neurochem,* 129**,** 898-915.

Seino, S. & T. Miki (2004) Gene targeting approach to clarification of ion channel function: studies of Kir6.x null mice. *J Physiol,* 554**,** 295-300.

Seniuk, N. A., W. G. Tatton & C. E. Greenwood (1990) Dose-dependent destruction of the coeruleus-cortical and nigral-striatal projections by MPTP. *Brain Res,* 527**,** 7-20.

Sheehan, J. P., R. H. Swerdlow, S. W. Miller, R. E. Davis, J. K. Parks, W. D. Parker & J. B. Tuttle (1997) Calcium homeostasis and reactive oxygen species production in cells transformed by mitochondria from individuals with sporadic Alzheimer's disease. *J Neurosci,* 17**,** 4612-22.

Sheets, P. L., B. A. Suter, T. Kiritani, C. S. Chan, D. J. Surmeier & G. M. Shepherd (2011) Corticospinal-specific HCN expression in mouse motor cortex: I(h)-dependent synaptic integration as a candidate microcircuit mechanism involved in motor control. *J Neurophysiol,* 106**,** 2216-31.

Sherer, T. B., R. Betarbet & J. T. Greenamyre (2002a) Environment, mitochondria, and Parkinson's disease. *Neuroscientist,* 8**,** 192-7.

Sherer, T. B., R. Betarbet, A. K. Stout, S. Lund, M. Baptista, A. V. Panov, M. R. Cookson & J. T. Greenamyre (2002b) An in vitro model of Parkinson's disease: linking mitochondrial impairment to altered alpha-synuclein metabolism and oxidative damage. *J Neurosci,* 22**,** 7006-15.

Sherer, T. B., R. Betarbet, C. M. Testa, B. B. Seo, J. R. Richardson, J. H. Kim, G. W. Miller, T. Yagi, A. Matsuno-Yagi & J. T. Greenamyre (2003) Mechanism of toxicity in rotenone models of Parkinson's disease. *J Neurosci,* 23**,** 10756-64.

Sherman, M. Y. & A. L. Goldberg (2001) Cellular defenses against unfolded proteins: a cell biologist thinks about neurodegenerative diseases. *Neuron,* 29**,** 15-32.

Shin, K. S., B. S. Rothberg & G. Yellen (2001) Blocker state dependence and trapping in hyperpolarization-activated cation channels: evidence for an intracellular activation gate. *J Gen Physiol,* 117**,** 91-101.

Singleton, A. B., M. J. Farrer & V. Bonifati (2013) The genetics of Parkinson's disease: progress and therapeutic implications. *Mov Disord,* 28**,** 14-23.

Slesinger, P. A., M. Stoffel, Y. N. Jan & L. Y. Jan (1997) Defective gamma-aminobutyric acid type B receptor-activated inwardly rectifying K+ currents in cerebellar granule cells isolated from weaver and Girk2 null mutant mice. *Proc Natl Acad Sci U S A,* 94**,** 12210-7.

Sonsalla, P. K., G. D. Zeevalk, L. Manzino, A. Giovanni & W. J. Nicklas (1992) MK-801 fails to protect against the dopaminergic neuropathology produced by systemic 1-methyl-4-phenyl-1,2,3,6-tetrahydropyridine in mice or intranigral 1-methyl-4-phenylpyridinium in rats. *J Neurochem,* 58**,** 1979-982.

Spencer, J. P., P. Jenner, S. E. Daniel, A. J. Lees, D. C. Marsden & B. Halliwell (1998) Conjugates of catecholamines with cysteine and GSH in Parkinson's disease: possible mechanisms of formation involving reactive oxygen species. *J Neurochem,* 71**,** 2112-22.

Spillantini, M. G., R. A. Crowther, R. Jakes, M. Hasegawa & M. Goedert (1998) alpha-Synuclein in filamentous inclusions of Lewy bodies from Parkinson's disease and dementia with lewy bodies. *Proc Natl Acad Sci U S A,* 95**,** 6469-73.

Spillantini, M. G., M. L. Schmidt, V. M. Lee, J. Q. Trojanowski, R. Jakes & M. Goedert (1997) Alpha-synuclein in Lewy bodies. *Nature,* 388**,** 839-40.

Stranahan, A. M. & M. P. Mattson (2010) Selective vulnerability of neurons in layer II of the entorhinal cortex during aging and Alzheimer's disease. *Neural Plast,* 2010**,** 108190.

Striessnig, J., A. Koschak, M. J. Sinnegger-Brauns, A. Hetzenauer, N. K. Nguyen, P. Busquet, G. Pelster & N. Singewald (2006) Role of voltage-gated L-type Ca2+ channel isoforms for brain function. *Biochem Soc Trans,* 34**,** 903-9.

Sulzer, D., J. Bogulavsky, K. E. Larsen, G. Behr, E. Karatekin, M. H. Kleinman, N. Turro, D. Krantz, R. H. Edwards, L. A. Greene & L. Zecca (2000) Neuromelanin biosynthesis is driven by excess cytosolic catecholamines not accumulated by synaptic vesicles. *Proc Natl Acad Sci U S A,* 97**,** 11869-74.

Sulzer, D. & D. J. Surmeier (2013) Neuronal vulnerability, pathogenesis, and Parkinson's disease. *Mov Disord,* 28**,** 41-50.

Sulzer, D. & L. Zecca (2000) Intraneuronal dopamine-quinone synthesis: a review. *Neurotox Res,* 1**,** 181-95.
Surmeier, D. J., J. N. Guzman & J. Sanchez-Padilla (2010) Calcium, cellular aging, and selective neuronal vulnerability in Parkinson's disease. *Cell Calcium,* 47**,** 175-82.
Surmeier, D. J. & P. T. Schumacker (2013) Calcium, bioenergetics, and neuronal vulnerability in Parkinson's disease. *J Biol Chem,* 288**,** 10736-41.
Szydlowska, K. & M. Tymianski (2010) Calcium, ischemia and excitotoxicity. *Cell Calcium,* 47**,** 122-9.
Taira, T., Y. Saito, T. Niki, S. M. Iguchi-Ariga, K. Takahashi & H. Ariga (2004) DJ-1 has a role in antioxidative stress to prevent cell death. *EMBO Rep,* 5**,** 213-8.
Takahashi, N., L. L. Miner, I. Sora, H. Ujike, R. S. Revay, V. Kostic, V. Jackson-Lewis, S. Przedborski & G. R. Uhl (1997) VMAT2 knockout mice: heterozygotes display reduced amphetamine-conditioned reward, enhanced amphetamine locomotion, and enhanced MPTP toxicity. *Proc Natl Acad Sci U S A,* 94**,** 9938-43.
Talbot, K. & K. E. Davies (2001) Spinal muscular atrophy. *Semin Neurol,* 21**,** 189-97.
Tanner, C. M. (1992) Epidemiology of Parkinson's disease. *Neurol Clin,* 10**,** 317-29.
Tatton, N. A. & S. J. Kish (1997) In situ detection of apoptotic nuclei in the substantia nigra compacta of 1-methyl-4-phenyl-1,2,3,6-tetrahydropyridine-treated mice using terminal deoxynucleotidyl transferase labelling and acridine orange staining. *Neuroscience,* 77**,** 1037-48.
Terzioglu, M. & D. Galter (2008) Parkinson's disease: genetic versus toxin-induced rodent models. *FEBS J,* 275**,** 1384-91.
Tokimasa, T. & T. Akasu (1990) Cyclic AMP regulates an inward rectifying sodium-potassium current in dissociated bull-frog sympathetic neurones. *J Physiol,* 420**,** 409-29.
Toulorge, D., S. Guerreiro, A. Hild, U. Maskos, E. C. Hirsch & P. P. Michel (2011) Neuroprotection of midbrain dopamine neurons by nicotine is gated by cytoplasmic Ca2+. *FASEB J,* 25**,** 2563-73.
Travagli, R. A. & R. A. Gillis (1994) Hyperpolarization-activated currents, IH and IKIR, in rat dorsal motor nucleus of the vagus neurons in vitro. *J Neurophysiol,* 71**,** 1308-17.
Trimmer, P. A., T. S. Smith, A. B. Jung & J. P. Bennett (1996) Dopamine neurons from transgenic mice with a knockout of the p53 gene resist MPTP neurotoxicity. *Neurodegeneration,* 5**,** 233-9.
Tsay, D., J. T. Dudman & S. A. Siegelbaum (2007) HCN1 channels constrain synaptically evoked Ca2+ spikes in distal dendrites of CA1 pyramidal neurons. *Neuron,* 56**,** 1076-89.
Uhl, G. R., J. C. Hedreen & D. L. Price (1985) Parkinson's disease: loss of neurons from the ventral tegmental area contralateral to therapeutic surgical lesions. *Neurology,* 35**,** 1215-8.
Uhl, G. R., D. Walther, D. Mash, B. Faucheux & F. Javoy-Agid (1994) Dopamine transporter messenger RNA in Parkinson's disease and control substantia nigra neurons. *Ann Neurol,* 35**,** 494-8.
Ulrich, D. (2002) Dendritic resonance in rat neocortical pyramidal cells. *J Neurophysiol,* 87**,** 2753-9.
Uversky, V. N., J. Li & A. L. Fink (2001) Evidence for a partially folded intermediate in alpha-synuclein fibril formation. *J Biol Chem,* 276**,** 10737-44.
van der Merwe, C., Z. Jalali Sefid Dashti, A. Christoffels, B. Loos & S. Bardien (2015) Evidence for a common biological pathway linking three Parkinson's disease-causing genes: parkin, PINK1 and DJ-1. *Eur J Neurosci,* 41**,** 1113-25.
van Duijn, C. M., M. C. Dekker, V. Bonifati, R. J. Galjaard, J. J. Houwing-Duistermaat, P. J. Snijders, L. Testers, G. J. Breedveld, M. Horstink, L. A. Sandkuijl, J. C. van Swieten, B. A. Oostra & P. Heutink (2001) Park7, a novel locus for autosomal recessive early-onset parkinsonism, on chromosome 1p36. *Am J Hum Genet,* 69**,** 629-34.
van Ginneken, A. C. & W. Giles (1991) Voltage clamp measurements of the hyperpolarization-activated inward current I(f) in single cells from rabbit sino-atrial node. *J Physiol,* 434**,** 57-83.
Van Laar, V. S., A. J. Mishizen, M. Cascio & T. G. Hastings (2009) Proteomic identification of dopamine-conjugated proteins from isolated rat brain mitochondria and SH-SY5Y cells. *Neurobiol Dis,* 34**,** 487-500.

Varastet, M., D. Riche, M. Maziere & P. Hantraye (1994) Chronic MPTP treatment reproduces in baboons the differential vulnerability of mesencephalic dopaminergic neurons observed in Parkinson's disease. *Neuroscience,* 63**,** 47-56.

Vila, M., V. Jackson-Lewis, S. Vukosavic, R. Djaldetti, G. Liberatore, D. Offen, S. J. Korsmeyer & S. Przedborski (2001) Bax ablation prevents dopaminergic neurodegeneration in the 1-methyl- 4-phenyl-1,2,3,6-tetrahydropyridine mouse model of Parkinson's disease. *Proc Natl Acad Sci U S A,* 98**,** 2837-42.

Volman, S. F., S. Lammel, E. B. Margolis, Y. Kim, J. M. Richard, M. F. Roitman & M. K. Lobo (2013) New insights into the specificity and plasticity of reward and aversion encoding in the mesolimbic system. *J Neurosci,* 33**,** 17569-76.

von Lewinski, F. & B. U. Keller (2005) Ca2+, mitochondria and selective motoneuron vulnerability: implications for ALS. *Trends Neurosci,* 28**,** 494-500.

Wainger, B. J., M. DeGennaro, B. Santoro, S. A. Siegelbaum & G. R. Tibbs (2001) Molecular mechanism of cAMP modulation of HCN pacemaker channels. *Nature,* 411**,** 805-10.

Wallace, B. A., K. Ashkan, C. E. Heise, K. D. Foote, N. Torres, J. Mitrofanis & A. L. Benabid (2007) Survival of midbrain dopaminergic cells after lesion or deep brain stimulation of the subthalamic nucleus in MPTP-treated monkeys. *Brain,* 130**,** 2129-45.

Wang, M., B. P. Ramos, C. D. Paspalas, Y. Shu, A. Simen, A. Duque, S. Vijayraghavan, A. Brennan, A. Dudley, E. Nou, J. A. Mazer, D. A. McCormick & A. F. Arnsten (2007) Alpha2A-adrenoceptors strengthen working memory networks by inhibiting cAMP-HCN channel signaling in prefrontal cortex. *Cell,* 129**,** 397-410.

Wang, W. T., Y. H. Wan, J. L. Zhu, G. S. Lei, Y. Y. Wang, P. Zhang & S. J. Hu (2006) Theta-frequency membrane resonance and its ionic mechanisms in rat subicular pyramidal neurons. *Neuroscience,* 140**,** 45-55.

Wang, X., M. H. Yan, H. Fujioka, J. Liu, A. Wilson-Delfosse, S. G. Chen, G. Perry, G. Casadesus & X. Zhu (2012) LRRK2 regulates mitochondrial dynamics and function through direct interaction with DLP1. *Hum Mol Genet,* 21**,** 1931-44.

Warrick, J. M., H. Y. Chan, G. L. Gray-Board, Y. Chai, H. L. Paulson & N. M. Bonini (1999) Suppression of polyglutamine-mediated neurodegeneration in Drosophila by the molecular chaperone HSP70. *Nat Genet,* 23**,** 425-8.

Wells, J. E., K. C. Rowland & E. K. Proctor (2007) Hyperpolarization-activated channels in trigeminal ganglia innervating healthy and pulp-exposed teeth. *Int Endod J,* 40**,** 715-21.

Williams, D. R., H. C. Watt & A. J. Lees (2006) Predictors of falls and fractures in bradykinetic rigid syndromes: a retrospective study. *J Neurol Neurosurg Psychiatry,* 77**,** 468-73.

Williams, S. R. & G. J. Stuart (2000) Site independence of EPSP time course is mediated by dendritic I(h) in neocortical pyramidal neurons. *J Neurophysiol,* 83**,** 3177-82.

Wu, S., W. Gao, C. Xie, X. Xu, C. Vorvis, F. Marni, A. R. Hackett, Q. Liu & L. Zhou (2012) Inner activation gate in S6 contributes to the state-dependent binding of cAMP in full-length HCN2 channel. *J Gen Physiol,* 140**,** 29-39.

Xiang, W., J. C. Schlachetzki, S. Helling, J. C. Bussmann, M. Berlinghof, T. E. Schäffer, K. Marcus, J. Winkler, J. Klucken & C. M. Becker (2013) Oxidative stress-induced posttranslational modifications of alpha-synuclein: specific modification of alpha-synuclein by 4-hydroxy-2-nonenal increases dopaminergic toxicity. *Mol Cell Neurosci,* 54**,** 71-83.

Xiong, N., J. Huang, Z. Zhang, J. Xiong, X. Liu, M. Jia, F. Wang, C. Chen, X. Cao, Z. Liang, S. Sun, Z. Lin & T. Wang (2009) Stereotaxical infusion of rotenone: a reliable rodent model for Parkinson's disease. *PLoS One,* 4**,** e7878.

Xue, W. N., Y. Wang, S. M. He, X. L. Wang, J. L. Zhu & G. D. Gao (2012) SK- and h-current contribute to the generation of theta-like resonance of rat substantia nigra pars compacta dopaminergic neurons at hyperpolarized membrane potentials. *Brain Struct Funct,* 217**,** 379-94.

Yang, L., R. T. Matthews, J. B. Schulz, T. Klockgether, A. W. Liao, J. C. Martinou, J. B. Penney, B. T. Hyman & M. F. Beal (1998) 1-Methyl-4-phenyl-1,2,3,6-tetrahydropyride neurotoxicity is attenuated in mice overexpressing Bcl-2. *J Neurosci,* 18**,** 8145-52.

Yang, Q., P. Kuzyk, I. Antonov, C. J. Bostwick, A. B. Kohn, L. L. Moroz & R. D. Hawkins (2015) Hyperpolarization-activated, cyclic nucleotide-gated cation channels in Aplysia: Contribution to classical conditioning. *Proc Natl Acad Sci U S A,* 112**,** 16030-5.

Yang, Y., S. Gehrke, Y. Imai, Z. Huang, Y. Ouyang, J. W. Wang, L. Yang, M. F. Beal, H. Vogel & B. Lu (2006) Mitochondrial pathology and muscle and dopaminergic neuron degeneration caused by inactivation of Drosophila Pink1 is rescued by Parkin. *Proc Natl Acad Sci U S A,* 103**,** 10793-8.

Yao, X., H. Y. Kwan & Y. Huang (2005) Regulation of TRP channels by phosphorylation. *Neurosignals,* 14**,** 273-80.

Ying, S. W., F. Jia, S. Y. Abbas, F. Hofmann, A. Ludwig & P. A. Goldstein (2007) Dendritic HCN2 channels constrain glutamate-driven excitability in reticular thalamic neurons. *J Neurosci,* 27**,** 8719-32.

Ying, S. W., G. R. Tibbs, A. Picollo, S. Y. Abbas, R. L. Sanford, A. Accardi, F. Hofmann, A. Ludwig & P. A. Goldstein (2011) PIP2-mediated HCN3 channel gating is crucial for rhythmic burst firing in thalamic intergeniculate leaflet neurons. *J Neurosci,* 31**,** 10412-23.

Yu, F. H. & W. A. Catterall (2004) The VGL-chanome: a protein superfamily specialized for electrical signaling and ionic homeostasis. *Sci STKE,* 2004**,** re15.

Yu, F. H., V. Yarov-Yarovoy, G. A. Gutman & W. A. Catterall (2005) Overview of molecular relationships in the voltage-gated ion channel superfamily. *Pharmacol Rev,* 57**,** 387-95.

Zamponi, G. W., J. Striessnig, A. Koschak & A. C. Dolphin (2015) The Physiology, Pathology, and Pharmacology of Voltage-Gated Calcium Channels and Their Future Therapeutic Potential. *Pharmacol Rev,* 67**,** 821-70.

Zesiewicz, T. A., K. L. Sullivan & R. A. Hauser (2006) Nonmotor symptoms of Parkinson's disease. *Expert Rev Neurother,* 6**,** 1811-22.

Zhang, W., K. Phillips, A. R. Wielgus, J. Liu, A. Albertini, F. A. Zucca, R. Faust, S. Y. Qian, D. S. Miller, C. F. Chignell, B. Wilson, V. Jackson-Lewis, S. Przedborski, D. Joset, J. Loike, J. S. Hong, D. Sulzer & L. Zecca (2011) Neuromelanin activates microglia and induces degeneration of dopaminergic neurons: implications for progression of Parkinson's disease. *Neurotox Res,* 19**,** 63-72.

Zucca, F. A., E. Basso, F. A. Cupaioli, E. Ferrari, D. Sulzer, L. Casella & L. Zecca (2014) Neuromelanin of the human substantia nigra: an update. *Neurotox Res,* 25**,** 13-23.

Zuo, L. & M. S. Motherwell (2013) The impact of reactive oxygen species and genetic mitochondrial mutations in Parkinson's disease. *Gene,* 532**,** 18-23.